Effect of Calreticulin and JAK2V617F driver mutations on mitotic progression in myeloproliferative neoplasms

Von der Fakultät für Mathematik, Informatik und Naturwissenschaften der RWTH Aachen University zur Erlangung des akademischen Grades einer Doktorin der Naturwissenschaften genehmigte Dissertation

vorgelegt von

Master of Science (M.Sc.)

Kristin Joana Holl

Aus

Dinslaken, Deutschland

Berichter*:* Univ.-Prof. Dr. rer. nat. Wolfram Antonin

Univ.-Prof. Dr. phil. nat. Gabriele Pradel

Tag der mündlichen Prüfung*:* 23.08.2024

Table of content

Table of content 1
List of figures 3
List of tables 4
Abbreviations 5
Summary 10
Zusammenfassung 11
1. Introduction 13
1.1 Haematopoiesis 13
1.2 Myeloproliferative neoplasm (MPN) 15
1.3 Mitosis 18
1.3.1 Spindle assembly checkpoint 21
1.3.2 Consequences of chromosome segregation errors 23
1.4 Aim of the thesis 26
2. Material and Methods 27
2.1 Material 27
2.1.1 Cell lines 27
2.1.2 Vectors 27
2.1.3 Antibodies 28
2.1.4 Chemicals 29
2.1.5 Software 31
2.1.6 Devices 31
2.2 Methods 32
2.2.1 Cells and their culture treatments 32
2.2.2 Drug treatments 34
2.2.3 Live cell microscopy experiments 35
2.2.4 Immunofluorescence staining experiments 38

2.2.7 Western Blot and gel electrophoresis....39
2.2.6 Flow cytometry experiments....42
3. Results....43
3.1 Effect of ph. neg. MPN mutations in mitotic timing and chromatin segregation 43
3.1.1 Stress-sensitive and error-prone mitosis in CALRdel52 and JAK2V617F transduced 32D^{MPL} cells....45
3.2 Effect of ph. neg. MPN mutations on spindle assembly checkpoint....48
3.2.1 SAC Challenge in 32D^{MPL} cells....48
3.2.2 Time-dependent degradation of Cyclin B1 in 32D^{MPL} cells....51
3.3 Effect of ph. neg. MPN mutations in mitotic timing, chromatin segregation and on spindle assembly checkpoint in human cell models....58
3.3.1 Effects of the mutations CALRdel52 and JAK2V617F on the SAC of human TF-1....58
3.3.2 Effect on mitotic duration and chromatin segregation in CALRdel52 and JAK2V617F transduced TF-1 cells....60
3.3.3 Kinetochore Recruitment of SAC factors in TF-1 cells....62
3.4 Effect of CALRdel52 and JAK2V617F on mitosis of non-haematopoietic cells 64
4. Discussion....67
5. Outlook on further work....73
6. Bibliography....75
7. Appendix....87
8. This thesis would not have been possible without the input of the following people:....93
9. Acknowledgments....94
10. Publications as part of the doctoral thesis....95
Eidesstattliche Erklärung....96

List of figures

Figure 1: Schematic overview of the haematopoiesis. 14
Figure 2: Frequency distribution of the occurrence of disease-causing driver mutations in ph. neg. MPN. 16
Figure 3: Overview of the driver mutations 17
Figure 4. Overview of the different phases of mitosis 19
Figure 5. Overview of SAC reaction in mitosis 22
Figure 6: Chromosome segregation errors and their follow up problems 24
Figure 7: Mitotic time and errors of 32D^{MPL} cells: 44
Figure 8: Mitotic time and errors of 32D^{MPL} cells after doxorubicin or NMS-P715 treatment: 46
Figure 9: Spindle assembly challenge effect on the CALRdel52 and JAK2V617F mutation in 32D^{MPL} cells 49
Figure 10: Difference in expression level of Cyclin B1 over time: 51
Figure 11: Mitotic slippage induced by degradation of Cyclin B1 after time dependent nocodazole treatment: 53
Figure 12: Difference in expression level of key factors in 32D^{MPL} cells: 55
Figure 13: Kinetochore recruitment of SAC factors in 32D^{MPL} cells: 57
Figure 14: Effect of CALRdel52 and JAK2V617F mutation on SAC in TF-1^{MPL} cells. 59
Figure 15: Mitotic time and errors of TF-1^{MPL} cells: 61
Figure 16: Effect of CALRdel52 and JAK2V617F mutation on recruitment of SAC factors: 63
Figure 17: Mitotic time and mitotic errors of HeLa cells transduced with different vectors: 65
Supplemental Figure 18: vector sheets for transfection and transduction 87
Supplemental Figure 19: Overview of results of the first cytometry experiment 89

List of tables

Table 1: Cell lines that were used in this thesis 27
Table 2: Construct names of used vectors 27
Table 3: Antibody used for Western Blot and Immunofluorescence staining 28
Table 4: Chemicals used for all experiments 29
Table 5: Software used for analysing the data.....31
Table 6: Used devices for cell culturing and data generation 31
Table 7: Composition of the different percentages gels for one SDS gel 40
Table 8: List of seeded cells per measured time 41
Supplemental Table 9: Raw compression of Cyclin B1 / GAPDH between 0 h and 3h of nocodazole incubation 88
Supplemental Table 10: Results of the Cyclin B1 time course experiments 88
Supplemental Table 11: Results of cytometry analysis 90
Supplemental Table 12: Exact data from SAC factor western Blotting experiments..90
Supplemental Table 14: Mitotic time and errors of $32D^{MPL}$ cells after doxorubicin NMS-P715 treatment 91
Supplemental Table 13: Signal ratio between the different SAC factors and CREST 92

Abbreviations

°C	Degree centigrade
µM	Micromolar
AB	Antibody
AML	Acute myeloid leukemia
ANOVA	Analysis of variance
APC	Allophycocyanin
APC/C	Anaphase promoting complex/cyclosome
approx.	Approximal
APS	Ammonium persulfate
B	Bursa of Fabricius
B/F/B	Break/fusion/bridge
BSA	Bovine Serum albumin
Ca	Calcium
$CaCl_2$	Calcium chloride
CDC	Cell division cycle protein
CDK1	Cyclin-dependent kinase
cDNA	Complementary DNA
CENP	Centromere-associated protein
cGAS	Cyclic GMP-AMP synthase
CIN	Chromosomal instability
CLP	Common lymphoid progenitors
cm	Centimetre
CML	Chronic myeloid leukaemia

CMP	Common myeloid progenitor
CO_2	Carbon dioxide
CPC	Chromosomal passenger complex
CRM1	Chromosomal region maintenance
Cy	Cyanine
DAPI	4′,6-diamidino-2-phenylindole
DMEM	Dulbecco's modified Eagle's medium
DMSO	Dimethylsulfoxid
DNA	Deoxyribonucleic acid
DTT	Dithiothreitol
Eco	Ecotropic
EDTA	Ethylenediaminetetraacetic acid
e.g.	exempli gratia
eGFP	Enhanced green fluorescent protein
ET	Essential thrombocythemia
EV	Empty vector
expo	Exposition time
FCS	Fetal calf serum
G phase	Gap phase
GAPDH	Glycerinaldehyd-3-phosphat-Dehydrogenase
GFP	green fluorescent protein
GM-CSF	Granulocyte /macrophage colony-stimulating factor
GMF	Granulocyte-macrophage progenitor)
H	Histones
h	Hour

HeLa	Henrietta Lacks
HSC	Haematopoietic stem cells
HSPC	Haematopoietic stem and progenitor cells
i.e.	For example
IG	Immunoglobulin
JAK2	Janus kinase 2
JH	Janus homology domain
KMN	KNL1-MIS12-NDC80
kDa	Kilodalton
L	Leucine
LED	Light-emitting diodes
LSD	Lysine-specific histone demethylase
LT	Long-term
M	Molar
M phase	Mitotic phase
mA	Milliampere
MAD	Mitotic arrest deficient
MAP	Mitogen-activated protein
MCC	Mitotic Control Point Complex
MEM	Minimum Essential Medium
MEP	Megakaryocyte-erythroid progenitors
$MgCl_2$	Magnesium chloride
min	Minutes
mL	Millilitre
MPL	Myeloproliferative leukemia protein

MPN	Myeloproliferative neoplasm
MPP	Multipotent progenitor cells
MPS	monopolar spindle
MYT1	Myelin transcription factor 1
NaCl	Natrium chloride
NDC80	Nuclear division cycle
ng	Nanogram
NH_4CL	Ammonium chloride
NPC	Nuclear pore complex
PBS	Phosphate-buffered saline
PenStrep	Penicillin-Streptomycin
PFA	Paraformaldehyde
Ph. neg.	Philadelphia negative
PLK1	Polo-like kinase 1
PMF	Primary myelofibrosis
PMSCV	Plasmid Murine Stem Cell Virus
PP1	Protein phosphatase-1
PP2A	Protein phosphatase 2A
PV	Polycythaemia vera
ROI	Region of Interest
rh GM-CSF	Recombinant Human Granulocyte Macrophage Colony Stimulating Factor
rpm	Revolutions per minute
RPMI	Roswell Park Memorial Institute
RT	Room temperature

S-phase	Synthesis phase
SAC	Spindle apparatus checkpoint
SCF	Stem cell factor
SDS	Sodium dodecyl sulfate
ST	Short-term
STATs	Signal transducer and activator of transcription proteins
STING	Stimulator of interferon genes
T	Triton x-100 (in experiments)
T	Thymus (in introduction)
TEMED	Tetramethylethylenediamine
TIFF	Tag Image File Format
TPOR	Thrombopoietin receptor
TRIS	Tris(hydroxymethyl)aminomethane
W	Tryptophan

Summary

Myeloproliferative neoplasms (MPN) are diseases of haematopoietic stem cells caused by somatic mutations and clonal expansion of mutated haematopoietic stem and progenitor cells (HSPC). MPNs manifest in various clinical pictures. The most commons are chronic myeloid leukaemia (CML), essential thrombocythemia (ET), polycythaemia vera and primary myelofibrosis (PMF). The present work focuses on Philadelphia-negative MPNs caused by mutations in the Janus Kinase 2 (JAK2) and the calreticulin (CALR).

The prevailing working model assumes that the influence of the cellular microenvironment and the acquisition of additional mutations lead to heterogeneous diseases caused by these driver mutations. In the present study, I demonstrate an increased incidence of chromatin segregation defects in haematopoietic cells with stable expression of the mutations CALRdel52 or JAK2V617F. In addition, my studies on murine 32D^{MPL} and human erythroleukemic TF-1^{MPL} cells showed a correlation between the expression of CALRdel52 or JAK2V617F and a defective spindle assembly checkpoint (SAC). This contributes to defective mitosis, which can lead to aneuploidy and tumorigenesis. Overall, this promotes defective mitosis. Further analysis showed that when CALRdel52 or JAK2V617F is expressed, there is a correlation between a defective SAC and an imbalance in the recruitment of SAC factors to mitotic kinetochores. I observed a premature degradation of Cyclin B1 during mitosis in 32D^{MPL} cells with CALRdel52 or JAK2V617F mutations, which is associated with a weakening of the SAC. My analysis results on the duration of mitosis in non-haematopoietic cells support the hypothesis and shows the importance of a defective SAC for non-error-free mitosis.

In summary, my research results showed that CALRdel52 or JAK2V617F MPN driver mutations alter mitotic regulation potentially impacting karyotype stability, which could be an important factor for the pathogenesis of MPN.

Zusammenfassung

Myeloproliferative Neoplasien (MPN) sind Erkrankungen hämatopoetischer Stammzellen, die durch somatische Mutationen und klonale Expansion mutierter hämatopoetischer Stamm- und Vorläuferzellen (HSPC) verursacht werden. MPN äußert sich in unterschiedlichen Krankheitsbildern. Die häufigsten sind chronische myeloische Leukämie (CML), essentielle Thrombozythämie (ET), Polycythaemia vera und primäre Myelofibrose (PMF). Die vorliegende Arbeit befasst sich mit Philadelphia-negative MPNs, die durch Mutationen in der Janus Kinase 2 (JAK2) und in Calreticulin (CALR) verursacht werden.

Das gegenwärtig vorherrschende Arbeitsmodell geht davon aus, dass der Einfluss der zellulären Mikroumgebung und der Erwerb zusätzlicher Mutationen zu den heterogenen Krankheiten führen, die alle durch dieselben Treibermutationen verursacht werden. In der vorliegenden Studie konnte ich eine erhöhte Inzidenz von Chromatinsegregationsdefekten in hämatopoetischen Zellen mit stabiler Expression der CALRdel52 bzw. JAK2V617F Treibermutation nachweisen. Darüber hinaus zeigten meine Studien an murinen $32D^{MPL}$- und humanen erythroleukämischen $TF\text{-}1^{MPL}$ -Zellen eine Korrelation zwischen der Expression von CALRdel52 bzw. JAK2V617F und einem defekten Spindelassemblierungs-Checkpoint (SAC). Dies trägt zu einer gestörten Mitose bei, was zur Aneuploide und Tumorbildung führen kann. Weitere Analysen haben gezeigt, dass bei der Expression von CALRdel52 oder JAK2V617F ein Zusammenhang zwischen einem defekten SAC und einem Ungleichgewicht in der Rekrutierung von SAC-Faktoren an mitotische Kinetochore besteht. In $32D^{MPL}$-Zellen, die CALRdel52- oder JAK2V617F exprimieren, konnte ich einen vorzeitigen Abbau von Cyclin B1 während der Mitose beobachten, der mit einer Schwächung des SAC einhergeht. Meine Analyseergebnisse zur Dauer der Mitosen in nicht-hämatopoetischen Zellen untermauern darüber hinaus die Hypothese, dass ein defekter SAC eine nicht fehlerfreie Mitose hervorrufen kann.

Zusammenfassend zeigen meine Forschungsergebnisse, dass CALRdel52 oder JAK2V617F MPN-Treibermutationen die mitotische Regulierung verändern und sich möglicherweise auf die Stabilität des Karyotyps auswirken können, was ein wichtiger Faktor in der Pathogenese der MPN sein könnte.

1. Introduction

1.1 Haematopoiesis

Haematopoiesis is the process of blood formation. In humans and mice, haematopoiesis begins in the embryonic yolk sac, where the blood islands are located, then migrates first to the embryonic liver and finally, after its formation, to the bone marrow and thymus (reviewed in (Cumano and Godin 2007)).

The lifespan of mature blood cells is relatively short, thus haematopoiesis needs to ensure that the body has sufficient blood cells at all times (Bryder et al. 2006). The origin of formation of mature blood cells in adults mostly takes place in the bone marrow, more precisely in the haematopoietic stem cells (HSC). Stem cell factor (SCF) is an important factor for the regulation and localization of HSC in the bone marrow niche. This increases the adhesion of the HSC in the niche and enables the HSC that circulate in the blood to return to the niche through the concentration gradient that arises in collaboration with the chemokine SDF-1 ((Nervi et al. 2006) and reviewed in (Broudy 1997)). Stem cells differ in the presence or absence of certain surface proteins, so-called differentiation clusters, which are specific to the respective stem cell group, e.g. the hematopoietic progenitor cell antigen CD34 is first expressed in the short-term (ST)-HSCs [Figure 1]. Multipotent progenitor cells (MPP) differ from ST-HSC in the expression of CD135, a receptor for growth factors that is important for cell proliferation, differentiation, and survival. The whole further development process is strictly controlled by an interplay of interleukins and cytokines (Bryder et al. 2006) as well as by signalling pathways within the cell (e.g. Wnt signalling pathway) (Staal and Clevers 2005).

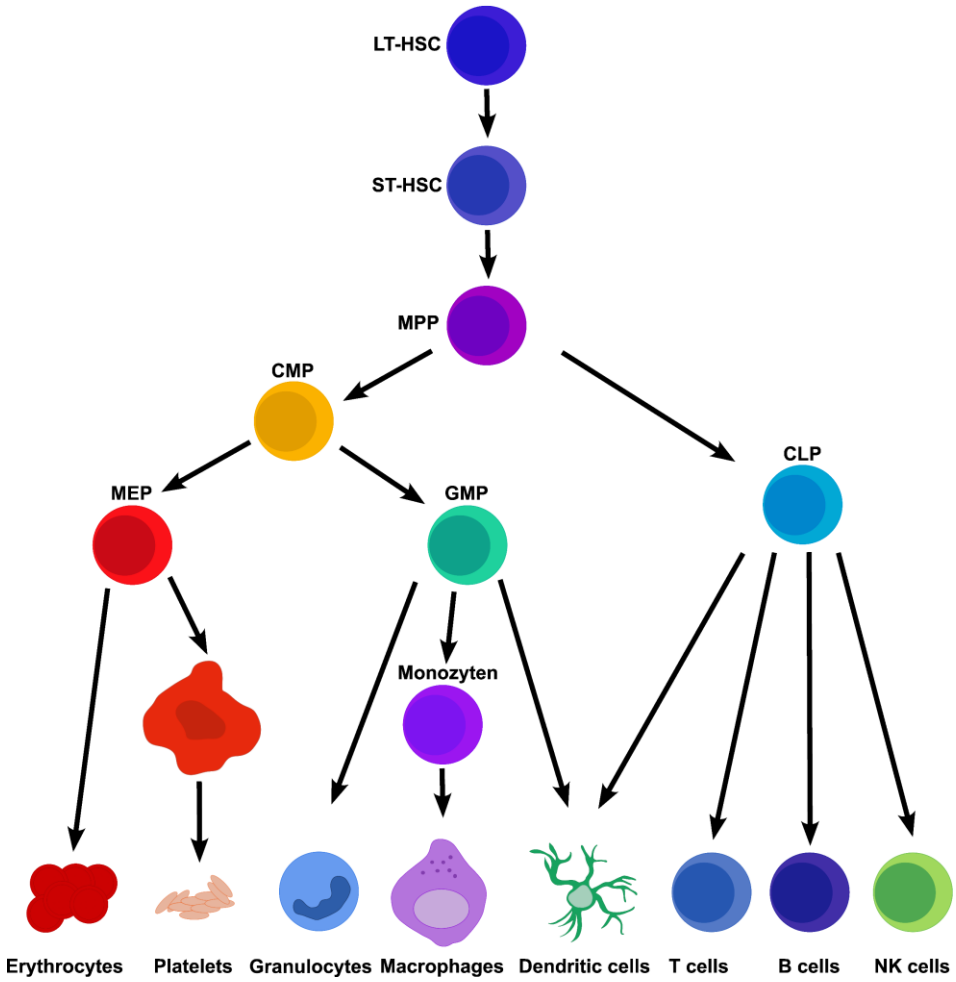

Figure 1: Schematic overview of the haematopoiesis. The origin of haematopoiesis lies in the haematopoietic stem cells with a long cell lifespan (LT-HSCs), from which the haematopoietic stem cells with a short cell lifespan (ST-HSCs) develop. The last ones can differentiate into multipotent progenitor cells (MPPs). In the next steps the general lymphoid progenitor cells (CLP) can further differentiate into lymphocytes (B, T, NK cells), while the myeloid progenitor cells (CMP) can differentiate further into granulocytes/macrophage precursors (GMP) or megakaryocytes/ erythrocyte precursors (MEP). GMP differentiate via different precursor cells into different granulocytes and macrophages. While the macrophages develop from monocytes, the granulocytes can mature into neutrophilic, eosinophilic and basophilic granulocytes. The MEP differentiate into either megakaryocyte, which matures into platelets, or into erythrocytes. An exception that can develop from both branches is dendritic cells, they can develop from monocytes or CLP. Modified from Blank et al. 2008.

Although the paradigmatic model for the haematopoietic lineage tree is the predominant model, recent studies using modern analytical methods show that the haematopoietic lineage tree more closely resembles the dynamic behaviour of a Waddington landscape (Kucinski et al. 2023).

1.2 Myeloproliferative neoplasm (MPN)

Myeloproliferative neoplasms (MPNs) are haematopoietic stem cell disorders caused by somatic mutations and clonal expansions of mutated haematopoietic stem and progenitor cells (HSPCs). MPNs are typically divided into several categories, the most common being are chronic myeloid leukemia (CML), essential thrombocythemia (ET), polycythemia vera, and (PV) primary myelofibrosis (PMF) (reviewed in (Arber et al. 2016)).

CML differs from the other three MPNs. A key feature of this disease is a fusion of the BCR (chromosome 9) and ABL (chromosome 22) genes, the so-called Philadelphia chromosome. CML is characterised by the uncontrolled growth of myeloid precursor cells of the white blood cells, mostly mature granulocytes and their precursors (Score et al. 2010).

The other three (ET, PV and PMF) belong to the Philadelphia-negative (ph. neg.) MPN, other less frequent representatives are chronic neutrophilic leukemia or chronic eosinophilic leukemia ((Kirschner et al. 2019) and reviewed in (Pizzi et al. 2021)). There are various ways of differentiating between these ph. neg. MPNs, one of them being classified according to the most severely affected blood cell type. ET patients usually have a disproportionate number of platelets. In contrast PV patients have an increased proportion of red blood cells in the blood volume. PMF is characterised by the growth of mutated cells in the bone marrow, leading to changes in the bone marrow and thus to the myelofibrosis that gives it its name (Marneth and Mullally 2020, Gotoh 2022).

At the genetic level, the ph. neg. classic MPNs are characterised by various driver mutations. The driver mutations JAK2V617F and CALRdel52 have been known since 2005 (JAK2V617F) (Levine et al. 2005) and 2013 (CALRdel52) (Klampfl et al. 2013), and several new bystander mutations have been discovered in patients in recent years (reviewed in (Baumeister et al. 2021)). The most common driver mutation, JAK2V617F, has a point mutation at the amino acid position 617 in the Janus kinase 2 (JAK2). This point mutation changes valine to phenylalanine and is present in 95 % of all PV patients and over half of all PMF and ET patients (Levine et al. 2005, Kagoya et al. 2014) [Figure 2]. There exist other mutations in JAK2 linked to ph. neg. MPNs, for example, the JAK2exon12, which is characterised by an isolated erythrocytosis

phenotype (Scott et al. 2007). The second most common mutation is in the CALR gene. These are either insertions or deletions of base pairs in exon 9. The two best-known mutations at are the insertion of 5 base pairs (CALRint5 / type 1) and the deletion of 52 base pairs (CALRdel52 / type 2). These mutations result in a one base pair frameshift and lead to an earlier CALR stop codon and the loss of the amino acid sequence KDEL (Lys-Asp-Glu-Leu). In 25 - 35 % of ET and PMF patients a CALR gene mutation is present (Klampfl et al. 2013, Nangalia et al. 2013). Another common driver mutation is in the gene encoding for the thrombopoietin receptor (TPOR), also referred to as myeloproliferative leukemia protein (MPL). This is a point mutation in position 515 resulting in a tryptophan to leucine (W515L) exchange (Beer et al. 2008). In 5 % to 12 % of the ET and PMF patients, none of the above-mentioned mutations are present, in which case we speak of a triple-negative mutation (Milosevic Feenstra et al. 2016).

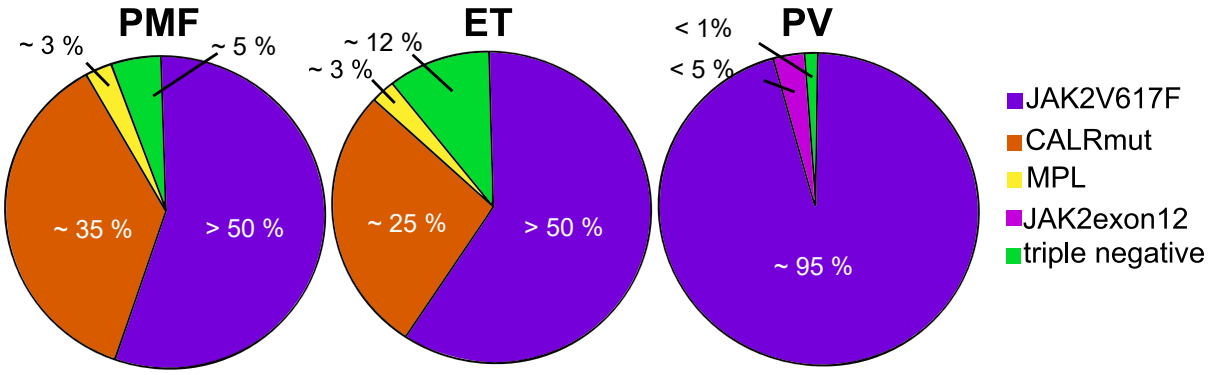

Figure 2: Frequency distribution of the occurrence of disease-causing driver mutations in ph. neg. MPN. (Modified from (Langabeer 2016).

The driver mutations in the JAK2, CALR, and MPL genes all influence the JAK2-related signalling pathways [Figure 3]. In the JAK2-related signalling pathways, the activation is as follows: A ligand binds to the receptor binding site, resulting in dimerization or aggregation of several receptor subunits, which in turn promotes transphosphorylation of JAK2 and its attachment to the cytoplasmic part of the subunits. Activation of JAK2 leads to tyrosine phosphorylation of the receptor, which enables the binding of different signal transducer and activator of transcription (STATs). These are then phosphorylated by JAK and form a dimer after detachment from the receptor. This STAT dimer can bind DNA in the nucleus, serves as a promoter, and regulates the

transcription of various genes that are important for the proliferation and survival of the cell (reviewed in (Guijarro-Hernández and Vizmanos 2021, Pandey et al. 2022)).

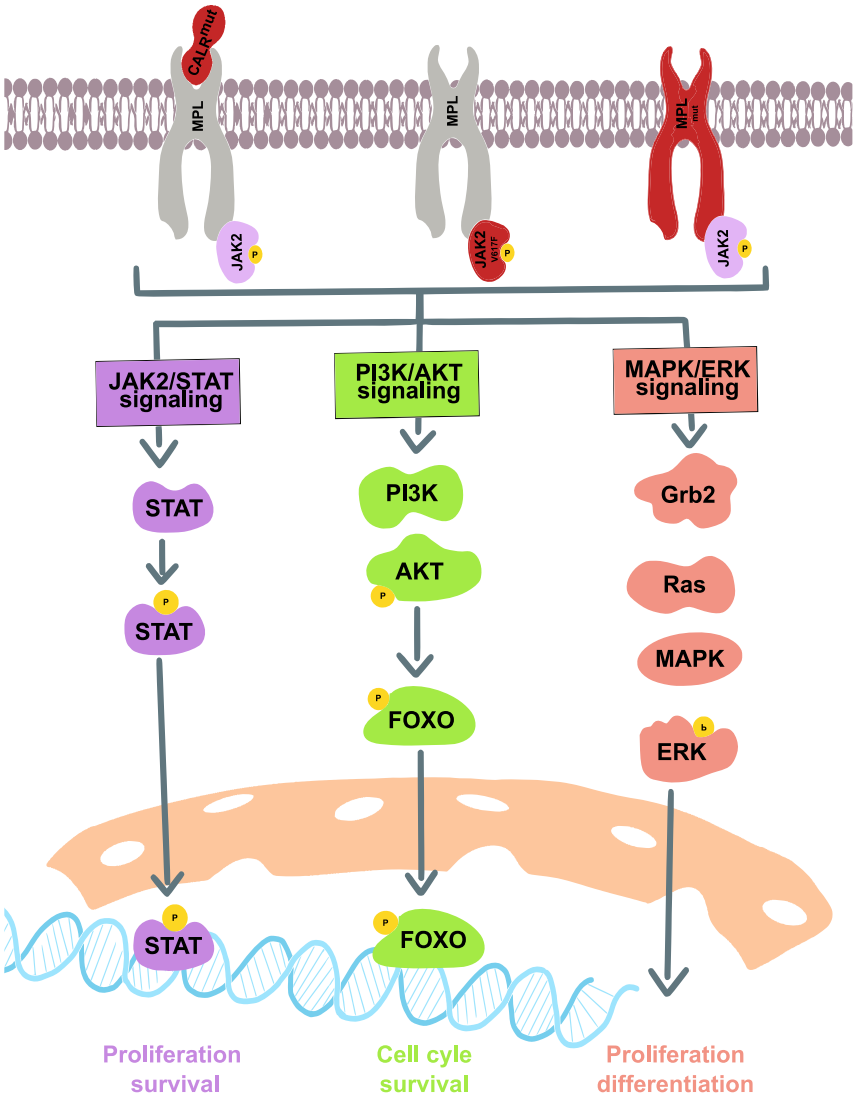

Figure 3: Overview of the driver mutations JAKV617F, CALR^{mut} and MPL^{mut} on active JAK2-related canonical signalling pathways in ph. neg. MPN, which lead to constitutive activation of the JAK2/STAT, PI3K/AKT, and MAPK/ERK signalling pathways. These promote the transport of certain transcription factors into the cell nucleus, where they lead to increased proliferation and cell survival via the upregulation of target genes. Adapted from Guijarro-Hernández and Vizmanos 2021

In the MPL gene, which codes for the TPOR, the W515L mutation, leads to increased activation and dimerization of the receptor (Beer et al. 2008).

The point mutation (V617F) of JAK2 results in a disturbance of the autoinhibition of JAK2, so that the Janus homology domain 2 (JH2) pseudo kinase domain loses its physiological inhibitory function against JH1, whereby JAK2 can also be active without

ligand binding to the receptor. This destabilisation of the folding of the JH2 domain is an direct results of the exchange of valine for phenylalanine at amino acid position 617 (reviewed in (Hu et al. 2021)).

CALR is a Ca^{2+}-binding chaperone that, together with calnexin, regulates protein folding during endoplasmic reticulum stress, particularly Ca^{2+} homeostasis. In addition to these two roles, CALR is also involved in many other cellular functions, such as proliferation, apoptosis or stress response, and is involved in many different signalling pathways (Nangalia et al. 2013). Mutant CALRs have an altered C-terminus, resulting in the loss of the KDEL motif and several Ca^{2+}-binding sites. This allows mutant CALR to be transported to the cell membrane where it can bind to the thrombopoietin receptor (TPOR/MPL) and lead to ligand-independent activation (Nangalia et al. 2013, Han et al. 2016).

1.3 Mitosis

The cell cycle is divided into different phases. These phases can be broadly divided into mitosis (M phase) and interphase. In interphase, the cell body grows, and the genetic material is duplicated. In mitosis, the cell divides, and the genetic material is divided into two identical daughter cells.

The interphase can be divided into G0, G1, S and G2 phase (Voorhees et al. 1976).The G0 phase is also known as the resting phase. Cells can remain in this phase for a relatively long time and return to the G1 phase through stimulation with mitogenic factors (Patt and Quastler 1963). In the G1 phase, there is an increase in cell volume due to increased protein biosynthesis in the cytoplasm and in the cell organelles. Nucleosides triphosphates and mRNA are synthesised in preparation for cell division. The progression of the cell cycle in the G1 phase is controlled by the activity of Cyclin-dependent kinases (CDK) 4 and 6. The binding of Cyclin D leads to the formation of the Cyclin D/CDK4/6 complex and its activation leads to the inactivation of the inhibition of transcription factors that are important for the transition from G1 to S in further steps of the cascade (reviewed in (Bretones et al. 2015)). Whether a cell can transition from the G1 to the S phase is checked at the G1/S checkpoint. This involves checking the

DNA for possible damage and checking whether cell growth has been completed. If the checkpoint conditions are fulfilled, the cell can enter the S phase and DNA replication begins (reviewed in (Ligasova et al. 2023)).

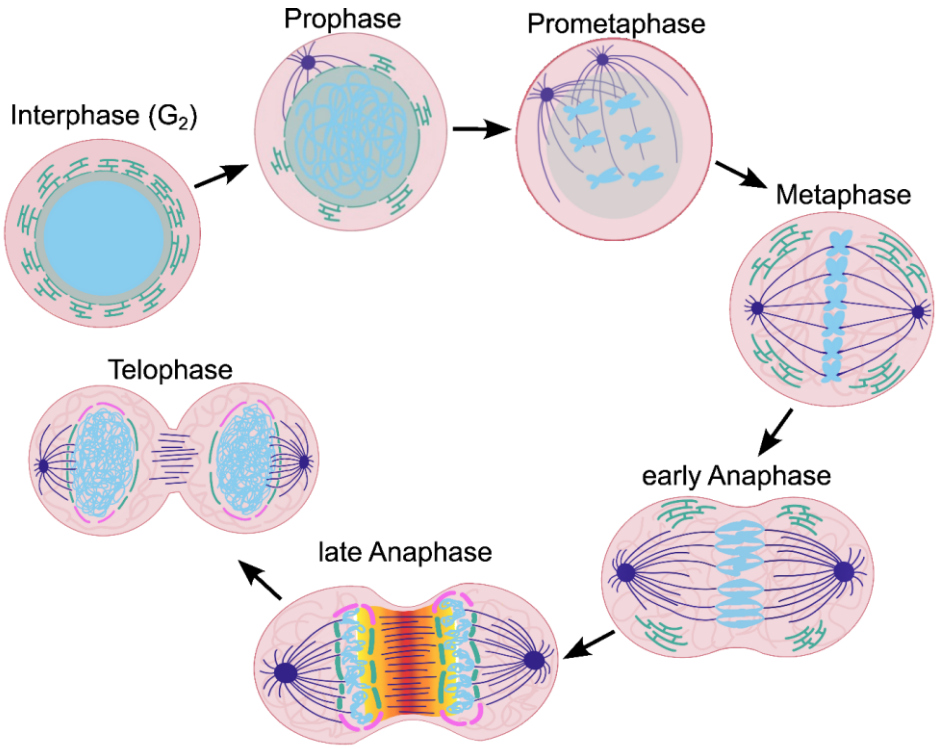

Figure 4. Overview of the different phases of mitosis starting from the interphase (G_2): The colour changes from red to yellow in late anaphase represent the phosphorylation gradient caused by the localisation of Aurora B at the central spindle. Adapted from Moreno et al. 2023.

In the subsequent G2 phase, preparation for cell division (mitotic phase) takes place, in which the proteins important for mitosis are synthesised. In addition, at the end of the G2 phase and before mitosis begins, the DNA synthesised in the S phase is checked for defects (G2/M checkpoint). Faulty DNA leads to the termination of the cell cycle and the activation of DNA repair enzymes. In the case of significant defects, the cell is driven into apoptosis to prevent genetic instability and thus the development of cancer. If the control mechanism is defective, cells with DNA damage can still enter into mitosis (reviewed in (Ligasova et al. 2023)).

During mitosis, the cell undergoes cytological and morphological changes. Mitosis is divided into different subphases: pro-, prometa-, meta-, ana-, and telophase [Figure 4].

In prophase, chromosome condensation begins, which largely interrupts transcription (Martinez-Balbás et al. 1995). Throughout the condensation of the chromatids, further preparatory processes take place in the cell, including the gradual disintegration of the nuclear envelope into individual components. In addition, the spindle apparatus begins to form whereby the activity and enlargement of the centrosomes is controlled by polo kinases (Nunes and Ferreira 2021). These steps continue in prometaphase, when the microtubule spindle begins to form and can already penetrate through the emerging gaps in the nuclear envelope into the nucleoplasm and interact with the chromosomes, mainly the kinetochores (O'Toole et al. 2003). As a result, the chromosomes begin to migrate towards the metaphase plates. In metaphase, the chromosomes get aligned in the metaphase plate and the correct links between centrosomes and kinetochores via microtubules are consolidated. This process is controlled by the spindle assembly checkpoint (SAC), which interrupts cell division until the chromosomes are properly connected to the spindle. This ensures that no errors occur later during chromatin segregation (reviewed in (Hayward et al. 2019)). When all chromatids are correctly bound to the centrosomes via kinetochores, the division of the sibling chromatids occurs in early anaphase by spindle traction forces that counteract the action of the cohesin complex (de Regt et al. 2022). In addition, the chromosomes reach their maximum compaction in this phase, dependent on Aurora B (Mora-Bermudez et al. 2007). In late anaphase, decondensation of the chromosomes begins by the action of phosphatases (reviewed in (Vagnarelli 2021)) and manifold other factors (Magalska et al. 2014, Schooley et al. 2015). They reverse the mitotic phosphorylation of kinases and counteract chromatin compaction, allowing the formation of the new nuclear envelope around the decondensed chromatin mass to form a diffusion barrier between cytoplasm and nucleoplasm. During telophase, the remaining spindle microtubules in the nucleus are disassembled, the nucleolus is restored, and the nuclear envelope is reformed. As this process goes on, nuclear pore complexes (NPCs), which are responsible for transport between the cytoplasm and nucleus, are timely reassembled in the nuclear envelope. In addition, the chromosomes are further decondensed and the constriction of the furrow to separate the two daughter cells is further focussed. The complete separation of the two daughter cells takes place during cytokinesis. Then, an actin-myosin ring forms below the plasma membrane (reviewed in (Mierzwa and Gerlich 2014)), which is in conjunction with a complicated network of protein interactions responsible for this cell separation (reviewed in (Moreno-Andres et al.

2023)). Finally, the two resulting daughter cells have a fully functional nucleus and can re-enter the interphase.

1.3.1 Spindle assembly checkpoint

The spindle assembly checkpoint (SAC) is one of several important checkpoints in the cell division that prevent genomic instability, aneuploidy (reviewed in (Hayward et al. 2019)), and chromothripsis (Zhang et al. 2015). The main task of the SAC is to monitor the correct linking of all chromatids via kinetochores with the microtubules of the spindle apparatus and to interrupt mitosis in the event of errors. After the correction of these errors the chromatin segregation can be continued.

When unbound kinetochores are recognised by monopolar spindle 1 (MPS1), the cell cycle inhibitor mitotic checkpoint complex (MCC) is formed in several steps (Abrieu et al. 2001) [Figure 5]. MPS1 is the main organiser of the signalling cascade, and its recruitment is promoted by two factors: indirectly by the Aurora B kinase, a catalytic subunit of the chromosomal passenger complex (CPC), and by direct phosphorylation by the CDK1-cyclin B1 complex, which is involved in many reactions within the checkpoint. Indirect recruitment by Aurora B is based on the fact that Aurora B can loosen incorrectly attached kinetochore-microtubule bonds and phosphorylate the KNL1-MIS12-NDC80 complex (KMN) as long as there is no tension on the microtubule attachment (Saurin et al. 2011, Hayward et al. 2019).

Subsequently, the MPS1 phosphorylates the Met-Glu-Leu-Thr (MELT) motif of the outer kinetochore protein KNL1 of the nuclear division cycle (NDC80) complex (Ji et al. 2015). This creates binding sites on KNL1 for BUB1-BUB3 complexes (Primorac et al. 2013) and additionally the mitotic arrest deficient 1 (MAD1)-MAD2 complex is recruited by MPS1-phosphorylations of BUB1 and MAD1 (Hayward et al. 2019).

The BUB1-BUB3 complex can recruit BUBR1 and BUB3, two members of the inhibitory MCC complex. In addition to these two, MAD2 and cell division cycle 20 (CDC20) also belong to the MCC (Visintin et al. 1997). In addition to the spatial proximity of the components, an important prerequisite for the formation of MCC is that MAD2 is in the closed state (C-MAD2) and not in the open state (O-MAD2). For this purpose, O-MAD2 must be converted at the MAD1-MAD2 complex (De Antoni et al. 2005).

After the MCC is formed, it binds to the anaphase-promoting complex/cyclosome (APC/C) and inhibits its activation through two functions: by blocking the ubiquitin ligase binding site and influencing the conformation of APC/C.

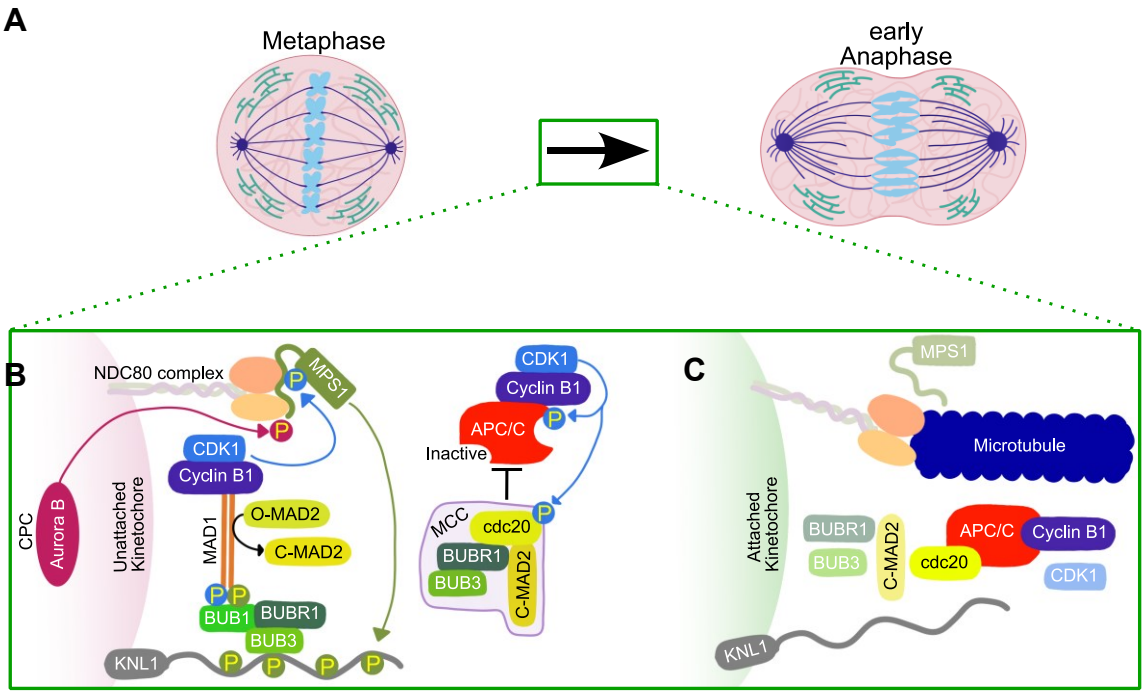

Figure 5. Overview of SAC action in mitosis : A) SAC is the checkpoint between metaphase and early anaphase B) Schematic representation of the SAC process at unbound kinetochores with the most important factors involved and their phosphorylation. First, Aurora B and Cyclin B1-CDK1 phosphorylate MPS1, which then phosphorylates several MELT motifs on KNL1; in addition, the phosphorylation of BUB1 by Cyclin B1-CDK1 ensures that MSP1 can also phosphorylate BUB1, resulting in the recruitment of MAD1, which ensures the conversion of MAD2 from an open (O) to a closed (C) state. C) After binding of all kinetochores to microtubules, the synthesis of MCC is inhibited, resulting in the activation of APC/C and the loss of the SAC factors at the kinetochore, which leads to chromosome segregation. Partly adapt from Moreno et al. 2023 (A) and Hayward et al. 2019 (B-C).

When all kinetochores are bound, MCC is no longer formed and the inhibitory effect of MCC on APC/C is stopped (reviewed in (Hayward et al. 2019)). The APC/C-MCC complex can be degraded by the following mechanisms: through the ubiquitination of CDC20 (Reddy et al. 2007) and through the conversion of C-MAD2 into O-MAD2 by the SAC antagonist MAD2L1BP and the thyroid receptor-interacting protein 13 (TRIP13). Both mechanisms lead to a disassembly of the MCC (Alfieri et al. 2018). As

a result, APC/C is activated and can ubiquitinate securin, an inhibitor of the protease separase, and Cyclin B1, a part of the Cyclin B1 kinase CDK1 complex (Alfieri et al. 2016). The ubiquitination of these two is essential for the progression of the cell cycle, as the presence of Cyclin B1 ensures that the mitotic state is maintained and separase action allows sister chromatin segregation.

1.3.2 Consequences of chromosome segregation errors

Error-free chromosome segregation during cell division is important to prevent genomic instability, genetic disorders and cancer (Pampalona et al. 2016). As shown in Figure 6, chromatin segregation defects such as chromosome bridges or lagging chromosomes can occur during cell division [Figure 6].

There are different types of chromosome bridges, including anaphase bridges and interphase bridges. Anaphase bridges consist of thin strands of chromatin that remain connected between sister chromatins, preventing the sister chromatids from being completely separated. Interphase bridges occur when anaphase bridges are not resolved during mitosis (reviewed in (Hawdon et al. 2021)). Chromosomal bridges can also originate in G2 phase, for example, when double-stranded bridges are repaired by fusion between two sister chromosomes. As a result, these cannot separate during chromosome division and the resulting tension during chromosome division can lead to chromosome breakage (Lo et al. 2002). This can lead to the so-called break/fusion/bridge cycle (B/F/B), which was already described by Barbara McClintock in 1941 (reviewed in (Simovic and Ernst 2022), original from (McCLINTOCK 1941)) and is associated with chromosomal instability (CIN) and tumour formation (reviewed in (Jiang and Chan 2024)). Chromosome breaks in the B/F/B cycle can lead to free chromosome fragments and thus to structural CIN. Structural CIN are structural changes in the genome that are associated with replication stress and the lack of a functional repair system for double-strand breaks (Burrell et al. 2013). The chromosomal fragments resulting from the breaking of chromosomal bridges can also lead to activation of the cyclic GMP-AMP synthase (cGAS)-interferon gene stimulator (STING) signalling pathway. Under normal conditions, the cGAS-STING signalling

pathway is activated by unprotected cytoplasmic DNA and inhibited during mitosis by Aurora B-dependent safety mechanisms (reviewed in (Moreno-Andres et al. 2023)). However, disruption of these safety mechanisms can lead to activation of the cGAS-STING signalling pathway and thus to the development of inflammation.

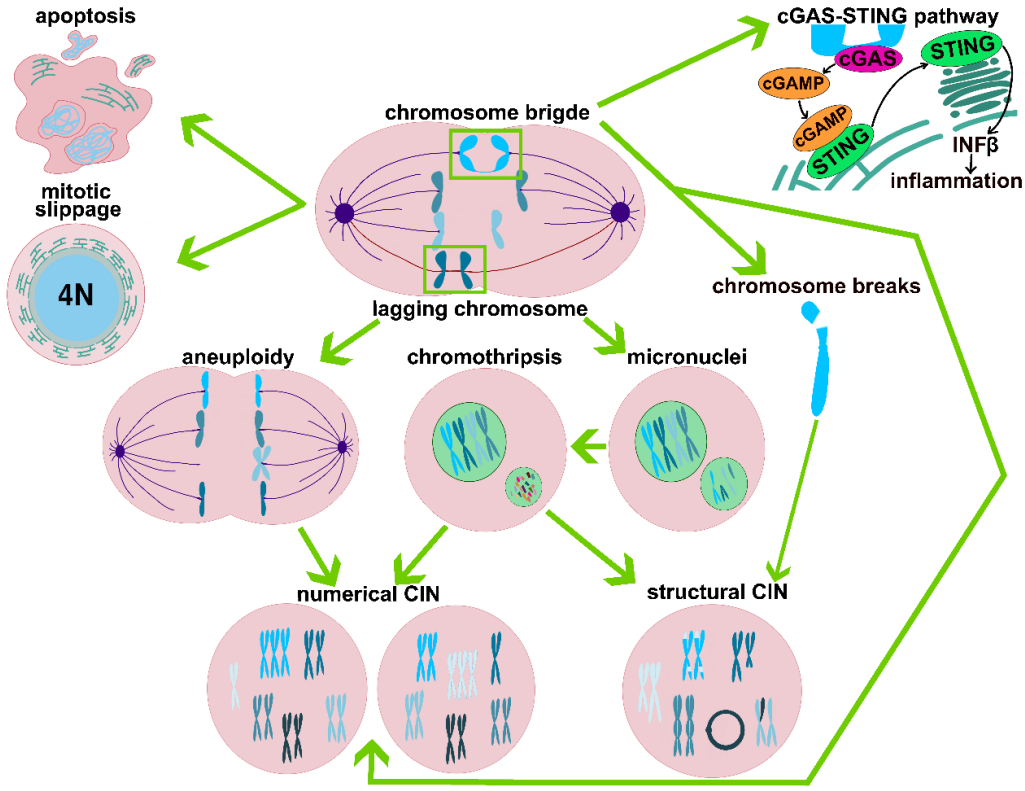

Figure 6: Chromosome segregation errors and their follow-up problems Chromosomal bridges and lagging chromosomes normally block the progression of mitosis and drive the cell into apoptosis; if the blocked cells escape the blockade, a so-called mitotic slippage occurs. Faulty mitotic chromosome segregation can lead to numerical CIN and aneuploidy. Micronuclei can be caused by lagging chromosomes and lead to chromothripsis. Numerical CIN can result from both aneuploidy and chromothripsis. Structural CIN can result from both chromothripsis and chromosome breaks. In addition, the proinflammatory cGAS-STING signalling pathway can be triggered by host DNA outside the nuclear region. Modified from Moreno et al. 2023

In addition to the chromosome bridges already discussed, the lagging chromosome is also a trigger for the development of CIN. Lagging chromosomes are caused by various connection defects between microtubules and kinetochores, the best known of which is an adhesion defect of a kinetochore between the two poles (merotelic microtubule-kinetochore adhesion) (Thompson and Compton 2011). The remaining chromosomes can lead to aneuploidy, for example, if two sister chromatids do not

separate. In aneuploidy, the chromosomes are unevenly distributed among the daughter cells or there is a loss or accumulation of chromosome arms (reviewed in (Ben-David and Amon 2020)). Although aneuploidy can occur naturally in certain tissues in rare cases, it is usually a product of CIN and can therefore be considered a sign of defective chromosome segregation (Potapova and Gorbsky 2017, Ben-David and Amon 2020). Normally, the SAC serves as a protective mechanism to prevent the progression of chromosomal errors by, among other things, repairing DNA damage. However, if there are disruptions in their interaction, cancer-causing factors such as aneuploidy can arise (reviewed in (Moreno-Andres et al. 2023)). In addition to the development of aneuploidy, the lack of integration of lagging chromosomes can also lead to the formation of micronuclei. These consist of chromosome fragments or even whole chromosomes surrounded by a nucleus-like membrane (reviewed in (Fenech et al. 2011)) and can lead to chromothripsis. This type of chromoanagenesis is the result of a single catastrophic event that leads to massive genomic rearrangements. In addition, carcinogenesis is favoured by subsequent structural CIN (Zhang et al. 2015)

Under normal circumstances, the occurrence of chromosome segregation errors leads to apoptosis of the affected cell. Under pathogenic conditions, however, mitosis can be terminated without cell division, a process known as mitotic slippage. Cells that return to interphase in this way can, for example, be polyploid, which can lead to genomic instability. Which of the two events occurs depends, among other things, on the relationship between Cyclin B1 activity and pro-apoptotic signalling. This model of "competing networks and thresholds" suggests that mitotic slippage occurs when Cyclin B1 concentration decreases faster than pro-apoptotic signalling increases and thus falls below the mitotic exit threshold (Ghelli Luserna di Rora et al. 2019). An increase in pro-apoptotic signalling and thus a shift in the balance in this direction would be a possible therapeutic approach for the treatment of cancer (reviewed in (Moreno-Andres et al. 2023)).

In summary, long-term increased DNA damage or errors in DNA repair can lead to aneuploidy, CIN, and cGAS-STING-associated inflammatory processes, which are associated with the development and growth of tumours (reviewed in (Hanahan and Weinberg 2011)).

1.4 Aim of the thesis

The stability of the karyotype, the maintenance of chromosomal integrity and the molecular balance of gene expression as well as the precise subcellular positioning of mitotic regulators play an important role in error-free mitosis. Mitotic defects can contribute to the progression and poor prognosis of various haematological cancers. CIN and karyotype aberrations lead to karyotype evolution, increase tumour aggressiveness and promote tumour adaptation in solid tumours and other haematopoietic neoplasms (Wilhelm et al. 2020). In solid tumours, a connection between defects in mitotic regulators and the malignant transformation of cells has been demonstrated (reviewed in (Moreno-Andres et al. 2023)). For example, overexpression of Cyclin B1 was observed in lung and breast cancer and overexpression of CDC20 in other types of cancer (Aaltonen et al. 2009, Huang et al. 2009). A more detailed investigation of mitotic regulators in MPNs could therefore also lead to new therapeutic approaches. In addition, the cytology and molecular status of mitosis in ph. neg. MPN has not yet been studied in detail, although a karyotype abnormality is found at diagnosis in up to 33% of cases (in PMF) (Tefferi et al. 2014).

In addition, little is known about how and by what means the phase transition from chronic to acute disease state occurs in ph. neg. MPN. It is also unclear whether the driver mutations CALRdel52 and JAK2V617F contribute to this progression by enhancing the disruption of mitotic homeostasis.

My hypothesis is therefore that at least some of the driver mutations in ph. neg. MPN disrupt mitotic progression and regulation and cause chromatin segregation defects. This can lead to instability of the karyotype, which favours this progression and leukemic transformation.

2. Material and Methods

2.1 Material

2.1.1 Cell lines

Table 1: Cell lines that were used in this thesis

Cell line	**Provider**
32D H2B-mCherry empty vector-EGFP	From Haematology Uniklink Aachen
32D H2B-mCherry CALRDdel52-EGFP	From Haematology Uniklink Aachen
32D H2B-mCherry JAK2V617F-EGFP	From Haematology Uniklink Aachen
TF-1 H2B-mCherry empty vector-EGFP	From Haematology Uniklink Aachen
TF-1 H2B-mCherry CALRDdel52-EGFP	From Haematology Uniklink Aachen
TF-1 H2B-mCherry JAK2V617F-EGFP	From Haematology Uniklink Aachen
HeLa Clon-1 EGFP	Anja Scheufen (Biochemistry and Molecular Cell Biology, Uniklink Aachen)

2.1.2 Vectors

Table 2: Construct names of used vectors

Construct name	**Cloning provider**
PMSCV Empty vector IG EGFP	From Haematology Uniklink Aachen
PMSCV CALRdel52 IG EGFP	From Haematology Uniklink Aachen
PMSCV JAK2V617F IG EGFP	From Haematology Uniklink Aachen
PMSCV MPC HA IHRES Puro	From Haematology Uniklink Aachen

2.1.3 Antibodies

Table 3: Antibodies used for Western Blot [WB], Immunofluorescence staining [IF], and cytometry [C]

Antibody	**Catalogue No.**	**Concentration**	**Company**
Actin	691001	1:10000 [WB]	MP Biomedicals
APC-Cy7	405716	1:200 [C]	Abcam plc
Aurora B	ab 45145	1:2000 [WB]	Abcam plc.
Aurora B	BD611083	1:100 [IF]	BD Biosciences
BUBR1	ab172581	1:1000 [WB] 1:100 [IF]	Abcam plc.
CDC20	ab183479	1:2000 [WB] 1:500 [IF]	Abcam plc.
CENP-E	SAB3701429	1:100 [IF]	Sigma-Aldrich Chemie GmbH
CREST	AI 15-234	1:500 [IF]	Antibodies incorporated
Cyclin B1	ab181593	1:1000 [WB]	Abcam plc.
Cyclin B1	MA5-14319	1:1000 [IF]	Invitrogen
GAPDH	sc-32233	1:500 [WB]	Santa Cruz Bio-technology, Inc.
Goat anti-Human IgG Alexa®Fluor 647	#A-21244	1:1000 [IF]	Invitrogen
Goat anti-Mouse IgG Alexa®Fluor 488	#A-11001	1:1000 [IF]	Invitrogen
Goat Anti-Mouse IgG Peroxidase Conjugate	401215	1:5000 [WB]	Sigma-Aldrich
Goat anti-Rabbit IgG Alexa®Fluor 488	#A-11008	1:1000 [IF]	Invitrogen
Goat Anti-Rabbit IgG Peroxidase Conjugate	401353	1:5000 [WB]	Sigma-Aldrich

Hoechst 33342	130-111-569	1.5 µl / 1 mio cells [C]	Miltenyi Biotec B.V. & Co. KG
MAD1	ab175245	1:500 [WB] 1:100 [IF]	Abcam plc.
MAD2xl	SA0503	1:1000 [WB] 1:50 [IF]	Ag Antonin (Uniklink Aachen)
MPS1	A01132-1	1:1000 [WB] 1:500 [IF]	bosterbio
PLK1	05-844	1:500 [WB]	Millipore
PP2A-Ca/b	sc-56950	1:500 [WB]	Santa Cruz Bio-technology

2.1.4 Chemicals

Table 4: Chemicals used for all experiments

Chemical	**Company**
10 % Bromphenol	Merck KGaA
30 % Acrylamide	Carl Roth GmbH + Co. KG
Acetic acid	VWR International GmbH
Albumin Fraction V (BSA)	Carl Roth GmbH + Co. KG
Alpha MEM	Gibco | Thermo Fisher Scientific
Ammonium chloride [NH_4Cl]	Carl Roth GmbH + Co. KG
Ammonium persulfate (APS)	Sigma-Aldrich Chemie GmbH
Calcium chloride dihydrate [$CaCl_2 . 2H_20$]	AppliChem GmbH
Di-Sodium hydrogen phosphate dihydrate [$Na_2HPO_4 \cdot 2H_2O$]	Merck KGaA
CyroSure Dimethylsulfoxid (DMSO)	WAK-Chemie Medical GmbH
Dithiothreitol (DTT)	Thermo Fisher Scientific

Dulbecco's modified Eagle's medium (DMEM)	Gibco | Thermo Fisher Scientific
Doxorubicin	Calbiochem-Novabiochem GmbH
Ethanol absolute	Otto Fischer GmbH & Co KG
Fetal calf serum (FCS)	Gibco | Thermo Fisher Scientific
Glycine	MP Biomedicals Germany GmbH
Magnesium chloride hexahydrate [$MgCl_2$. $6H_2O$]	VWR International GmbH
Methanol	VWR International GmbH
Mowiol 40 88	Carl Roth GmbH + Co. KG
MPS1like inhibitor NMS-P715	Merck KGaA
Nocodazole	EMD Chemicals, Inc.
Non-fat dried milk powder	AppliChem GmbH
Paraformaldehyde	Sigma-Aldrich Chemie GmbH
PBS	Gibco | Thermo Fisher Scientific
PenStrep	Gibco | Thermo Fisher Scientific
Ponceau S (C.I.27195)	Carl Roth GmbH + Co. KG
Potassium chloride [KCl]	AppliChem GmbH
Potassium dihydrogen phosphate [KH_2PO_4]	Merck KGaA
Recombinant Human Granulocyte Macrophage Colony Stimulating Factor (rh GM-CSF)	ImmunoTools GmbH
RPMI1640	PAN-Biotech GmbH
SDS pellets	Carl Roth GmbH + Co. KG
Sucrose	AppliChem GmbH
Sodium chloride [NaCl]	VWR International GmbH
TEMED	Bio-Rad Laboratories GmbH
Tris buffer	Carl Roth GmbH + Co. KG
Triton® X-100	AppliChem GmbH
Trypan blue	Gibco | Thermo Fisher Scientific
Trypsin	Gibco | Thermo Fisher Scientific

Tween-20	Carl Roth GmbH + Co. KG
Unstained Protein Standard, Broad Range (10-200 kDa)	New England Biolabs GmbH
WEHI 3B culture supernatant	From Haematology Uniklink Aachen

2.1.5 Software

Table 5: Software used for analysing the data

Software	**Company/ developer**
ImageJ (Fiji)	Schindelin et al. (2012)
Cell cognition	Michael Held et al. (2010)
NIS-Element	Nikon
FlowJo™	Becton Dickinson
Graphpad Prism	Domatics
Excel	Microsoft Corporation

2.1.6 Devices

Table 6: Used devices for cell culturing and data generation

device	**company**
Eclipse Ti2-E (Inversmicroscope)	Nikon
MCO-19AIC (Incubator)	Sanyo
Gallios (flow cytometer)	Beckman Coulter
HERAsafe KS 18 (Workbench)	Thermo Scientific
Vortex-Genie 2 (Vortex)	Scientific Industries Inc.
Hydroserie S (water bath)	LAUDA
Z 400 K (Centrifuge)	HERMLE LaborTechnik GmbH

2.2 Methods

2.2.1 Cells and their culture treatments

The original murine bone marrow 32D cells (DSMZ, Braunschweig, Germany) have been modified in several steps to adapt them to ph. neg. MPN disease patient cells, as described before (Czech et al. 2019). First, the cells were transduced with the pMSCV-MPL-HA vector [Supplemental Figure 18 B]. The 32D^{MPL} cells were then transduced with retroviruses containing the fluorophore EGPF and either the cDNA of JAK2V617F or CALRdel52 [Supplemental Figure 18 C-D]. In addition, a control cell line was established that contained only an empty vector (EV) with the enhanced green fluorescent protein (EGFP) fluorophore instead of the complementary DNA (cDNA) [Supplemental Figure 18 A]. To visualise the chromatin, H2B-mCherry was also transduced into all three cell lines. These modifications of the cells were carried out and provided by the Department of Haematology at Aachen University Hospital. The culture medium for the 32D^{MPL} cells was either RPMI1640 with 10 % fetal calf serum (FCS), 1 % penicillin and streptavidin (PenStrep) and 10 % WEHI culture supernatant (WEHI) for the experiments and for culturing the 32D^{MPL} EV cells or RPMI1640 with only 10 % FCS and 1 % PenStrep for culturing of the 32D^{MPL} CALRdel52 and 32D^{MPL} JAK2V617F cells. Once a week, the cells were centrifuged for 5 min at 1000 rpm to remove cell fragments and the pellet was resuspended in 10 ml of medium before passaging. The passaging of these cell lines was done every 2 to 3 days.

The TF-1^{MPL} H2B-mCherry cell lines [EV, CALRdel52, JAK2V617F] are originally human erythroleukemia cells (Olschok et al. 2023). Compared to the production of the 32D^{MPL} cell lines, an additional step was required for the transduction of the TF-1 cells: The original human TF-1 cells (DSMZ, Braunschweig, Germany) were transduced with the ecotropic receptor Scl7a1 (Eco). This receptor is necessary for the cells to accept murine vectors. The further transduction steps of the TF-1 eco cells correspond to those of the 32D^{MPL} cells [Supplemental Figure 18 A, C-D] and were also carried out in the Department of Haematology at Aachen University Hospital. The culture medium for TF-1^{MPL} cells was RPMI1640 with 10 % FCS, 1 % PenStrep and 5 ng/ml recombinant human granulocyte-macrophage colony-stimulating factor (rh GM-CSF). Once a week, the cells were centrifuged for 5 min at 1000 rpm and the pellet was

resuspended in 10 ml of medium before passaging. Passaging of these cell lines was performed every 2 to 3 days.

The HeLa cell line is one of the most prominent human immortalized cancer cell lines, which is named after Henrietta Lachs (Beskow 2016). The used HeLa cell line also stable expressed H2B-mCherry, which was produced by Anja Scheufen (Biochemistry and Molecular Cell Biology, Uniklink Aachen). The culture medium for these cells was Dulbecco's modified Eagle's medium (DMEM) with 10 % FCS and 1 % PenStrep. Passaging of these suspension cells was performed every 2 - 3 days by removing the culture medium, washing the cells with 8 mL PBS and adding 2 mL trypsin/ ethylenediaminetetraacetic acid (EDTA) for approximately 3 min to disrupt cell-matrix and cell-cell contacts. The detachment was stopped by adding 8 mL of culture medium. The number of cells was counted using a Neubauer counting chamber. During counting, the remaining cells were centrifuged at 1000 rpm for 5 minutes. The pellet was resuspended in an appropriate volume with a concentration of $1*10^6$ cells per mL.

No distinction was made between cell lines in the procedure for freezing and thawing the different cell lines. The description of the method therefore applies to all cell lines used in this study. For freezing, the cells were first centrifuged at 1000 rpm for 5 min. The pellet was then suspended in the appropriate culture medium containing 10 % DMSO. Subsequently, 1 x 10^6 cells were added to each cryo-tube. These cryo-tubes were then placed in a box and frozen slowly (1 °C per minute) in the - 80 °C freezer and finally transferred to the - 150 °C freezer for long-term storage. The thawing process of the cells was initiated one week before the first experiment. The cells stored at - 150 °C were thawed under room temperature conditions (approx. 20 °C). Approximately 1 ml of the thawed cell suspension was mixed with 10 ml of preheated culture medium (approx. 37 °C). The cells were then washed for 5 min at 1000 rpm and the supernatant was discarded. The pellet was dissolved in 10 ml of fresh culture medium and placed in a Petri dish. All cell lines were cultured on 10 cm Petri plates and maintained in an incubator at 37 °C and 5 % CO_2.

2.2.2 Drug treatments

In the experiments with 32D^{MPL} and TF-1^{MPL} cells, different drugs were used to investigate the functionality of certain mitotic mechanisms and factors.

To test the functionality of the SAC, a concentration of 100 ng/ml nocodazole (dissolved in DMSO) was used (Burrell et al. 2013), and the same concentration was used in the cytometer experiments to observe the accumulation and degradation of Cyclin B1. In the immunofluorescence fixation experiments, the concentration was increased to 200 ng/ml (dissolved in DMSO) according to Brito and Rieder (Brito and Rieder 2006) to arrest the maximum amount of cells in the prometaphase. This allowed the recruitment of important SAC factors to be observed. The same concentration was used in the Western blot experiments to induce spindle-less mitosis and to observe the changes in the expression of important mitotic factors.

Doxorubicin is a chemotherapeutic agent used to treat various types of cancer (e.g., breast cancer (reviewed in (Sun et al. 2022)), acute lymphoblastic leukaemia (Kantarjian et al. 2004) or non-Hodgkin's lymphoma (Herting et al. 2014) and has three main mechanisms: incorporation into the DNA, which inhibits nucleic acid synthesis; inhibition of topoisomerase II, which causes strand breaks in the DNA helix, and formation of reactive oxygen species that damage the DNA. In all experiments, doxorubicin was used at a final concentration of 200 ng/ml to observe the mitotic effects of DNA damage (Hintzsche et al. 2018).

NMS-P715 is an anti-mitotic drug that inhibits the checkpoint kinase MPS1, which leads to an interruption of mitotic progression. A final concentration of 3 µM (dissolved in DMSO) was used in all experiments to observe the mitotic effects on SAC dysfunction (Waenphimai et al. 2022).

2.2.3 Live cell microscopy experiments

For all live cell experiments, the cells were seeded in glass-bottom 18-well or ibiTreat polymer 8-well chambers (Ibidi, Gräfeling, Germany) and kept under incubator conditions throughout the experiment to provide a constant environment for the cells.

The Nikon Ti2 Eclipse microscope with the LED light engine SpectraX (Lumecor, Beaverton, USA) in fluorescence-widefield mode of an X-light spinning disk (CrestOptics, Roma, Italy) was used for all live cell microscopy experiments. To have the same conditions throughout the measurement the incubation chamber of the microscope was set at 37°C and with the help of an environmental control system UNO-T-H-CO2 (Okölab, Ottaviano, Italy) the air pressure was set at 0.63 bar and 0.3 for CO_2. The time between measure points was 1.5 min for 32D^{MPL} and TF-1^{MPL} and 3 min for HeLa.

2.2.3.1 Analysis of mitotic timing and chromatin segregation defects in 32D^{MPL} and TF-1^{MPL} cells

The two cell types (32D^{MPL} and TF-1^{MPL}) were prepared as indicated above. Cells were first seeded into the wells of an 18-well chamber. The whole chamber was then incubated for 1 h at 37 °C and 5 % CO_2 in the incubator of the Nikon Ti2 Eclipse microscope. The recording settings were as follows:

For the mitotic timing and chromatin segregation defects investigations the 20x 0.75NA objective of the Nikon Ti2 Eclipse microscope was used with the filter sets of mCherry (5 % laser intensity and 500 ms exposition) and GPF (5 % laser intensity and 100 ms exposition) for a total time of 20 h per experiment.

During the recording time of 20 h, at different positions images were taken every 1.5 min. These were then saved position by position in one file and had to be broken down again into the individual positions and images for analysis using the Nikon NIS elements programme (https://www.microscope.healthcare.nikon.com/products/software/nis-elements; 23.02.2024; 22:26). These images were then further analysed

using CellCognition (http://www. cellcognition.org/software/cecoganalyzer; 23.02.2024; 22:27). CellCognition is an automated, computer-assisted analysis programme that uses machine learning to evaluate data from living cells and is ,therefore, a high-content screening programme (Held et al. 2010). As described by Held et al., the programme must first be trained on the chromatin morphologies of the cells used. For this purpose, I determined the phenotype of the chromatin of cells in all phases of the cell cycle as well as the signal of dead cells and artifacts from several hundred trajectories. This scheme was then used to analyse all images of the respective experiment with CellCognition. It became clear that the automatic tracking algorithm would recognise many faulty trajectories due to the high mobility of the cells and it was decided to carry out the analysis semi-automatically. Therefore, the mitotic trajectories determined by CellCognition were sorted out using a further method, whereby erroneous trajectories were discarded without bias. For this purpose, an R-Studio code was used, which was provided by Dr Ramona Jühlen (Institute of Biochemistry and Molecular Cell Biology, Faculty of Medicine, RWTH Aachen University, Aachen, Germany). The frequency and type of chromatin segregation errors were determined by visual evaluation and classification of image galleries of valid mitotic trajectories.

2.2.3.2 Quantification of mitotic timing and chromatin segregation defects in transfected HeLa cells

One day before transfection, the HeLa cells were counted in a Neubauer chamber and seeded in an 8-well chamber. The transfection of the cells was performed with the same vectors (pMSCV Empty vector IG EGFP, pMSCV CALRdel52 IG EGFP, pMSCV JAK2V617F IG EGFP and pMSCV MPC HA IHRES Puro) [Supplemental Figure 18], that were used for the production of stably transduced $32D^{MPL}$ cells.

The preparation of the transfection solution was performed according to the protocol described by the manufacturer jetPRIME. The amount of construct DNA was mixed with jetPRIME buffer depending on the DNA concentration using the vortexer. Then jetPRIME reagent was added and vortexed again. The mix was then incubated for

10 min at RT. Finally, the mix was added to the cells. After 4 h incubation in the incubator [37 °C and 5 % CO_2], the transfection medium was replaced by the standard medium to reduce the toxicity of the transfection medium. The 8-well chamber plate was then placed in the Nikon Ti2 eclipse microscope and incubated for another hour before the recording was started. The recording settings were as follows:

To measure mitotic timing and chromatin segregation defects in Hela cells the 20x 0.75NA objective of the Nikon Ti2 Eclipse microscope was used with the filter sets of mCherry (3 % laser intensity and 100 ms exposition) and GPF (2 % laser intensity and 200 ms exposition) for a total time of 37 h per experiment.

The evaluation of the mitotic time and the mitotic errors occurring between 12 and 28 hours after the start of the experiment were determined manually with Fiji ImageJ (https://imagej.net/software/fiji/; 23.02.2024; 22:28) (Schindelin et al. 2012). This time range was chosen since most GPF fluorescence-positive mitotic cells were counted in this range in the first experiment. In the analysis, the number of frames from the beginning of prometaphase to the beginning of anaphase was counted in 20 cells per experiment and condition. It was found that the PMSCV JAK2V617F IG EGFP vector was not transfected into the HeLa cells and therefore only cells transfected with the control vector (with or without MPL) and the CALRdel52 vector (with or without MPL) were compared with an untreated control in this experiment.

2.2.3.3 Spindle assembly checkpoint challenge

$32D^{MPL}$ cells and TF-1^{MPL} cells were prepared in the same way. First, the three respective cell lines were seeded into an 18-well chamber (Ibidi, Gräfeling, Germany) and placed in the incubator of the Nikon Ti2 Eclipse microscope. After 30 min of incubation, nocodazole was added to the cells at a final concentration of 100 ng/ml and incubated for another 30 min (Burrell et al. 2013). The recording settings were as follows:

For the spindle assembly checkpoint challenge the 20x 0.75NA objective of the Nikon Ti2 Eclipse microscope was used with the filter set of mCherry (5 % laser intensity and 500 ms exposition) for a total time of 20 h per experiment.

The images were analysed with ImageJ, whereby the duration and fate of the mitotic arrest were determined visually. The arrest time of chromatin condensation was determined from entry into prophase to mitotic slip/chromatin segregation. Cells that were in mitotic arrest until the end of the recording were not considered.

The number of cells analysed per experiment was based on the lowest number of condensed cells found in a cell line in an experiment. Consequently, the number of cells analysed was 20 cells per cell line and experiment for the $32D^{MPL}$ cells and 10 cells per experiment and cell line for the $TF\text{-}1^{MPL}$ cells.

2.2.4 Immunofluorescence staining experiments

Immunofluorescence staining of cells is a method of visualising specific cellular components with the aid of an antibody-fluorescence interaction and is used, for example, for the microscopic analysis of cellular structures and interactions within the cell (Jonkman et al. 2020).

One day before fixation, the cells were changed to RPMI 1640 WEHI medium. Three hours before the fixation process, 200 ng/ml nocodazole was added to the cells. The cells were then washed three times with PBS and spun down onto Sigma P-1399 Poly L-lysine hydrobromide-coated glass plates (1000 rpm and 5 min). Then the cells were fixed with 4 % PFA for 10 min at RT. Subsequently, the samples were washed three times with PBS (see appendix for PBS buffer) containing 0.1 % Triton X-100; 1 mM $MgCl_2$; and 0.1 mM $CaCl_2$ (PBS-T++). Thereafter the samples were quenched with 50 mM NH_4Cl in PBS for 5 min at RT. In the next step, the samples were blocked with 3 % BSA in PBS-T++ for 30 min at RT. After that, the samples were incubated with the respective primary antibodies in 3 % BSA in PBS-T++ for 2 h at RT. Thereafter the samples were washed again three times with PBS-T++. Then the respective secondary antibody in 3 % BSA in PBS-T++ was added to the samples and incubated for 2 h at RT in the dark. Finally, the samples were washed three more times with PBS-T++ and mounted on microscopy slides with Mowiol. Images were taken at random positions and the number of images was chosen to image a wide spectrum of mitotic cells. Imaging of the fixed and stained samples was performed on the Nikon Eclipse Ti2

microscope in the fluorescence-confocal mode of an X-light spinning disk (CrestOptics, Roma, Italy). The settings were as follows:

Lambda Oil 60x NA 1.4 objective was used with the filter sets of mCherry (25 % laser intensity and 1 s exposition), GFP (18 % laser intensity and 2 s exposition), and Cy5 (50 % laser intensity and 3 s exposition) with Z-stacks spanning the height of the cell monolayer from random sample field.

The images were opened in ImageJ and with the help of a FiJi Batch macro. The Nikon image files ".nd" were first converted into the open standardised TIFF file format. Then the projections of each channel were created by summing the intensity of each z-stack image. In these images, the mitotic cells were identified and cut out with the help of a ROI manager. Then, the ROIs with mitotic cells were then loaded into Cellprofiler (https://cellprofiler.org/; 23.02.2024; 22:30). CellProfiler is an analysis software that makes it possible to analyse microscopic images in a standardised and automatic way according to a self-created pipeline (Carpenter et al. 2006). First, chromatin and kinetochores of the images were identified. An artificial cytoplasmic ring was determined by taking the area of the H2B-mCherry signal, expanding it by 10 µm, and subtracting the area of the H2B-mCherry signal from it. This artificial cytoplasmic ring served as a background subtraction to deduce the background. The intensities of kinetochores and chromatin were determined in all images, as well as the size of chromatin and kinetochores. The mean values of these intensities of the respective objects were calculated and further analysed and plotted in Excel (Microsoft Corporation, Redmond, USA), and GraphPad Prism software version 9.0 (GraphPad Inc., La Jolla, USA).

2.2.7 Western Blot and gel electrophoresis

Firstly, gel electrophoresis is carried out. This method is used to separate DNA or proteins from a DNA or protein mixture (e.g. cell extract) according to their molecular size (Lee et al. 2012). Western blotting is a protein analytical method in which proteins are transferred from a gel to a membrane and specific proteins can then be visualised

by antibody enzyme binding. This complex is detected by a chemiluminescence reaction of the enzyme with a substrate (Tie et al. 2021).

The gels for the gel electrophorese were prepared depending on which pore size was needed. The pore size determines, which proteins with which molecule size remain in the gel and can then be detected, e.g. in 10 % SDS geld proteins between 15 – 100 kDa can be detected [Table 7: Composition of the different percentages gels for one SDS gel.

Table 7: Composition of the different percentages gels for one SDS gel

	10%	12%	15%	stack
H_20	1.6	1.3	0.9	0.68
30% acrylamide	1.3	1.6	2.0	0.17
1.5M TRIS pH8.8	1.0	1.0	1.0	- / -
1.5M TRIS pH6.8	- / -	- / -	- / -	0.13
10% SDS	0.04	0.04	0.04	0.01
TEMED	0.002	0.002	0.002	0.001
10% APS	0.04	0.04	0.04	0.01

Only in the time course experiments different numbers of cells have to be seeded to obtain similar numbers of protein extracts in the end. In all other expression experiments, a cell density of 1 million cells per ml was selected to produce of the cell extracts [Table 8].

The extracts of all experiments were made as follows: The cells were centrifugated at 1000 rpm for 5 min. The pellets were washed with PBS for 5 min, spun down at 1000 rpm, and mixed with 2x loading dye + 1 mM DTT. Thereafter the pellets were heated at 95 °C for 5 min and the cell extracts were stored at - 20°C.

For gel electrophoresis, the gels were first placed in an electrophoresis chamber and then approximately 800 ml of Laemmli buffer was added. The samples and unstained protein standard were added as a marker. The electrophoresis was run at 15 mA per gel for 10 - 15 minutes until it reached the end of the stacking gel, then the current was

increased to 25 mA per gel and run for 20 - 30 minutes until the running front reached the end of the gel.

Table 8: List of seeded cells per measured time

time points	Cell density [cells/ml]	Total amount per plate
0 h	500.000	4 Mio.
3 h	580.000	4,64 Mio.
6 h	660.000	5,28 Mio.
9 h	750.000	6 Mio.
12 h	830.000	6,64 Mio.
15 h	910.000	7,28 Mio
18 h	1.000.000	8 Mio.

For the Western Blot a TRIS/Glycine buffer and a nitrocellulose membrane was used. The setting for the transfer was 3 h at 100 mA at 4 °C. Then the membrane was coloured with a Ponceau solution to show the band and the marker lines. After that the membrane was blocked with 5 % milk buffer (5 % milk powder in PBS-T), and then the 1. AKs were added and incubated at 4 °C overnight on a shaker. On the next day the membrane was washed with PBS-T and the secondary antibodies were added. The membrane was analysed with a chemiluminescent detector (ImageQuant LAS-4000 system, Fuji) by adding ECL.

The analysis of the western blot images was performed with the gel analysis tool from FiJi ImageJ. This allows the intensity and size of the acquisition bands to be determined. It displays the values and removes the background noise. The plug-in works as follows: First the image is opened in ImageJ and then the area of the bands to be analysed is marked with the rectangular marker function. The plug-in then creates a 2D profile that considers the intensity and size of the bars. The area of each band was separated by drawing lines and the area of each peak was then used for the analysis between each band.

2.2.6 Flow cytometry experiments

Flow cytometry is a cell analysis technique in which cells are analysed according to their size and structure. In fluorescence-activated flow cytometry, the cells are first fluorescently labelled, which enables further classification. In addition to its routine use in diagnostics, this method also enables the quantitative analysis of cells at different stages of the cell cycle (reviewed in (Ligasova et al. 2023)).

In these experiments, cells were first blocked with 100 ng/ml nocodazole at different times (0 h, 2 h, 6 h, 9 h). The cells were then washed twice with PBS at 1000 rpm for 2 min, fixed slowly with 95 % EtOH by slow shaking on a vortex, and stored overnight at - 20 °C. On the next day the ethanol was separated from the cells by centrifugation (1000 rpm, 2 min, 4 °C), and the cells were again washed twice with PBS (1000 rpm, 2 min, 4 °C). The cells were then incubated with the first antibody for 30 min on ice. After two more washes with PBS (1000 rpm, 2 min, 4 °C), the cells were incubated with the second antibody for 30 min on ice. After another wash with PBS (1000 rpm, 2 min, 4°C), the cells were incubated in PBS supplemented with RNase A (100 ng/ml), and Hoechst33342 (10 µl per 1 million cells) was added to the cells 15 min before the start of a measurement. Each measurement was performed on a Gallios flow cytometer (Beckman Coulter, Brea, USA) at the Department of Haematology, University Hospital Aachen. In addition to the standard channels, the fluorescence intensities of DNA (Hoechst33342) and Cyclin B1 (APC-Cy7) were measured.

The analysis was performed using FlowJo™ (Becton Dickinson, Franklin Lakes, USA). This software enables data from different flow cytometers to be analysed. For the analysis the following procedure was chosen: First, cells that had not formed clusters were selected using the forward scatter and sideward scatter representation. Subsequently, the cells that showed a higher Hoechst33342 signal than the negative control and were within the normal distribution of Hoechst33342 were selected (Coquelle et al. 2006). The cells obtained by gating served as the basis for further analysis between the samples. A distinction was made between G1 phase, S phase, G2M phase, and mitotic slippage within the incubation times of nocodazole in the diagram of Hoechst 33342 (x-axis) versus CyclinB-APC-Cy7 (y-axis). For the percentage distribution, the analysed phases were added and set as 100 % and the respective percentage values of the three cell lines in the respective phases were determined.

3. Results

Defects in mitosis are one of the main causes of chromosomal instability involved in the development and progression of cancer (Bakhoum and Cantley 2018). Time-lapse microscopy in living cells is a technique that allows exploring the various phenotypes of defective mitosis while pinpointing their possible molecular causes (Piltti et al. 2018). Therefore, we performed long-term live-cell imaging of cells to investigate the duration of mitosis and the correctness of chromatin segregation in cells expressing control, CALRdel52 or JAK2V617F constructs. Live-cell imaging of murine 32D^{MPL} cells, human TF-1^{MPL} or HeLa cells was done for a duration of 20 h (32D^{MPL} and TF-1^{MPL}) or 40 h (HeLa). The Western Blot and flow cytometry were used to study the molecular status of mitosis.

3.1 Effect of ph. neg. MPN mutations in mitotic timing and chromatin segregation

To investigate the effect of CALRdel52 and JAK2V617F on mitosis in murine 32D^{MPL}, we determined the chromatin segregation and mitosis duration by long-term live cell imaging over 20 h and measured via image analysis. Eleven independent experiments were performed with approximately 100 cells each. Significant differences between the control cell line [15.2 ± 4.7 min] and the two mutant cell lines (CALRdel52 [15.9 ± 4.8 min] and JAK2V617F [15.9 ± 4.3 min]) (two-tailed t-test) could not be detected [Figure 7 A].

The effect of the mutations on the accuracy of chromatin segregation was addressed by measuring the number of chromosome bridges, lagging chromosomes and telophase micronuclei in the 32D^{MPL}. The error rate of chromosome bridges the control cell line was 10.3 ± 2.1 %, while the two mutated cell lines had an error rate of 12.4 ± 3.3 % (CALRdel52) and 13.5 ± 3.6 % (JAK2V617F) [Figure 7 B].

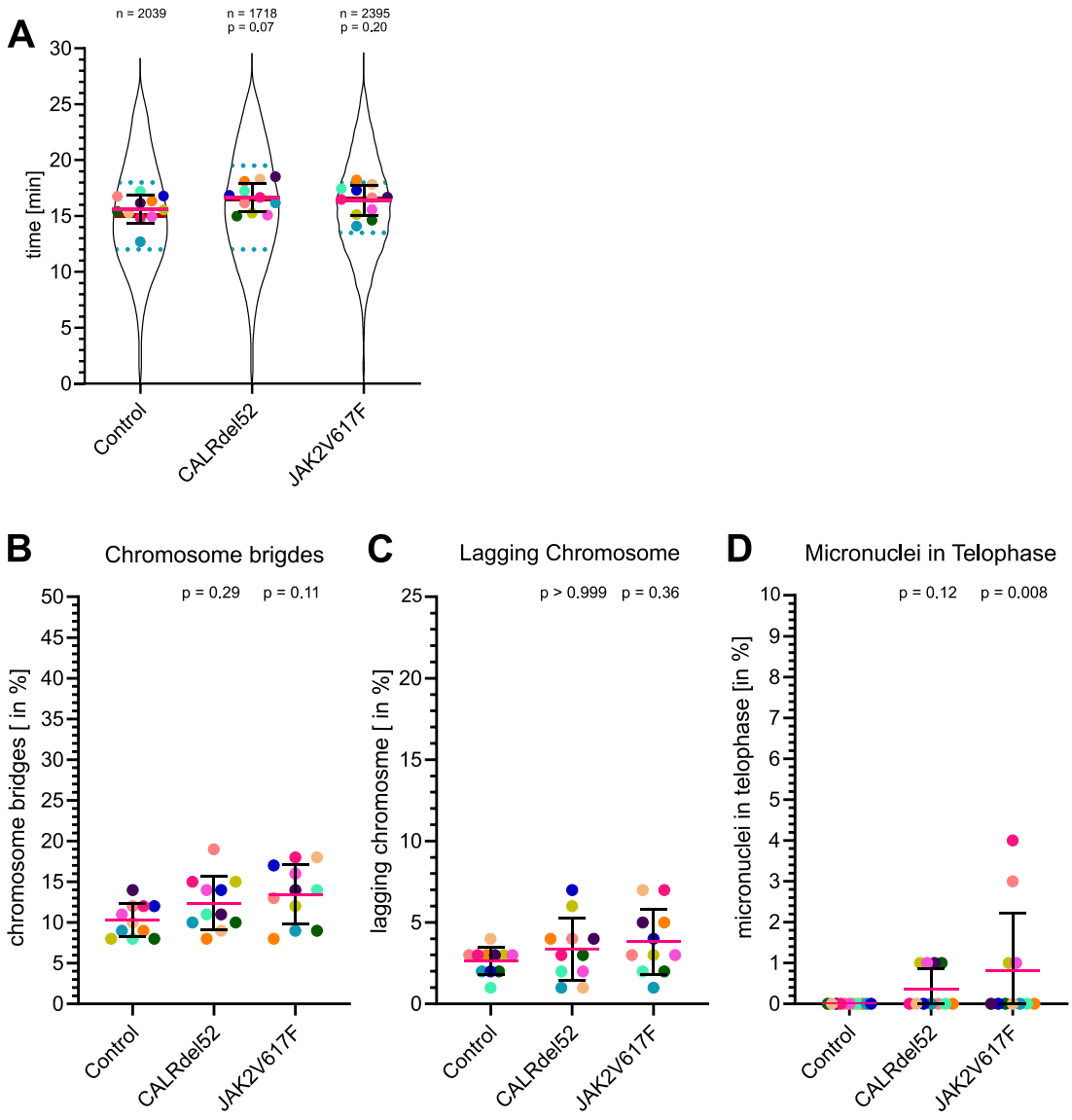

Figure 7: Mitotic time and errors of 32D^{MPL} cells: A) The superplots show the mitotic timing of the control, CALRdel52 and JAK2V617F transduced 32D^{MPL} cells expressing H2B-mCherry. The violin-shaped structure represents the distribution of all individual measurements (n = 1718 - 2039). The mean values of the individual experiments are shown as coloured dots [n = 11]. The pink bar shows the mean of all experiments, and the black bars show the standard deviations. The red line indicates the median and the blue dashed line the quartiles. The significances between the untreated control and all other conditions, and between the controls and the mutations cell lines in each treatment were analysed by one-Way ANOVA (Kruskal-Wallis with Dunn´s post-test). B - D) Graphs show the percentages of different mitotic errors (chromatin bridges, lagging chromosomes and micronuclei) of the control, CALRdel52 and JAK2V617F transduced 32D^{MPL} cells expressing H2B-mCherry. Approximal 100 events were analysed in each mitotic time experiment. The mean values of the individual experiments are shown as coloured dots [n = 11]. The pink bar shows the mean of all experiments, and the black bars show the standard deviations. The significance between the individual controls and

the other two cell lines were analysed using Fisher's exact test. The red numbers show the conditions that differ significantly from the control. (Partly modified from Holl et al. 2024)

The rate of lagging chromosome was 2.6 ± 0.8 % for the control cell line, 3.4 ± 1.9 % for the CALRdel52 and 3.8 ± 2.0 % for the JAK2V617F [Figure 7 C]. Although no significant differences were found between the control and the two mutant cell lines (CALRdel52 and JAK2V617F) for the chromosome bridges and lagging chromosomes, the mutant lines showed increased number of these mitotic errors. I found no micronuclei in the control cell line, while the two cell lines expressing the JAK2V617F and CALRdel52 had a percentage of defects of 0.4 ± 0.5 % (CALRdel52) and 0.8 ± 1.4 % (JAK2V617F), [Figure 7 D]. While CALRdel52 cells showed no differences with control cells, the number of micronuclei was significantly higher in the JAK2V617F cells concerning the control cell line ($p < 0.01$, Fisher´s exact test).

In summary, the two cell lines expressing the JAK2V617F and CALRdel52 showed a tendency towards increased number of mitotic errors. As even small increase in karyotype aberrations have been linked to carcinogenesis (reviewed in (Simonetti et al. 2019)) I pursued the functional characterization of the mitotic process and its defects in the presence of CALRdel52 and JAK2V617F mutations.

3.1.1 Stress-sensitive and error-prone mitosis in CALRdel52 and JAK2V617F transduced 32D^{MPL} cells

As the general influence of the CALRdel52 and JAKV617F mutations on mitosis time and the number of chromosome segregation defects had been established, the next step was to test the robustness of the SAC in 32D^{MPL} cells. For this purpose, the cells were treated with 200 nM doxorubicin or 3 µM NMS-P715. Damage or malfunction of the SAC should normally lead to termination of mitosis and apoptosis of the cell. Doxorubicin is an anthracycline that leads to the formation of DNA double-strand breaks. Normally this leads to apoptosis of the cells, but if the DNA repair mechanism is disrupted, chromosome segregation errors and aneuploidy may occur (Forrest et al. 2012).

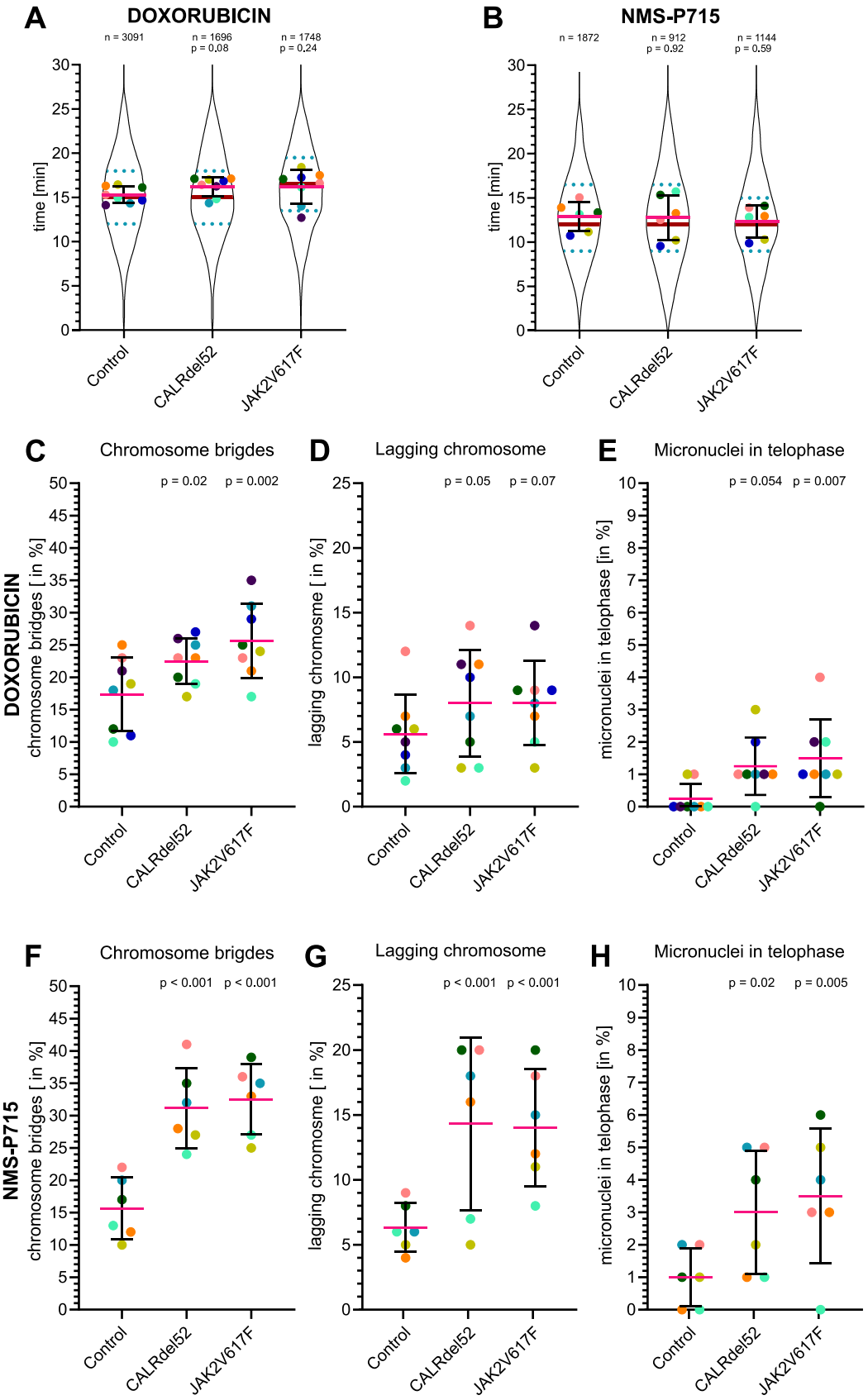

Figure 8: Mitotic time and errors of 32D^{MPL} cells after doxorubicin or NMS-P715 treatment: A - B) These superplots show the mitotic timing of the control, CALRdel52 and JAK2V617F transduced 32D^{MPL} cells treated with 200 nM doxorubicin or 3 µM NMS-P715 expressing H2B-

mCherry. The violin-shaped structure represents the distribution of all individual measurements (n = 912 - 3091). The mean values of the individual experiments are shown as coloured dots [n = 8 or 6]. The pink bar shows the mean of all experiments, and the black bars show the standard deviations. The red line indicates the median and the blue dashed line the quartiles. The significances between the untreated control and all other conditions, and between the controls and the mutations cell lines in each treatment were analysed by one-way ANOVA (Kruskal-Wallis with Dunn´s post-test). C - H) These graphs show the percentages of different mitotic errors (chromatin bridges, lagging chromosomes and micronuclei) of the control, CALRdel52 and JAK2V617F transduced 32D^{MPL} cells expressing H2B-mCherry. Approximal 100 events were analysed in each mitotic time experiment. The mean values of the individual experiments are shown as coloured dots [n = 8 or 6]. The pink bar shows the mean of all experiments, and the black bars show the standard deviations. The significance between the individual controls and the other two cell lines were analysed using Fisher's exact test. The red numbers show the conditions that are differ significantly from the control. (Partly modified from Holl et al. 2024)

NMS-P715 is a small molecule MPS-1 inhibitor that accelerates mitosis and inhibits the correct localisation of kinetochore components, which leads to increased aneuploidy and ultimately drives the cell into apoptosis. If the SAC is weakened or defective, cells with segregation defects can continue to divide and undergo mitotic slippage (Colombo et al. 2010).

The mean mitotic time after induction of DNA damage by doxorubicin treatment in CALRdel52 cells (15.9 ± 4.8 min) and JAK2V617F cells (15.9 ± 4.3 min) was similar to the mitotic time in control cells (15.2 ± 4.7 min) [Figure 8 A] (two-tailed t-test). Also, after addition of the antimitotic agent NMS-P715, which induces SAC dysfunction, no difference in mitotic time could be detected between CALRdel52 cells (12.7 ± 5.1 min), JAK2V617F cells (12.5 ± 4.8 min), and control cells (12.8 ± 4.6 min) [Figure 8 B].

From the comparison of the three chromatin segregation defects, it can be deduced that the chromosome bridge error rates in 32D^{MPL} cells with CALRdel52 or JAK2V617F mutation increase significantly after induction of doxorubicin ($p < 0.02$, Fisher's exact test) [Figure 8 C]. Also, the chromosome bridge error rates and the number of lagging chromosomes in 32D^{MPL} cells with CALRdel52 or JAK2V617F mutation increase significantly after induction of SAC dysfunction by NMS-P715 ($p < 0.001$, Fisher's exact test) [Figure 8 F, G]. In addition, the number of telophase micronuclei for JAK2V617F-expressing cells is significantly increased after treatment with doxorubicin and NMS-

P715 ($p < 0.005$, Fisher's exact test) [Figure 8 E, H]. The measured values for each experiment are listed in the Appendix [Supplemental Table 13].

In summary, the increased chromatin segregation errors under treatment in CALRdel52 and JAK2V617F expressing 32D^{MPL} cells suggest a stress-sensitive and error prone mitosis.

3.2 Effect of ph. neg. MPN mutations on spindle assembly checkpoint

The observed phenotypes could be due to defects in the SAC. As mentioned earlier, the SAC ensures correct chromatid separation by delaying chromatin segregation until the chromatids are properly bound to the spindle microtubules via the kinetochore. To fulfill this task, a large number of proteins and their precise interaction are required (reviewed in (Hayward et al. 2019)). Both the presence of certain proteins at a certain time and their quantity at the kinetochore during activation of the SAC play a role. Any change in the SAC can have fundamental effects on mitosis and thus on the survival of the cell (reviewed in (Weaver and Cleveland 2005)).

3.2.1 SAC Challenge in 32D^{MPL} cells

Nocodazole is an antineoplastic agent that inhibits the polymerization of microtubules and thereby triggers mitotic arrest. Microtubules bind to chromatids via kinetochores during mitosis and are a driving force in chromatin segregation (Hoffman et al. 2001). Nocodazole-induced mitotic arrest is shorter in cells with weakened or defective SAC (reviewed in (Yamada and Gorbsky 2006)). I could observe nocodazole-induced arrest in all 32D^{MPL} cells. The arrest time in the control cells was 257 ± 45 min, while the arrest in the CALRdel52 cells lasted 210 ± 36 min and in the JAK2V617F cells 186 ± 35 min. Thus, a significantly shorter mitotic arrest was observed in both mutant

cell lines compared to the control cell line ($p < 0.05$, Kruskal-Wallis with Dunn's post-test) [Figure 9 A].

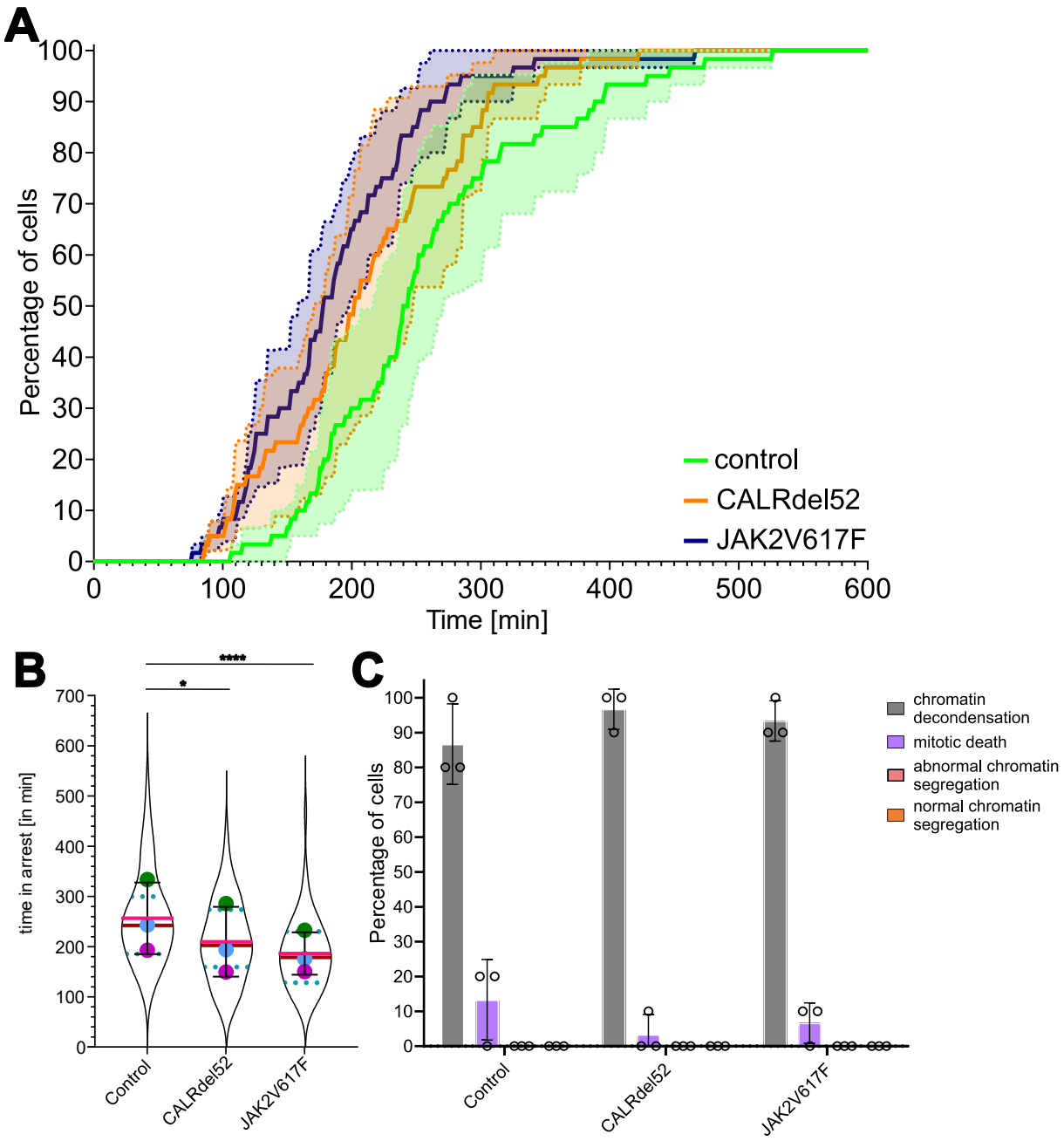

Figure 9: Spindle assembly challenge effect on the CALRdel52 and JAK2V617F mutation in 32D^{MPL} cells co-expressing H2B-mCherry after 100 ng/ml nocodazole treatment: A) The plots show the proportion of cells that leave mitosis at a specific time after mitotic entry. The bold lines show the mean values and the coloured areas show the SDs. B) The violin-shaped structure represents the distribution of all individual measurements (n = 60). The mean values of the individual experiments are shown as coloured dots [n =3]. The pink bar shows the mean of all experiments and the black bars show the standard deviations. The red line indicates the

*median and the blue dashed line the quartiles. The significances between the untreated control and all other conditions, and between the controls and the mutations cell lines in each treatment were analysed by one-way ANOVA (Kruskal-Wallis with Dunn´s post-test, * p < 0.05, **** p < 0.001). C) The fate of the nocodazole-induced mitotic arrest was determined in control or CALRdel52- or JAK2V617F transduced cells, which were divided in the following groups: spindle-less mitotic exit with direct chromatin decondensation (grey), cell death during mitotic arrest (violet), normal chromatin segregation (red) and abnormal chromatin segregation (orange). For each independent experiment 10 cells were analysed and the mean values of all three experiments are shown as dots. The mean of all experiments is shown as a column. The black bars indicate the deviation of the mean values. A two-way ANOVA with Dunnet post-test was used to test the significance, and no significant difference was found between the control and the two mutated cell lines. (Partly modified from Holl et al. 2024)*

Due to different signalling pathways, the results of mitotic arrest induced by microtubule inhibitors (such as nocodazole) differ between cancer and normal cell lines (reviewed in (Yamada and Gorbsky 2006)). The "competing networks and thresholds" model assumes that the cell fate decision is determined by whether the threshold for cell death or prolonged survival is reached first. This refers to the activation of pro-apoptotic caspases and the degradation of Cyclin B1, the latter leading to mitotic slippage (Gascoigne and Taylor 2008).

The percentage of cells that decondense is 86.7 ± 9.4 % in control cells, 96.7 ± 4.7 % in CALRdel52 cells, and 93.3 ± 4.7 % in JAK2V617F cells. The percentage of mitotic death in control cells is about 13.3 ± 9.4 %, while the percentage in the CALRdel52 cells is about 3.3 ± 4.7 % and in the JAK2V617F cells is about 6.7 ± 4.7 %. There was no significant change in the distribution of the fates between the two cell lines expressing JAK2V617F or CALRdel52 and the control cell line (two-way ANOVA with Dunnet post-test) [Figure 9 A, B].

In summary, I found a shortened mitotic arrest time in both mutant cell lines, which is consistent with a weakened or defective SAC ((Boyapati et al. 2007) and reviewed in (Brown and Geiger 2018)). The most common outcome of mitotic arrest was mitotic slippage, which could be due to accelerated destruction of Cyclin B1 in the presence of an unsatisfied SAC (Brito and Rieder 2006).

3.2.2 Time-dependent degradation of Cyclin B1 in 32D^{MPL} cells

Cyclin B1 in accumulated during G2 and early mitosis and degraded after satisfaction of the SAC. Premature Cyclin B1 degradation during mitosis is associated with a weakening of the SAC. Thus, we investigated whether Cyclin B1 accumulation and degradation differ between control cells and CALRdel52 or JAK2V617F cells after incubation with nocodazole. I used western blotting for a more general overview of the cyclin B1 phenotype and cytometry for a more detailed look at the different phases of the cell cycle. The incubation time in nocodazole is the shortest average mitotic arrest time of the cells before they undergo slippage.

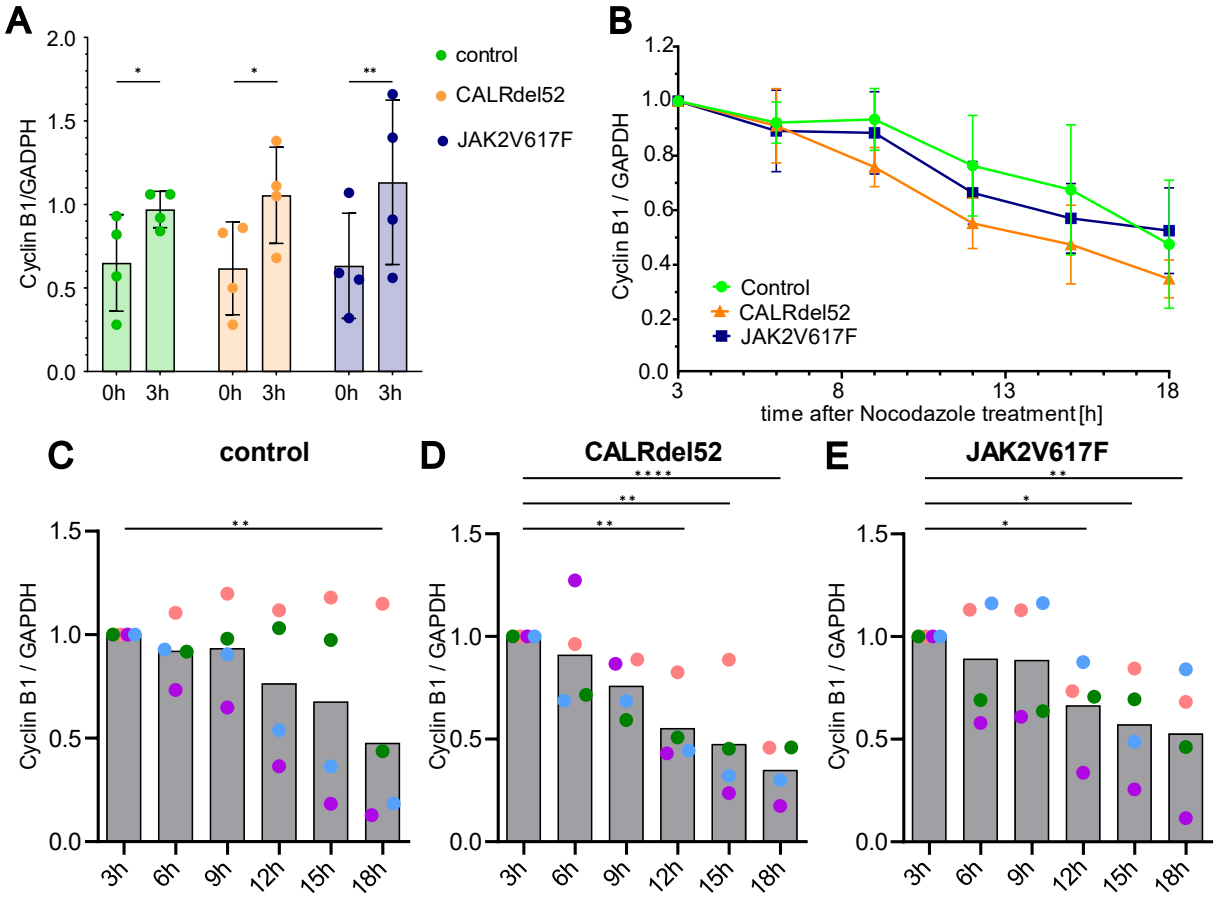

Figure 10: Difference in expression level of Cyclin B1 over time: A) The last graph shows the ratio between Cyclin B1 and GAPDH after expression of Cyclin B1 at 0 and 3 h of incubation (exact data are in [Supplemental Table 9]). A two-way ANOVA (Fishers LSD post-test) was used to test the significance (p<0.05; ** p<0.001). B) The line chart shows the development of all three cell lines over time in direct comparison (exact data are in [Supplemental Table 9]).*

C-E) The graphs show the ratio normalised to GAPDH after 3 hours of treatment with 200 ng/ml nocodazole of CALRdel52, JAK2V617 and control 32D^{MPL} cells stably expressing H2B-mCherry. The individual mean values of all three experiments are shown as coloured dots. The mean value of all experiments is shown as a grey column. Two-way ANOVA with Dunnett post-test (p<0.05; **p<0.01; ***p<0.001). (Partly modified from Holl et al. 2024)*

Similar accumulation was observed in all three cell lines [Figure 10 A]. Once accumulated, the amount of Cyclin B1 was determined at time points during 15h. A comparison between the cell lines showed that the degradation of Cyclin B1 in the cells expressing the CALRdel52 and JAK2V617F mutations is overall faster [Figure 10 B]. Within the respective cell line, Cyclin B1 is degraded over time in all three cell lines [Figure 10 C-E].

Cyclin B1 was degraded faster after its accumulation in the CALRdel52 and JAK2V617F cells, indicating a weakened SAC. This in turn may be the cause of defective mitosis in these cells.

Cytometry was used to further investigate the observed Cyclin B1 phenotype and the faster slippage of nocodazole-induced mitotic arrest. This method enables the cell cycle analysis by visualising the amount of cells in the G1, S and G2/M phases, as well as the among of cells that express Cyclin B1 (Nunez 2001). For the cytometric evaluation of Cyclin B1 expression after mitotic arrest, cell extracts were prepared after 0 h, 2 h, 6 h and 9 h induction of 100 ng/ml nocodazole.

Regarding the G1 and S phases, a similar time course can be seen in all three cell lines [Figure 11 B-C], although the JAK2V617F cells are initially less frequent in the S phase than the other two cell lines. In the G2/M phase, the proportion of control and CALRdel52 cells increases slowly over time, while the proportion of JAK2V617F cells increases more quickly, reaches a peak after 6 h and then falls again. So, the course of the JAK2V617F cell line differs from the course of the other cell lines [Figure 11 D]. In all three cell lines, the proportion of slippage triggered by the degradation of Cyclin B1 rises after 2 h of incubation time with nocodazole. In the two mutated cell lines the percentage of slippage after 9 h incubation with nocodazole was higher than in the control cells [Figure 11 E]. The exact percentages of each cell line in every phase can be found in the appendix [Supplemental Table 11].

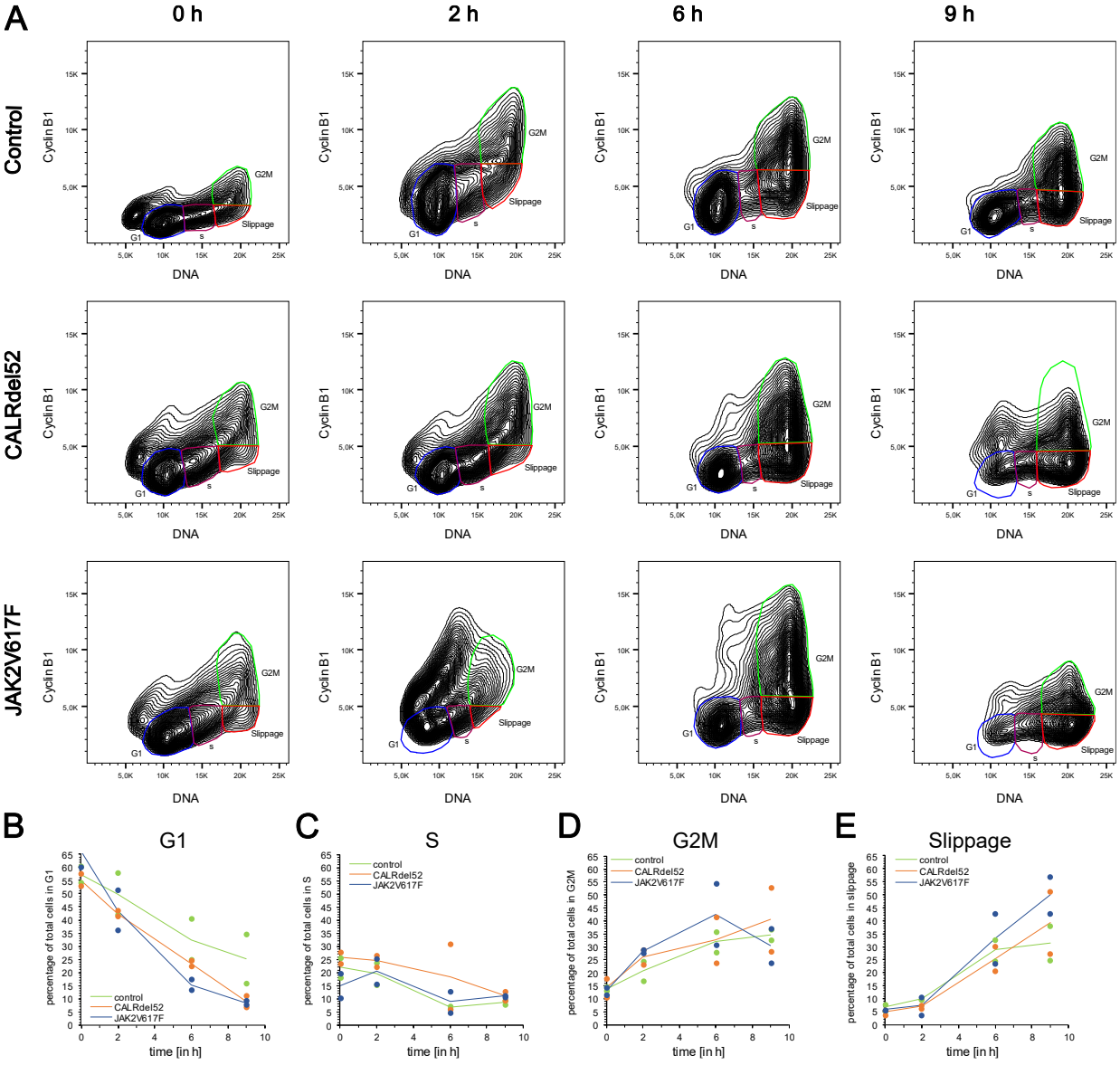

Figure 11: Mitotic slippage induced by degradation of Cyclin B1 after time-dependent nocodazole treatment: A) Example images of the contour plots from one of the two experiments used for analysis. The different colours show the different phases of the analysed mitoses and the slippage. Pictures of all the steps of the pipeline can be found in the appendix [Supplemental Figure 19]. B-E) The graphs show the progression of the percentage of total control, CALRdel52, and JAK2V617 32D^{MPL} cells stably expressing H2B-mCherry in the respective phase after the tested times of mitotic arrest by 100 ng/ml nocodazole treatment. The individual means of the two experiments are shown as coloured dots. The mean of both experiments is shown as a grey column.

In summary, a time-dependent increase in Cyclin B1 degradation after nocodazole-induced mitotic arrest was observed in Western Blotting in all three cell lines. In agreement, the cytometry experiments show that the percentage of slippage was higher in the CALRdel52 and JAK2V617F cells after 9 h of nocodazole-induced mitotic arrest.

3.2.2 Expression level of the different SAC factors in 32D^{MPL} cells

It is known that some SAC factors are partially downregulated in cancer cells ((Boyapati et al. 2007, Wolanin et al. 2010) and reviewed in (Schnerch et al. 2012)). Since the SAC is an interplay of the correct expression level and localisation of many different SAC factors, the downregulation of individual SAC factors can disturb the balance and promote the development of cancer (Lin et al. 2002). Therefore, we analysed by Western Blot the level of expression of several SAC proteins in whole protein extracts from cells treated with 200 ng/ml nocodazole for approximately 10 min and 18 hours. In both CALRdel52 and JAK2V617F cells, except for Cyclin B1, no significant difference was observed for any of the SAC factors compared to the control cells. After 18 h of nocodazole-induced arrest, the expression of Cyclin B1 was reduced in all three cell lines compared to 10 min ($p < 0.05$, Kruskal-Wallis test with Dunn´s post-test) [Figure 12 C]. In addition, a decrease was also observed in CDC20, Aurora B, and MAD1 after 18 h incubation with nocodazole, but this was not significant [Figure 12 A, B, D]. One possible reason for the observed decrease in the SAC factors mentioned could be that 32D^{MPL} mouse cells escape more quickly from mitotic arrest under experimental conditions with nocodazole. The exact expression ratios between the SAC factors and actin can be found in the appendix [Supplemental Table 12].

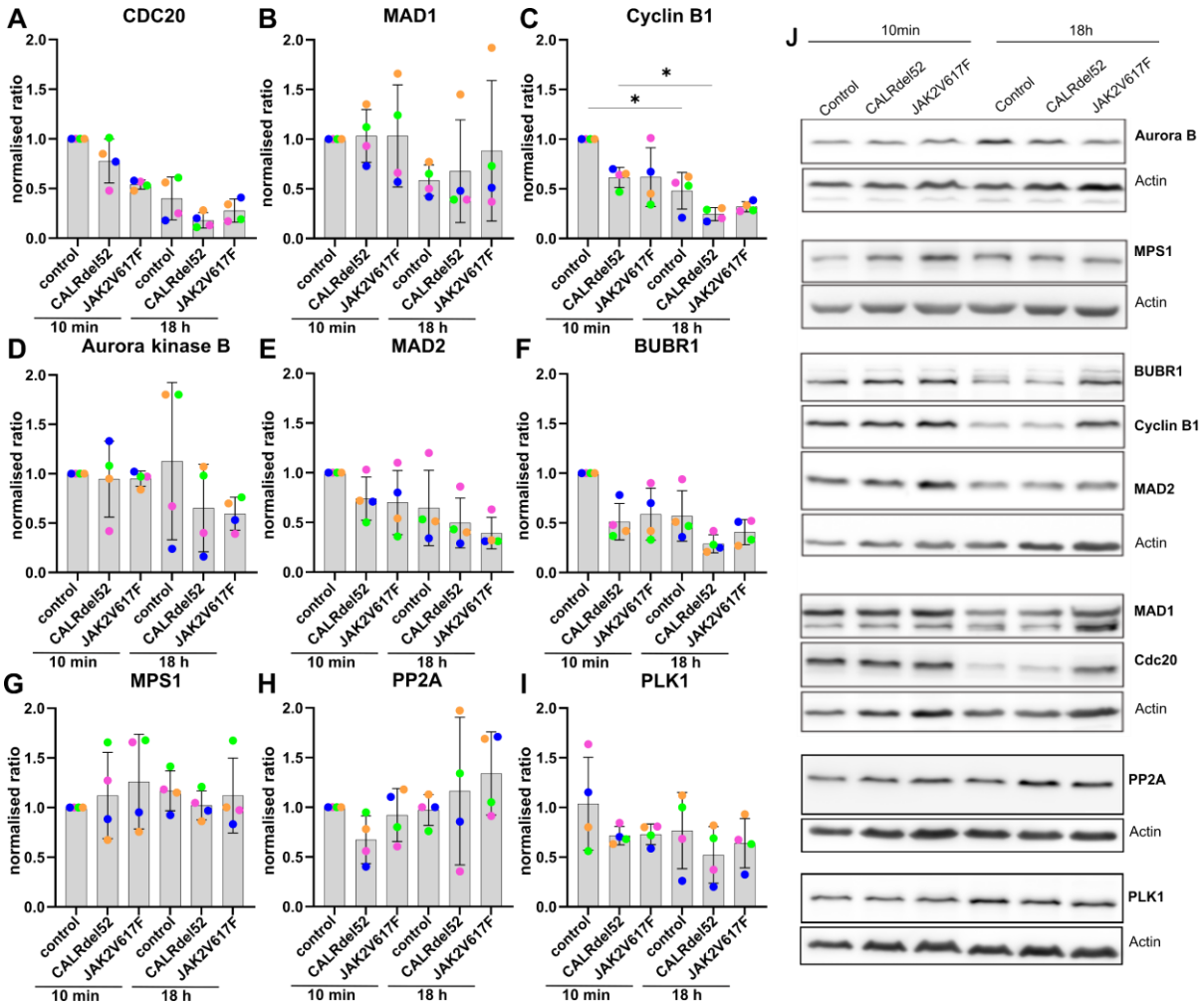

Figure 12: Difference in expression level of key factors in 32D^{MPL} cells: A-I) The graphs show the actin and 10 min control ratio normalized to the other time points after mitotic arrest by 200 ng/ml nocodazole treatment of CALRdel52, JAK2V617 and control 32D^{MPL} cells stably expressing H2B-mCherry. The individual mean values of all four experiments are shown as coloured dots. The mean value of all experiments is shown as a grey column. The black bars indicate the deviation of the mean values. A one-way ANOVA (Kruskal-Wallis test with Dunn´s post-test) was used to test the significance (p >0.05). The sample images of the corresponding Western Blot are shown in the appendix [Supplemental Table 12]. J) Example pictures of the western Blot. (Modified from Holl et al. 2024)*

The fact that no changes in the SAC factors were detected in the CALRdel52 and JAK2V617F cells, except of Cyclin B1, suggests that the influence of the two mutations on the SAC is properly not due to a change in the expression level of the analysed factors, but could ,in turn, be due to unbalance recruitment of SAC factors to the kinetochores during early mitosis (reviewed in (McAinsh and Kops 2023)).

3.2.3 Kinetochore recruitment of SAC factors in 32D cells

The functionality of the SAC can also be influenced by defective recruitment of its factors (reviewed in (Dou et al. 2019)). Both an increase and a decrease in the recruitment of SAC factors can weaken the SAC (Lok et al. 2020). The analysis of the kinetochore recruitment of SAC factors in $32D^{MPL}$ cells arrested with nocodazole was done by quantitative immunofluorescence. Altered kinetochore recruitment was observed in the CALRdel52 and JAK2V617F cells for several SAC factors compared to the control. In the CALRdel52 cells, significant changes could be detected in the kinetochore recruitment of MAD1, CENPE, Aurora B and BUBR1 ($p < 0.05$, two-tailed t-test) [Figure 13 A, B, F, H].In the JAK2V617F cells significant changes could be detected in the kinetochore recruitment of MAD1, CDC20, Cyclin B1 and BUBR1 ($p < 0.05$, two-tailed t-test) [Figure 13 A, C, D, H]. The exact signal intensity ratios between the SAC factors and CREST are shown in the appendix [Supplemental Table 14].

In summary, the unbalanced recruitment of the different SAC factors is consistent with the expectations of a weakened SAC. In CALRdel52 cells, an opposite effect of transduction was observed compared to JAK2V617F cells regarding the localisation of MAD1, CDC20 and Cyclin B1. For BUBR1 and MPS1, an equal trend was observed for both mutations. This suggests a change in an upstream regulatory network. Our first hypothesis was an abnormal expression in PLK1 or PP2A, which are among the most important mitotic regulators. However, since we could not detect any significant changes in the total protein expression of PLK1 or PP2A by Western blot, the JAK2V617F and the CALRdel52 mutations do not seem to affect the expression of PLK1 and PP2A in murine $32D^{MPL}$ cells [Figure 12 H, I].

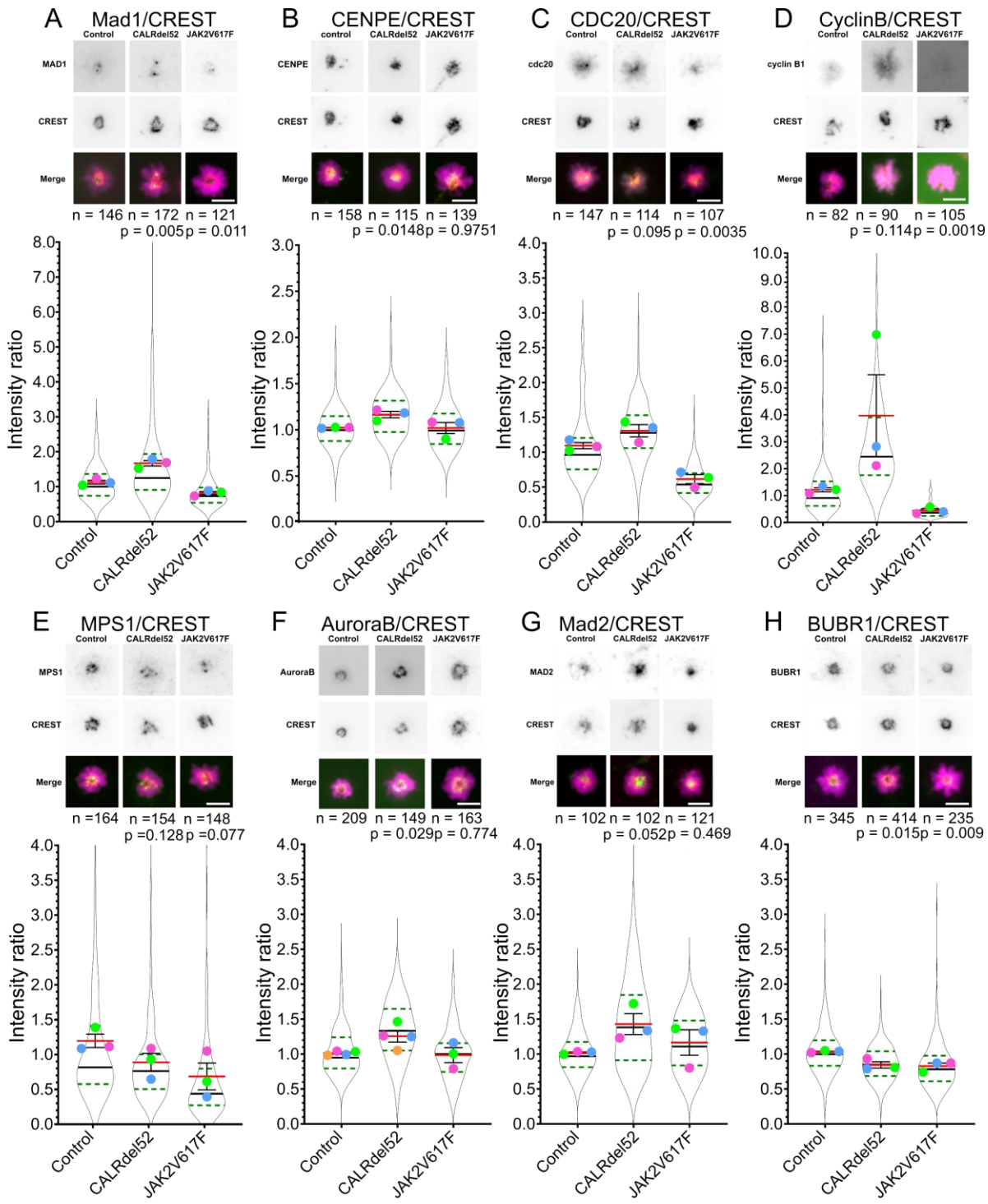

Figure 13: Kinetochore recruitment of SAC factors in 32D^{MPL} cells: A-H) The top rows of each indicated SAC factor are example images of control, CALRdel52 or JAK2V617F transduced 32D^{MPL} cells stably expressing H2B-mCherry (magenta) after 200 ng/ml nocodazole was arrested at the kinetochores by quantitative immunofluorescence. The SAC factors are green in the overlay and the internal standard CREST is red in the overlay. Below the sample pictures are the superplots showing the normalised intensity ratio between the SAC factors and the CREST. The violin-shaped structure represents the distribution of all individual measurements, the number of these is shown above each graph (n = x). The mean values of the individual

experiments are shown as coloured dots [n = 3 - 4]. The red bar shows the mean value of all experiments and the black bars show the standard deviations. The horizontal black line indicates the median and the green dashed line the quartiles. Significances between the untreated control and all other conditions were analysed using an unpaired two-tailed t-test ($p < 0.05$) over the means of the independent experiments. (Modified from Holl et al. 2024)

3.3 Effect of ph. neg. MPN mutations in mitotic timing, chromatin segregation and on spindle assembly checkpoint in human cell models

I have used so far 32D^{MPL} mouse cells, which is a common cell model for investigating haematopoietic diseases, as these mouse cells, for example, have sufficient similarity in myelopoiesis compared to human haematopoietic progenitor cells (Kagoya et al. 2014, Han et al. 2016, Zjablovskaja et al. 2018). To find out whether the mitotic effects induced by the two driver mutations CALRdel52 and JAK2V617F also occur in human cells, I validated key results in erythroleukemic TF-1^{MPL} cells.

3.3.1 Effects of the mutations CALRdel52 and JAK2V617F on the SAC of human TF-1

To further investigate nocodazole-induced mitotic arrest, I consider the effect of CARLdel52 and JAKV617F on TF-1^{MPL} compared to control cells. In the control cells, the nocodazole arrest is 313 ± 75 min, while in the CALRdel52 cells, it is 177 ± 22 min and in JAK2V617F it is 201 ± 24 min. In line with the 32D^{MPL} experiments, both mutated TF-1^{MPL} cell lines showed a significantly shorter mitotic arrest in comparison to the control cells ($p < 0.001$, Kruskal-Wallis with Dunn´s post-test) [Figure 14 A, B]. In contrast to the 32D^{MPL} experiments, the TF-1^{MPL} cells showed a more diversified progression after the nocodazole arrest. The most frequent consequences of mitotic exit are still chromatin decondensation and mitotic death.

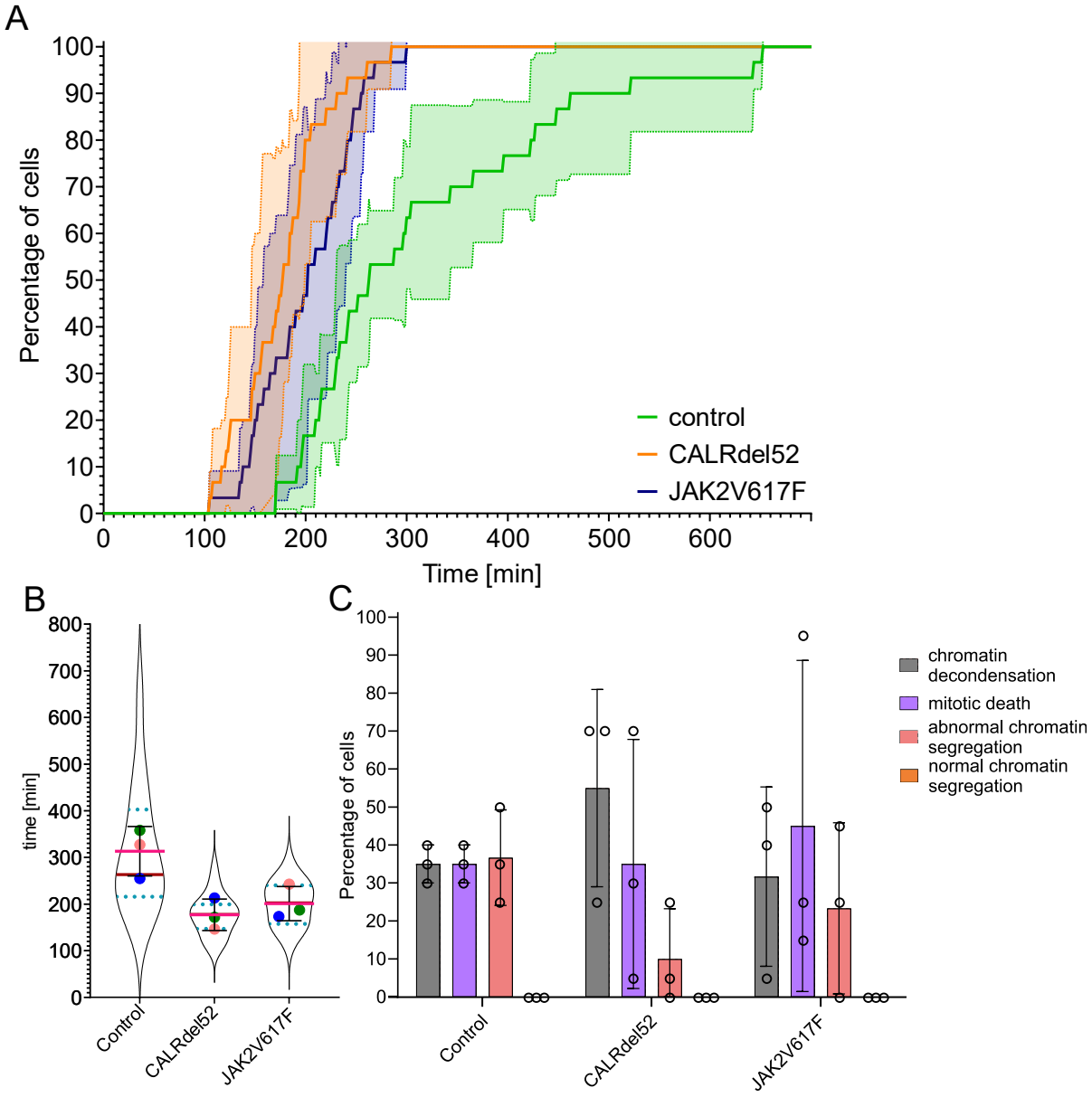

*Figure 14: Effect of CALRdel52 and JAK2V617F mutation on SAC in TF-1^{MPL} cells co-expressing H2B-mCherry after 100 ng/ml nocodazole treatment A) The Plots show the proportion of cells that leave mitosis at a specific time after mitotic entry. The bold lines show the mean values and the coloured areas show the SDs. B) The violin-shaped structure represents the distribution of all individual measurements (n = 30). The mean values of the individual experiments are shown as coloured dots [n =3]. The pink bar shows the mean of all experiments and the black bars show the standard deviations. The red line indicates the median and the blue dashed line the quartiles. The significances between the untreated control and all other conditions, and between the controls and the mutations cell lines in each treatment were analysed by one-way ANOVA (Kruskal-Wallis with Dunn´s post-test, *** p < 0.0005 **** p < 0.001). C) The fate of the nocodazole-induced mitotic arrest was determined in control or CALRdel52- or JAK2V617F transduced cells, which were divided into the following groups: spindle-less mitotic exit with direct chromatin decondensation (grey), cell*

death during mitotic arrest (violet), normal chromatin segregation (red) and abnormal chromatin segregation (orange). For each independent experiment, 10 cells were analysed and the mean values of all three experiments are shown as dots. The mean of all experiments is shown as a column. The black bars indicate the deviation of the mean values. A two-way ANOVA with Dunnett post-test was used to test the significance, and no significant difference was found between the control and the two mutated cell lines. (Modified from Holl et al. 2024)

However, compared to the 32D^{MPL} cells, fewer cells are affected by mitotic slippage. In contrast to the 32D^{MPL} experiments, abnormal chromatin segregation was observed in all three cell lines in the TF-1^{MPL} experiment [Figure 14 B]. In summary, the results indicate that CALRdel52 and JAK2V617F mutations also lead to a disruption of the SAC in human haematopoietic cells.

3.3.2 Effect on mitotic duration and chromatin segregation in CALRdel52 and JAK2V617F transduced TF-1 cells

Since the SAC challenge also suggests an influence of CALRdel52 and JAK2V617F in the TF-1^{MPL} cells, the next step was to observe the effect on mitosis and chromatin segregation. The mitotic time of the control cell line was 36.1 ± 21.4 min, while the two mutated cell lines had a time for passage through mitosis of 44.5 ± 32.6 min (CALRdel52) and 51.1 ± 48.8 min (JAK2V617F) [Figure 15 A]. Although there was no significant change in mitotic time between the two mutant cell lines and the control cell line, a tendency to prolong mitosis was observed, particularly in the JAK2V617F cells. In addition to the lagging chromosomes, the chromosome bridges, and the micronuclei, the number of misaligned chromosomes could also be classified in the experiments with TF-1^{MPL}. These are chromosomes that are not aligned with the metaphase plate and, like the other mitotic defects, can lead to CIN (Wilhelm et al. 2019). None of the four mitotic defects tested showed a significant difference between the two mutant cell lines and the control cell line (Fisher´s exact test).

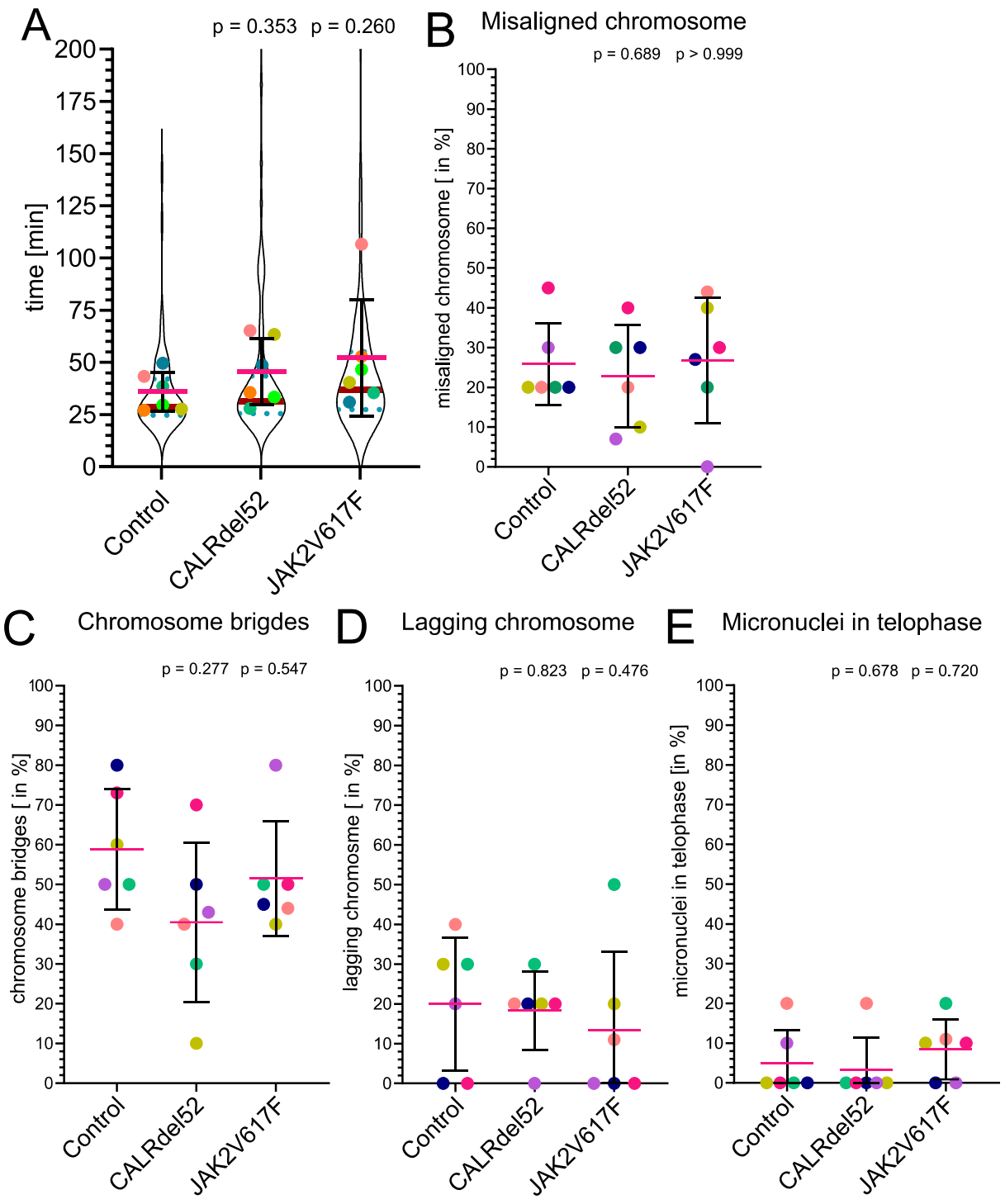

Figure 15: Mitotic time and errors of TF-1^{MPL} cells: A) The superplots shows the mitotic timing of the control, CALRdel52 and JAK2V617F transduced TF-1^{MPL} cells expressing H2B-mCherry. The violin-shaped structure represents the distribution of all individual measurements (n = 15 - 30). The mean values of the individual experiments are shown as coloured dots [n = 3]. The pink bar shows the mean of all experiments and the black bars show the standard deviations. The red line indicates the median and the blue dashed line the quartiles. The significances (p-value) between the control and mutated cell lines were detected through one-way ANOVA (Kruskal-Wallis with Dunn´s post-test). No significant difference was

found. B-E) These graphs show the percentages of different mitotic errors (misaligned chromosome, chromatin bridges, lagging chromosomes, and micronuclei in telophase) of the control, CALRdel52 and JAK2V617F transduced TF-1^{MPL} cells expressing H2B-mCherry. The mean values of the individual experiments are shown as coloured dots [n = 6]. The pink bar shows the mean of all experiments and the black bars show the standard deviations. The significance between the individual controls and the other two cell lines were analysed using Fisher's exact test. No significant difference was found.

High number of mitotic defects should be in principle a sign of a disturbed control mechanism. As I was able to determine a high number of mitotic defects in all three TF-1^{MPL} cell lines, it can be assumed that there is a general underlying problem within the TF-1 cells used. In contrast to the 32D cells (Anna Maria Agliano 2000), the TF-1 cells have a highly rearranged hyperdiploid karyotype (Winkelmann et al. 1995). The altered karyotype increases the susceptibility to errors during mitosis, which would explain the generally high incidence of chromatin segregation defects.

3.3.3 Kinetochore Recruitment of SAC factors in TF-1 cells

The influence of JAK2V617F and CALRdel52 mutations on the kinetochore recruitment of SAC factors in TF-1^{MPL} cells was investigated by measuring the recruitment of CDC20, Cyclin B1 and MAD1, which were prominently influenced in JAK2V617F 32D^{MPL} cells. The data from the MAD1 experiments are from Nathalie Brock's bachelor thesis, which I helped to supervise. We could not detect a significant change in kinetochore recruitment in any of the three SAC factors tested [Figure 16]. However, in all SAC factors, we observed a tendency towards an increase in the SAC factor CDC20 in JAK2V617F cells, while in the CALRdel52 cells a slight tendency towards a decrease. In both mutant cell lines a tendency towards an increase in the SAC factor Cyclin B1 could be observed.

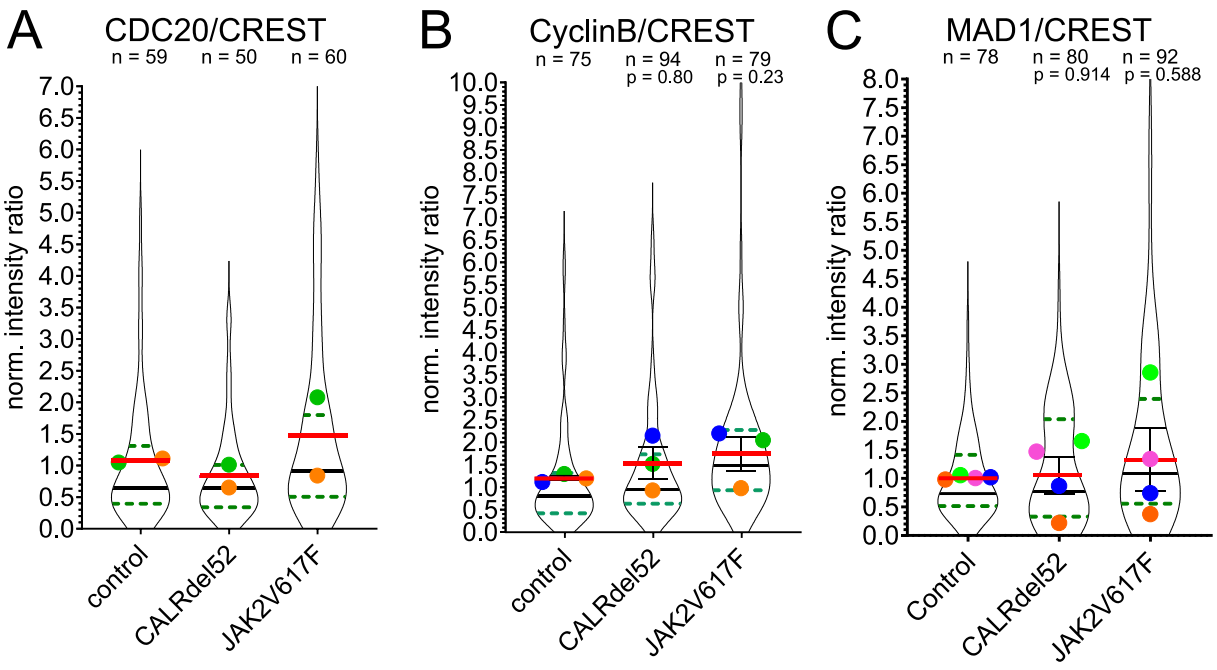

Figure 16: Effect of CALRdel52 and JAK2V617F mutation on recruitment of SAC factors: A-C) Superplots of the quantitative immunofluorescence from control, CALRdel52 or JAK2V617F transduced 32D^{MPL} cells stably expressing H2B-mCherry, after 200 ng/ml nocodazole arrest show the normalised intensity ratio between the SAC factors and the CREST. The violin-shaped structure represents the distribution of all individual measurements and the number of these measurements is shown above each graph (n = 50 - 92). The mean values of the individual experiments are shown as coloured dots [n = 2 - 3]. The red bar shows the mean value of all experiments and the black bars show the standard deviations. The horizontal black line indicates the median and the green dashed line the quartiles. (Two-tailed t-test)

The TF-1^{MPL} cells showed a less clear picture of the influence of the CALRdel52 and JAK2V617F mutations than the 32D^{MPL} cells, but there is a tendency to a dysregulation of the recruitment of the SAC-factors. As SAC is a very sensitive regulator and, many reactions take place in one region (reviewed in (Hayward et al. 2019)) even small changes can influence the function of the SAC. In addition, TF-1 cells in general show changes in karyotype and generally exhibit a high number of chromatin segregation errors [see experiment 3.3.1].

3.4 Effect of CALRdel52 and JAK2V617F on mitosis of non-haematopoietic cells

The prevailing working model explains how CALRdel52 and JAK2V617F mutations exert their main pathologic effect through the JAK-STAT pathway. For this, CALRdel52 needs the MPL receptor (Klampfl et al. 2013, Kagoya et al. 2014). Yet, it is unclear whether the changes I observed in mitosis occur via this pathway and/or by direct interaction with mitotic machinery, and whether the effects in 32D/TF-1 cells are generally transferable to non-hematopoietic cells.

To address this question, HeLa cells were transfected with the same CALRdel52 and JAK2V617F vectors as previously $32D^{MPL}$ and TF-1^{MPL} and additionally either with or without an MPL vector. However, after reiterated attempts, the transfection with the JAK2V617F vector could not be achieved [Figure 17 A].

Transfection with empty vector as well as with empty vector and CALRdel52 led to a similar mean mitotic time as with the non-transfected HeLa cells. When comparing the mitotic time after transfection with an empty vector and with CALRdel52, no significant change was observed, but a tendency towards a shorter mitotic time after transfection with CALRdel52. In contrast, when comparing transfection with empty vector and MPL with transfection with CALRdel52 and MPL, a tendency towards a longer mitotic time was observed [Figure 17 B].

The number of misaligned chromosomes was higher in all transfected HeLa cells than in the non-transfected HeLa cells. When comparing the empty vector and CALRdel52 as well as when comparing the two with additional MPL transfection, a similar average number of misaligned chromosomes was found between the two comparative transfections. In contrast, the number of chromosome bridges was lower in CALRdel52 as well as in CALRdel52 and MPL than in empty vector and empty vector with MPL.

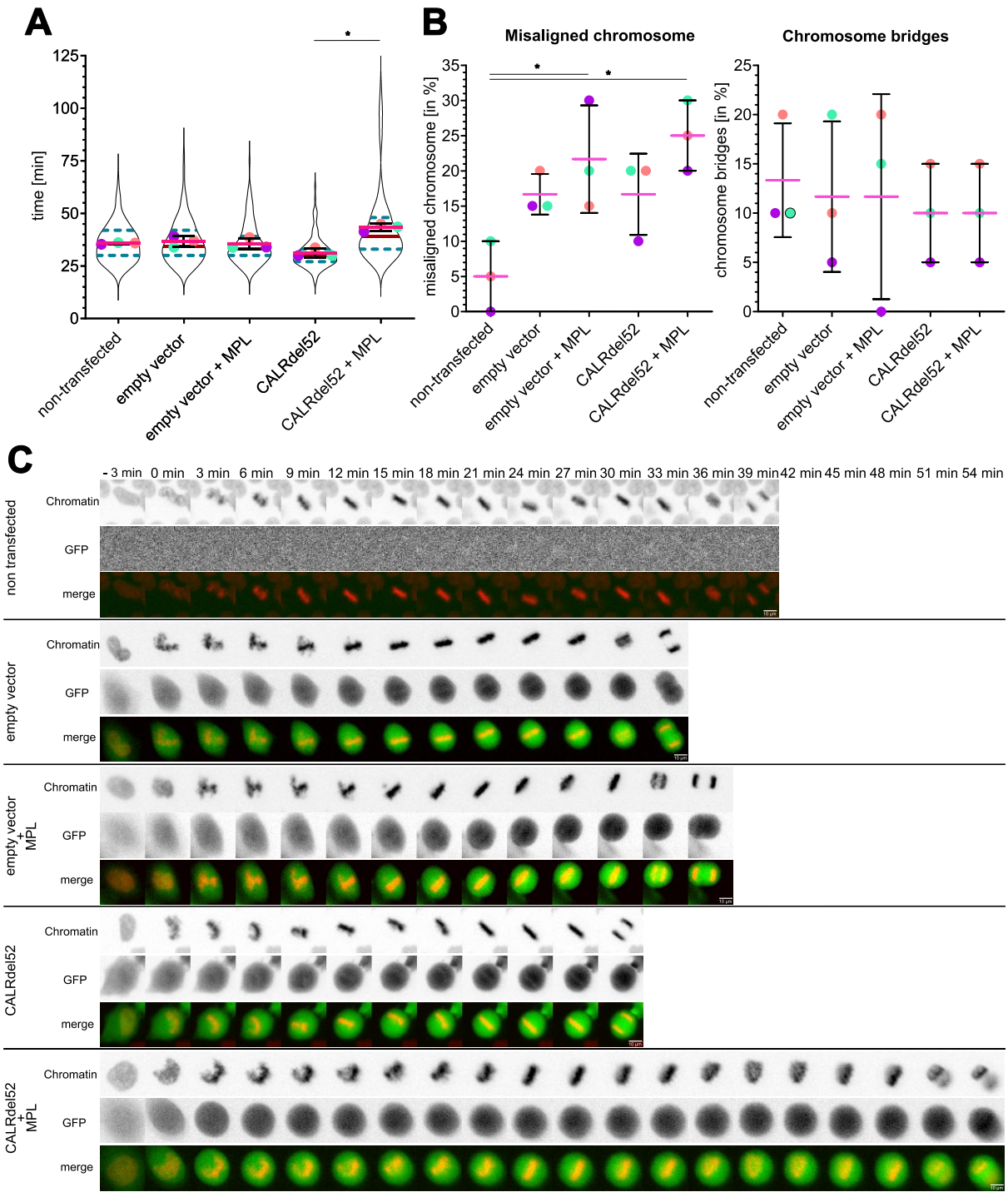

Figure 17: Mitotic time and mitotic errors of HeLa cells transduced with different vectors: A) The superplots show the mitotic timing of untreated HeLa cells and HeLa cells transduced with empty vector ± MPL and CALRdel52 ± MPL. The violin-shaped structure represents the distribution of all individual measurements (n = 99 - 120). The mean values of the individual experiments are shown as coloured dots [n = 3]. The pink bar shows the mean of all trials and the black bars show the standard deviations. The red line indicates the median and the blue dashed line the quartiles. The significands between the untreated control and all other conditions were analysed using one-way ANOVA (Kruskal-Wallis with Dunn´s post-test,

** p < 0.05, ** p < 0.01, *** p < 0.005, **** p < 0.001) B) The graph shows the percentage of mitotic errors of untreated HeLa cells and HeLa cells transduced with empty vector ± MPL and CALRdel52 ± MPL. The mean values of the individual experiments are shown as coloured dots [n = 3]. The pink bar shows the mean of all experiments and the black bars show the standard deviations. The significances between the untreated control and all other conditions were analysed by using Fisher´s exact test (* p < 0.05, ** p < 0.01, *** p < 0.005, **** p < 0.001) C) Example pictures of the mitotic timing after transfection of the individual vectors and non-transfection. The first row is the signal of H2B-mCherry (red in overlay), the second row is the signal of the EGPF (green in overlay) of the transfected vectors and the last row is the merge picture. The scale bar is 10 µm.*

In summary, a shortening of mitotic time was observed in HeLa cells after transfection with the CALRdel52 vector, whereas the mitotic time was prolonged when HeLa cells were co-transfected with CALRdel52 and MPL. This suggests that expression of the CALRdel52 mutation in non-haematopoietic cells, similar to TF-1^{MPL} cells, has a limited effect on mitotic time prolongation, both via the JAK-STAT signalling pathway and without this pathway. The lack of significant differences between the transfections with the empty vector and CALRdel52 concerning chromatin segregation defects could be because these are generally attributable to a toxic effect of the mouse plasmid used. However, it is more likely that the mitotic defects observed in haematopoietic cells are generally not transferable to non-haematopoietic cells.

4. Discussion

Philadelphia-negative (ph. neg.) MPNs rise due to different molecular defects caused by driver and bystander mutations. The characterisation of the most important canonical and non-canonical CALR and JAK signalling pathways in combination with the identification of driver mutations in JAK2, CALR, and MPL as well as bystander mutations provides a deeper insight into the pathogenesis of ph. neg. MPNs- However, little is known about how single mutations in haematopoietic stem and progenitor cells can lead to the development of aggressive diseases such as secondary AML (reviewed in (Greenfield et al. 2021)) or myelofibrosis (reviewed in (Vainchenker and Kralovics 2017)). There is evidence for an accumulation of an altered karyotype in the patients' cells already at diagnosis, which in turn indicates mitotic failure and would lead to a lower survival rate for patients. Nevertheless, the process of mitosis and chromosome segregation in ph. neg. MPN has not yet been studied in as much detail as in other corresponding diseases. My thesis addressed the question of whether CALRdel52 and JAK2V617F mutations perturb mitotic homeostasis, which could contribute to disease progression and phase transition from chronic to acute phase in ph. neg. MPN by promoting the formation of chromosome segregation defects.

When investigating the effects of CALRdel52 and JAK2V617F mutations on mitotic timing and chromatin segregation in murine 32D^{MPL} cells, both mutant cell lines showed an increased frequency of mitotic bridges, lagging chromosomes and micronuclei compared to the control cell line under stress conditions. Even a small increase in mitotic defects harms overall survival and can favour the formation of aneuploids and CIN, which promotes the development of tumours and their karyotype development (reviewed in (Simonetti et al. 2019)) as well as inflammation through activation of the cGAS-STING signalling pathway (Flynn et al. 2021). The massive genomic rearrangements caused by micronuclei-induced chromothripsis are a form of chromoanagenesis and the result of a single catastrophic event that favours carcinogenesis (Zhang et al. 2015). In a recently published paper Brierley et al. could show a link between chromothripsis and leukemic transformation in ph. neg. MPN (Brierley et al. 2023). In contrast to the findings in 32D^{MPL} cells, I found an overall high number of chromosome segregation errors in all three TF-1^{MPL} cell lines. This could be

because TF-1 cells have a highly rearranged hyper diploid karyotype (Winkelmann et al. 1995).

If mutations influence SAC activities, the first question that arises is the robustness of SAC activities against the influence of mutations. To this end, the formation of DNA double-strand breaks was stimulated in $32D^{MPL}$ cells using doxorubicin, and aneuploidy accumulation was induced using NMS-P715. This provoked the cells to undergo apoptosis. The results show that the CALRdel52 and JAK2V617F mutants in $32D^{MPL}$ cells lead to stress-sensitive and error-prone mitosis. This was characterised by an increased number of chromatin bridges, lagging chromosomes, and the appearance of micronuclei, raising the question of the influence of mutations in the SAC activity.

The activity of the SAC was tested by arresting the control and mutant cells of both $32D^{MPL}$ and TF-1^{MPL} cell lines with nocodazole and analysing how long it took the cells to escape from mitotic arrest. I observed that for both mutations the nocodazole-induced mitotic arrest was shortened compared to the control cells. This observation applies to both $32D^{MPL}$ and TF-1^{MPL} cells, suggesting that both mutations lead to a weakened or defective SAC (reviewed in (Brown and Geiger 2018)). When investigating cell fate after mitotic arrest, I found no difference between control cells and cells with CALRdel52 or JAK2V617F transduction in both $32D^{MPL}$ and TF-1^{MPL} cells, although they differed significantly in the duration of nocodazole-induced arrest time. This is consistent with observations in other cancer cells, e.g. Gascoigne and Taylor found no correlation between the length of mitotic arrest time and cell fate in 13 cancer lines (Gascoigne and Taylor 2008).

One reason for the observed weakening of the SAC could be an accelerated destruction of Cyclin B1 during mitosis. Cyclin B1 is an important regulatory protein that accumulates during G2 and early mitosis and is degraded after the SAC is satisfied. The premature degradation of Cyclin B1 during mitosis can be associated with a weakening of the SAC, whereas the expression of Cyclin B1 should be critical for cell fate after mitotic arrest. No difference in Cyclin B1 accumulation was observed in the Western Blot experiments between the control cells and the two mutant target lines, suggesting that mitotic arrest occurred timely in all the cases. Cyclin B1 levels subsequently decrease in the cell as they enter mitotic exit or escape the nocodazole-mediated-mitotic arrest (Choi et al. 2011). A detailed comparison of Cyclin B1

degradation between the control cell line and the mutant cell lines CALRdel52 and JAK2V617F shows a clear tendency towards faster Cyclin B1 degradation in the two mutant target lines. This indicates that the CALRdel52 and JAK2V617F mutant cells seem to have a defective SAC. To confirm this tendency, I performed cytometry experiments in which I was able to detect the time-dependent increase in Cyclin B1 degradation after nocodazole-induced mitotic arrest in the CALRdel52 and JAK2V617F cells. This suggests that one possible reason for the observed weakening of SAC by the mutations is the accelerated degradation of Cyclin B1. Since SAC is a tightly regulated process and an interplay of proteins, it is likely that the CALRdel52 and JAK2V617F mutations also affect other important SAC factors.

This raises the question of the influence of the mutations on the expression of certain SAC-relevant proteins, as it is known that the SAC factors BUBR1 and BUB1 are frequently downregulated in cells of AML patients (Schnerch et al. 2013). Reduced expression of BUB1, BUB3, BUBR1, and Mad2 is a hallmark of CML and leads to mitotic defects that result in CIN in mouse 32D cells (Wolanin et al. 2010). The expression levels of CDC20, MAD1, Cyclin B1, Aurora B, MAD2, BUBR1, MPS1, PP2A, and PLK1 from whole protein extracts were compared between 10 minutes and 18 hours of nocodazole-induced arrest. In the protein expression of the analysed critical SAC factors of the CALRdel52 and JAK2V617F expressing cells, I could not observe changes, except Cyclin B1. The changes in the expression level of cyclin B1 were consistent with previous studies on Cyclin B1 degradation after nocodazole-induced mitotic arrest. As no changes in the expression level of the other SAC factors have been found, the previously observed influence of CALRdel52 and JAK2V617F on the nocodazole-induced mitotic arrest could also be due to an influence on the localisation of the SAC factors or a dysregulation of the expression of SAC proteins in the regulatory cascade or mediated by a change in the activation status of these or other mitotic regulators such as CDK1, WEE1 and PP1.

Therefore, I focussed on the possibility that a defect in the SAC is due to inadequate recruitment of the SAC factors at their site of action. The SAC factors must be recruited to the unbound kinetochores in a balanced ratio, as an imbalance can lead to interruptions in the activation chain or defective phosphorylation (reviewed in (McAinsh and Kops 2023)). In my immunofluorescence experiments of kinetochore recruitment of SAC factors in mutant $32D^{MPL}$ cells, I found an imbalance of several SAC factors in

both mutant lines, consistent with expectations of a weakened SAC. It is striking that the upregulation of SAC factors occurred more frequently in CALRdel52 cells compared to the control cells, while downregulation of factors occurred mainly in JAK2V617F cells. This suggests that although the two mutations cause similar mitotic defects, the molecular mechanisms that mediate them are complex and different. In line with this, in my recently published work, we were also able to demonstrate an alteration in the mitotic regulatory network in cells from patients with ph. neg. MPN, revealing the correlation between defective SAC and the imbalance in the recruitment of SAC factors to kinetochores upon CALRdel52 and JAK2V617F expression, indicating that mitotic imbalance is a necessary prerequisite for the development of ph. neg. MPN (data not included in this thesis, (Holl et al. 2024)).

Are the observed effects with CALRdel52 and JAK2V617F generally transferable to non-haematopoietic cells and do they depend on the JAK-STAT signalling pathway? The fact that CALRdel52 can bind to MPL has already been shown in other studies (Chachoua et al. 2016), as has the link between the interaction of CALRdel52 with MPL and the development of MPN (Kotaro Shide et al. 2020). In experiments with HeLa cells, I observed an increase in mitotic time after transfection with CALRdel52 and the MPL receptor and a decrease in mitotic time in the absence of MPL. This indicates that CALRdel52 influences mitosis both independently and via the JAK-STAT signalling pathway. The fact that we have now also observed a change in mitosis time in non-haematopoietic cells supports our central hypothesis that CALRdel52 and JAK2V617F also influence chromatin segregation and thus promote chromatin segregation defects and that this may be dependent or independent of the JAK-STAT signalling pathway.

In summary, the data obtained in my studies show that CALRdel52 and JAK2V617F mutations disrupt the molecular control of mitosis in myeloid cells and lead to defects in chromatin segregation defects. This is likely due to impaired recruitment of various SAC factors.

Further research is needed to clarify more precisely the mechanism of action of CALRdel52 and JAK2V617F mutations on mitosis. In recent years, several research groups have uncovered a connection between chromosomal segregation errors and the activation of the cGAS-STING pathway. In cancer cells, the activation of cGAS-STING could trigger paracrine inflammatory processes (Harding et al. 2017,

Mackenzie et al. 2017, Flynn et al. 2021). Investigating the influence of chromosome segregation defects on the cGAS-STING signalling pathway could therefore lead to a better understanding of the inflammatory processes in ph. neg. MPN. However, performing these tests would exceed the time frame of this thesis.

Recent studies show that when the JAK2V617F driver mutation occurs at a young age, the likelihood of developing MPN later in life is increased due to genomic alterations (Williams et al. 2022). It is therefore plausible that even a small increase in chromatin segregation defects, as we observe, has pathologic potential after several mitotic divisions. This effect could be amplified by everyday environmental effects that favour the progression of MPN and a possible phase transition from chronic to acute. Further investigation on genetic factors and the influence of other environmental conditions is important to better understand the phase transition towards the acute form of the diseases and ultimately to be able to protect against it. This will contribute to a better overall treatment of the disease.

5. Outlook on further work

The present study demonstrated that chromatin segregation is disrupted in 32DMPL cells transduced with CALRdel52 and JAK2V617F. This results in a weakening of the SAC. This suggests that a phase transition from the chronic to the acute state in Philadelphia-negative MPNs is promoted through chromatin segregation errors in the cells. However, further research is required to elucidate the triggers of this phase transition and a number of other complex processes that need to be investigated within this field of research. In this study, $32D^{MPL}$ and TF-1^{MPL} cell models were used. However, the disease manifests itself in hematopoietic human stem and progenitor cells (HSPCs) and their lineages. The next possible step would be to investigate whether the previously mentioned changes can also be detected in the HSPCs. Particular attention should be paid to the following aspects: Mitotic timing, increase in chromosome segregation errors, changes in SAC integrity and kinetochore recruitment of SAC factors.

Despite my results, direct influence of CALRdel52 and JAK2V617F on the mitotic machinery cannot be completely ruled out. Therefore, a further point could be to find out whether CALRdel52 and JAK2V617F mutations localize on mitotic structures such as rod-shaped chromosomes, the centromeres, the kinetochores or the mitotic spindle.

Furthermore, phosphorylation during mitosis is of crucial importance (Moura and Conde 2019). The investigation of the phosphorylation status of SAC factors in CALRdel52 and JAK2V617F cells could provide information about the effects of the observed changes at the post-translational modification level. In addition, a possible change in the phosphorylation profile could lead to a possible target for drugs in the long term (Campos and Clemente-Blanco 2020).

As outlined at the beginning, chromatin segregation defects can result in activation of the cGAS-STING signalling pathway, leading to a general inflammatory response. At present, it is not possible to say whether cells with chromatin segregation defects induced by CALRdel52 and JAK2V617F are more susceptible to activate the cGAS-STING signalling pathway. The activation of the cGAS-STING signalling pathway and the inflammatory response it triggers are associated with tumour formation and metastasis (Flynn et al. 2021). It would therefore be of great interest to investigate

whether the CALRdel52 and JAK2V617F mutations can trigger a cGAS-STING-mediated inflammatory response and whether this can be reduced by certain drugs.

In addition to the research opportunities mentioned above, which are primarily concerned with the basic understanding of the effects of CALRdel52 and JAK2V617F mutations at the cellular level, it would also be of interest to investigate the effects of MPN treatments on mitosis in relation to CALRdel52 and JAK2V617F. There are currently several treatment options available that are used as therapy for various MPN diseases. One example is ruxolitinib (Gotoh 2022). There is still a considerable need for research into the effects on mitotic processes. It would also be interesting to investigate the effects of treatments in combination with anti-mitotic drugs.

With reference to the previous remarks, it can therefore be stated that there are still many questions in this area of research that have yet to be answered.

6. Bibliography

Aaltonen, K., Amini, R. M., Heikkila, P., Aittomaki, K., Tamminen, A., Nevanlinna, H. and Blomqvist, C. (2009). "High cyclin B1 expression is associated with poor survival in breast cancer." Br J Cancer **100**(7): 1055-1060.

Abrieu, A., Magnaghi-Jaulin, L., Castro, A., Kahana, J. A., Peter, M., Vigneron, S., Cleveland, D. W., Lorca, T. and Labbe, J.-C. (2001). "Mps1 Is a Kinetochore-Associated Kinase Essential for the Vertebrate Mitotic Checkpoint." Cell **106**: 83–93.

Alfieri, C., Chang, L. and Barford, D. (2018). "Mechanism for remodelling of the cell cycle checkpoint protein MAD2 by the ATPase TRIP13." Nature **559**(7713): 274-278.

Alfieri, C., Chang, L., Zhang, Z., Yang, J., Maslen, S., Skehel, M. and Barford, D. (2016). "Molecular basis of APC/C regulation by the spindle assembly checkpoint." Nature **536**(7617): 431-436.

Anna Maria Agliano, C. S., Ida Silvestri, Paola Gazzaniga, Laura Giuliani, Giuseppe Naso, and Luigi Frati (2000). "On chromosomal instability: what is the karyotype of your 32D Cl3 cell line?" Blood **95**.

Arber, D. A., Orazi, A., Hasserjian, R., Thiele, J., Borowitz, M. J., Le Beau, M. M., Bloomfield, C. D., Cazzola, M. and Vardiman, J. W. (2016). "The 2016 revision to the World Health Organization classification of myeloid neoplasms and acute leukemia." Blood **127**(20): 2391-2405.

Bakhoum, S. F. and Cantley, L. C. (2018). "The Multifaceted Role of Chromosomal Instability in Cancer and Its Microenvironment." Cell **174**(6): 1347-1360.

Baumeister, J., Chatain, N., Sofias, A. M., Lammers, T. and Koschmieder, S. (2021). "Progression of Myeloproliferative Neoplasms (MPN): Diagnostic and Therapeutic Perspectives." Cells **10**(12).

Beer, P. A., Campbell, P. J., Scott, L. M., Bench, A. J., Erber, W. N., Bareford, D., Wilkins, B. S., Reilly, J. T., Hasselbalch, H. C., Bowman, R., Wheatley, K., Buck, G., Harrison, C. N. and Green, A. R. (2008). "MPL mutations in myeloproliferative disorders: analysis of the PT-1 cohort." Blood **112**(1): 141-149.

Ben-David, U. and Amon, A. (2020). "Context is everything: aneuploidy in cancer." Nat Rev Genet **21**(1): 44-62.

Beskow, L. M. (2016). "Lessons from HeLa Cells: The Ethics and Policy of Biospecimens." Annu Rev Genomics Hum Genet **17**: 395-417.

Boyapati, A., Yan, M., Peterson, L. F., Biggs, J. R., Le Beau, M. M. and Zhang, D. E. (2007). "A leukemia fusion protein attenuates the spindle checkpoint and promotes aneuploidy." Blood **109**(9): 3963-3971.

Bretones, G., Delgado, M. D. and Leon, J. (2015). "Myc and cell cycle control." Biochim Biophys Acta **1849**(5): 506-516.

Brierley, C. K., Yip, B. H., Orlando, G., Goyal, H., Wen, S., Wen, J., Levine, M. F., Jakobsdottir, G. M., Rodriguez-Meira, A., Adamo, A., Bashton, M., Hamblin, A., Clark, S. A., O'Sullivan, J., Murphy, L., Olijnik, A. A., Cotton, A., Narina, S., Pruett-Miller, S. M., Enshaei, A., Harrison, C., Drummond, M., Knapper, S., Tefferi, A., Antony-Debre, I., Thongjuea, S., Wedge, D. C., Constantinescu, S., Papaemmanuil, E., Psaila, B., Crispino, J. D. and Mead, A. J. (2023). "Chromothripsis orchestrates leukemic transformation in blast phase MPN through targetable amplification of DYRK1A." bioRxiv.

Brito, D. A. and Rieder, C. L. (2006). "Mitotic checkpoint slippage in humans occurs via cyclin B destruction in the presence of an active checkpoint." Curr Biol **16**(12): 1194-1200.

Brown, A. and Geiger, H. (2018). "Chromosome integrity checkpoints in stem and progenitor cells: transitions upon differentiation, pathogenesis, and aging." Cell Mol Life Sci **75**(20): 3771-3779.

Bryder, D., Rossi, D. J. and Weissman, I. L. (2006). "Hematopoietic stem cells: the paradigmatic tissue-specific stem cell." Am J Pathol **169**(2): 338-346.

Burrell, R. A., McClelland, S. E., Endesfelder, D., Groth, P., Weller, M. C., Shaikh, N., Domingo, E., Kanu, N., Dewhurst, S. M., Gronroos, E., Chew, S. K., Rowan, A. J., Schenk, A., Sheffer, M., Howell, M., Kschischo, M., Behrens, A., Helleday, T., Bartek, J., Tomlinson, I. P. and Swanton, C. (2013). "Replication stress links structural and numerical cancer chromosomal instability." Nature **494**(7438): 492-496.

Campos, A. and Clemente-Blanco, A. (2020). "Cell Cycle and DNA Repair Regulation in the Damage Response: Protein Phosphatases Take Over the Reins." Int J Mol Sci **21**(2).

Carpenter, A. E., Jones, T. R., Lamprecht, M. R., Clarke, C., Kang, I. H., Friman, O., Guertin, D. A., Chang, J. H., Lindquist, R. A., Moffat, J., Golland, P. and Sabatini, D. M. (2006). "CellProfiler: image analysis software for identifying and quantifying cell phenotypes." Genome Biol **7**(10).

Chachoua, I., Pecquet, C., El-Khoury, M., Nivarthi, H., Albu, R. I., Marty, C., Gryshkova, V., Defour, J. P., Vertenoeil, G., Ngo, A., Koay, A., Raslova, H., Courtoy, P. J., Choong, M. L., Plo, I., Vainchenker, W., Kralovics, R. and Constantinescu, S. N. (2016). "Thrombopoietin receptor activation by myeloproliferative neoplasm associated calreticulin mutants." Blood **127**(10): 1325-1335.

Choi, H. J., Fukui, M. and Zhu, B. T. (2011). "Role of cyclin B1/Cdc2 up-regulation in the development of mitotic prometaphase arrest in human breast cancer cells treated with nocodazole." PLoS One **6**(8): e24312.

Colombo, R., Caldarelli, M., Mennecozzi, M., Giorgini, M. L., Sola, F., Cappella, P., Perrera, C., Depaolini, S. R., Rusconi, L., Cucchi, U., Avanzi, N., Bertrand, J. A., Bossi, R. T., Pesenti, E., Galvani, A., Isacchi, A., Colotta, F., Donati, D. and Moll, J. (2010). "Targeting the mitotic checkpoint for cancer therapy with NMS-P715, an inhibitor of MPS1 kinase." Cancer Res **70**(24): 10255-10264.

Coquelle, A., Mouhamad, S., Pequignot, M. O., Braun, T., Carvalho, G., Vivet, S., Metivier, D., Castedo, M. and Kroemer, G. (2006). "Enrichment of non-synchronized cells in the G1, S and G2 phases of the cell cycle for the study of apoptosis." Biochem Pharmacol **72**(11): 1396-1404.

Cumano, A. and Godin, I. (2007). "Ontogeny of the hematopoietic system." Annu Rev Immunol **25**: 745-785.

Czech, J., Cordua, S., Weinbergerova, B., Baumeister, J., Crepcia, A., Han, L., Maie, T., Costa, I. G., Denecke, B., Maurer, A., Schubert, C., Feldberg, K., Gezer, D., Brummendorf, T. H., Muller-Newen, G., Mayer, J., Racil, Z., Kubesova, B., Knudsen, T., Sorensen, A. L., Holmstrom, M., Kjaer, L., Skov, V., Larsen, T. S., Hasselbalch, H. C., Chatain, N. and Koschmieder, S. (2019). "JAK2V617F but not CALR mutations confer increased molecular responses to interferon-alpha via JAK1/STAT1 activation." Leukemia **33**(4): 995-1010.

De Antoni, A., Pearson, C. G., Cimini, D., Canman, J. C., Sala, V., Nezi, L., Mapelli, M., Sironi, L., Faretta, M., Salmon, E. D. and Musacchio, A. (2005). "The Mad1/Mad2 complex as a template for Mad2 activation in the spindle assembly checkpoint." Curr Biol **15**(3): 214-225.

de Regt, A. K., Clark, C. J., Asbury, C. L. and Biggins, S. (2022). "Tension can directly suppress Aurora B kinase-triggered release of kinetochore-microtubule attachments." Nat Commun **13**(1).

Dou, Z., Prifti, D. K., Gui, P., Liu, X., Elowe, S. and Yao, X. (2019). "Recent Progress on the Localization of the Spindle Assembly Checkpoint Machinery to Kinetochores." Cells **8**(3).

Fenech, M., Kirsch-Volders, M., Natarajan, A. T., Surralles, J., Crott, J. W., Parry, J., Norppa, H., Eastmond, D. A., Tucker, J. D. and Thomas, P. (2011). "Molecular mechanisms of micronucleus, nucleoplasmic bridge and nuclear bud formation in mammalian and human cells." Mutagenesis **26**(1): 125-132.

Flynn, P. J., Koch, P. D. and Mitchison, T. J. (2021). "Chromatin bridges, not micronuclei, activate cGAS after drug-induced mitotic errors in human cells." Proc Natl Acad Sci U S A **118**(48).

Forrest, R. A., Swift, L. P., Rephaeli, A., Nudelman, A., Kimura, K., Phillips, D. R. and Cutts, S. M. (2012). "Activation of DNA damage response pathways as a consequence of anthracycline-DNA adduct formation." Biochem Pharmacol **83**(12): 1602-1612.

Gascoigne, K. E. and Taylor, S. S. (2008). "Cancer cells display profound intra- and interline variation following prolonged exposure to antimitotic drugs." Cancer Cell **14**(2): 111-122.

Ghelli Luserna di Rora, A., Martinelli, G. and Simonetti, G. (2019). "The balance between mitotic death and mitotic slippage in acute leukemia: a new therapeutic window?" J Hematol Oncol **12**(1): 123.

Gotoh, A. (2022). "Philadelphia chromosome-negative myeloproliferative neoplasms: clinical aspects and treatment options." Int J Hematol **115**(5): 616-618.

Greenfield, G., McMullin, M. F. and Mills, K. (2021). "Molecular pathogenesis of the myeloproliferative neoplasms." J Hematol Oncol **14**(1): 103.

Guijarro-Hernández, A. and Vizmanos, J. L. (2021). "A Broad Overview of Signaling in Ph-Negative Classic Myeloproliferative Neoplasms." Cancers **13**(5).

Han, L., Schubert, C., Kohler, J., Schemionek, M., Isfort, S., Brummendorf, T. H., Koschmieder, S. and Chatain, N. (2016). "Calreticulin-mutant proteins induce megakaryocytic signaling to transform hematopoietic cells and undergo accelerated degradation and Golgi-mediated secretion." J Hematol Oncol **9**(1).

Hanahan, D. and Weinberg, R. A. (2011). "Hallmarks of cancer: the next generation." Cell **144**(5): 646-674.

Harding, S. M., Benci, J. L., Irianto, J., Discher, D. E., Minn, A. J. and Greenberg, R. A. (2017). "Mitotic progression following DNA damage enables pattern recognition within micronuclei." Nature **548**(7668): 466-470.

Hawdon, A., Aberkane, A. and Zenker, J. (2021). "Microtubule-dependent subcellular organisation of pluripotent cells." Development **148**(20).

Hayward, D., Alfonso-Perez, T., Cundell, M. J., Hopkins, M., Holder, J., Bancroft, J., Hutter, L. H., Novak, B., Barr, F. A. and Gruneberg, U. (2019). "CDK1-CCNB1 creates a spindle checkpoint-permissive state by enabling MPS1 kinetochore localization." J Cell Biol **218**(4): 1182-1199.

Hayward, D., Alfonso-Perez, T. and Gruneberg, U. (2019). "Orchestration of the spindle assembly checkpoint by CDK1-cyclin B1." FEBS Lett **593**(20): 2889-2907.

Held, M., Schmitz, M. H., Fischer, B., Walter, T., Neumann, B., Olma, M. H., Peter, M., Ellenberg, J. and Gerlich, D. W. (2010). "CellCognition: time-resolved phenotype annotation in high-throughput live cell imaging." Nat Methods **7**(9): 747-754.

Herting, F., Friess, T., Bader, S., Muth, G., Holzlwimmer, G., Rieder, N., Umana, P. and Klein, C. (2014). "Enhanced anti-tumor activity of the glycoengineered type II CD20 antibody obinutuzumab (GA101) in combination with chemotherapy in xenograft models of human lymphoma." Leuk Lymphoma **55**(9): 2151-2160.

Hintzsche, H., Montag, G. and Stopper, H. (2018). "Induction of micronuclei by four cytostatic compounds in human hematopoietic stem cells and human lymphoblastoid TK6 cells." Sci Rep **8**(1).

Hoffman, D. B., Pearson, C. G., Yen, T. J. and Salmon, E. D. (2001). "Microtubule-dependent Changes in Assembly of Microtubule Motor Proteins and Mitotic Spindle Checkpoint Proteins at PtK1 Kinetochores." Molecular Biology of the Cell **12**: 1995 - 2009.

Holl, K., Chatain, N., Krapp, S., Baumeister, J., Maie, T., Schmitz, S., Scheufen, A., Brock, N., Koschmieder, S. and Moreno-Andres, D. (2024). "Calreticulin and JAK2V617F driver mutations induce distinct mitotic defects in myeloproliferative neoplasms." Sci Rep **14**(1): 2810.

Hu, X., Li, J., Fu, M., Zhao, X. and Wang, W. (2021). "The JAK/STAT signaling pathway: from bench to clinic." Signal Transduct Target Ther **6**(1).

Huang, H. C., Shi, J., Orth, J. D. and Mitchison, T. J. (2009). "Evidence that mitotic exit is a better cancer therapeutic target than spindle assembly." Cancer Cell **16**(4): 347-358.

Ji, Z., Gao, H. and Yu, H. (2015). "Kinetochore attachment sensed by competitive Mps1 and microtubule binding to Ndc80C." Science **348**: 1260-1264.

Jiang, H. and Chan, Y. W. (2024). "Chromatin bridges: stochastic breakage or regulated resolution?" Trends Genet **40**(1): 69-82.

Jonkman, J., Brown, C. M., Wright, G. D., Anderson, K. I. and North, A. J. (2020). "Tutorial: guidance for quantitative confocal microscopy." Nat Protoc **15**(5): 1585-1611.

Kagoya, Y., Yoshimi, A., Tsuruta-Kishino, T., Arai, S., Satoh, T., Akira, S. and Kurokawa, M. (2014). "JAK2V617F+ myeloproliferative neoplasm clones evoke paracrine DNA damage to adjacent normal cells through secretion of lipocalin-2." Blood **124**(19): 2996-3006.

Kantarjian, H., Thomas, D., O'Brien, S., Cortes, J., Giles, F., Jeha, S., Bueso-Ramos, C. E., Pierce, S., Shan, J., Koller, C., Beran, M., Keating, M. and Freireich, E. J. (2004). "Long-term follow-up results of hyperfractionated cyclophosphamide, vincristine, doxorubicin, and dexamethasone (Hyper-CVAD), a dose-intensive regimen, in adult acute lymphocytic leukemia." Cancer **101**(12): 2788-2801.

Kirschner, M., Bornemann, A., Schubert, C., Gezer, D., Kricheldorf, K., Isfort, S., Brummendorf, T. H., Schemionek, M., Chatain, N., Skorski, T. and Koschmieder, S. (2019). "Transcriptional alteration of DNA repair genes in Philadelphia chromosome negative myeloproliferative neoplasms." Ann Hematol **98**(12): 2703-2709.

Klampfl, T., Gisslinger, H., Harutyunyan, A. S., Nivarthi, H., Rumi, E., Milosevic, J. D., Them, N. C., Berg, T., Gisslinger, B., Pietra, D., Chen, D., Vladimer, G. I., Bagienski, K., Milanesi, C., Casetti, I. C., Sant'Antonio, E., Ferretti, V., Elena, C., Schischlik, F., Cleary, C., Six, M., Schalling, M., Schonegger, A., Bock, C., Malcovati, L., Pascutto, C., Superti-Furga, G., Cazzola, M. and Kralovics, R. (2013). "Somatic mutations of calreticulin in myeloproliferative neoplasms." N Engl J Med **369**(25): 2379-2390.

Kotaro Shide, Kazuhiko Ikeda, Akuro Kameda, Masaaki Sekine, Goro Sashida, Yako Kamiunten, Keiichi Akizuki, Oshinori Ozono, Kenichi Nakamura, Kazuya Shimoda, Kenji

Nagata, Takako Yokomizo-Nakano, Sho Kubota, Masaya Ono, Tomonori Hidaka and Kubuki, Y. (2020). "Calreticulin haploinsufficiency augments stem cell activity and is required for onset of myeloproliferative neoplasms in mice." Blood.

Kucinski, I., Campos, J., Barile, M., Severi, F., Bohin, N., Moreira, P. N., Allen, L., Lawson, H., Haltalli, M. L. R., Kinston, S. J., O'Carroll, D., Kranc, K. R. and Gottgens, B. (2023). "A time- and single-cell-resolved model of murine bone marrow hematopoiesis." Cell Stem Cell.

Langabeer, S. E. (2016). "Chasing down the triple-negative myeloproliferative neoplasms: Implications for molecular diagnostics." JAKSTAT **5**(2-4): e1248011.

Lee, P. Y., Costumbrado, J., Hsu, C. Y. and Kim, Y. H. (2012). "Agarose gel electrophoresis for the separation of DNA fragments." J Vis Exp(62).

Levine, R. L., Wadleigh, M., Cools, J., Ebert, B. L., Wernig, G., Huntly, B. J., Boggon, T. J., Wlodarska, I., Clark, J. J., Moore, S., Adelsperger, J., Koo, S., Lee, J. C., Gabriel, S., Mercher, T., D'Andrea, A., Frohling, S., Dohner, K., Marynen, P., Vandenberghe, P., Mesa, R. A., Tefferi, A., Griffin, J. D., Eck, M. J., Sellers, W. R., Meyerson, M., Golub, T. R., Lee, S. J. and Gilliland, D. G. (2005). "Activating mutation in the tyrosine kinase JAK2 in polycythemia vera, essential thrombocythemia, and myeloid metaplasia with myelofibrosis." Cancer Cell **7**(4): 387-397.

Ligasova, A., Frydrych, I. and Koberna, K. (2023). "Basic Methods of Cell Cycle Analysis." Int J Mol Sci **24**(4).

Lin, S. F., Lin, P. M., Yang, M. C., Liu, T. C., Chang, J. G., Sue, Y. C. and Chen, T. P. (2002). "Expression of hBUB1 in acute myeloid leukemia." Leuk Lymphoma **43**(2): 385-391.

Lo, A. W., Sprung, C. N., Fouladi, B., Pedram, M., Sabatier, L., Ricoul, M., Reynolds, G. E. and Murnane, J. P. (2002). "Chromosome instability as a result of double-strand breaks near telomeres in mouse embryonic stem cells." Mol Cell Biol **22**(13): 4836-4850.

Lok, T. M., Wang, Y., Xu, W. K., Xie, S., Ma, H. T. and Poon, R. Y. C. (2020). "Mitotic slippage is determined by p31(comet) and the weakening of the spindle-assembly checkpoint." Oncogene **39**(13): 2819-2834.

Mackenzie, K. J., Carroll, P., Martin, C. A., Murina, O., Fluteau, A., Simpson, D. J., Olova, N., Sutcliffe, H., Rainger, J. K., Leitch, A., Osborn, R. T., Wheeler, A. P., Nowotny, M., Gilbert, N., Chandra, T., Reijns, M. A. M. and Jackson, A. P. (2017). "cGAS surveillance of micronuclei links genome instability to innate immunity." Nature **548**(7668): 461-465.

Magalska, A., Schellhaus, A. K., Moreno-Andres, D., Zanini, F., Schooley, A., Sachdev, R., Schwarz, H., Madlung, J. and Antonin, W. (2014). "RuvB-like ATPases function in chromatin decondensation at the end of mitosis." Dev Cell **31**(3): 305-318.

Marneth, A. E. and Mullally, A. (2020). "The Molecular Genetics of Myeloproliferative Neoplasms." Cold Spring Harb Perspect Med **10**(2).

Martinez-Balbás, M. A., Dey, A., Rabindran, S. K., Ozato, K. and Wu, C. (1995). "Displacement of Sequence-Specific Transcription Factors from Mitotic Chromatin." Cell **83**: 29-38.

McAinsh, A. D. and Kops, G. (2023). "Principles and dynamics of spindle assembly checkpoint signalling." Nat Rev Mol Cell Biol **24**(8): 543-559.

McCLINTOCK, B. (1941). "THE STABILITY OF BROKEN ENDS OF CHROMOSOMES IN ZEA MAYS." GENETIC **26**.

Mierzwa, B. and Gerlich, D. W. (2014). "Cytokinetic abscission: molecular mechanisms and temporal control." Dev Cell **31**(5): 525-538.

Milosevic Feenstra, J. D., Nivarthi, H., Gisslinger, H., Leroy, E., Rumi, E., Chachoua, I., Bagienski, K., Kubesova, B., Pietra, D., Gisslinger, B., Milanesi, C., Jager, R., Chen, D., Berg, T., Schalling, M., Schuster, M., Bock, C., Constantinescu, S. N., Cazzola, M. and Kralovics, R. (2016). "Whole-exome sequencing identifies novel MPL and JAK2 mutations in triple-negative myeloproliferative neoplasms." Blood **127**(3): 325-332.

Mora-Bermudez, F., Gerlich, D. and Ellenberg, J. (2007). "Maximal chromosome compaction occurs by axial shortening in anaphase and depends on Aurora kinase." Nat Cell Biol **9**(7): 822-831.

Moreno-Andres, D., Holl, K. and Antonin, W. (2023). "The second half of mitosis and its implications in cancer biology." Semin Cancer Biol **88**: 1-17.

Moura, M. and Conde, C. (2019). "Phosphatases in Mitosis: Roles and Regulation." Biomolecules **9**(2).

Nangalia, J., Massie, C. E., Baxter, E. J., Nice, F. L., Gundem, G., Wedge, D. C., Avezov, E., Li, J., Kollmann, K., Kent, D. G., Aziz, A., Godfrey, A. L., Hinton, J., Martincorena, I., Van Loo, P., Jones, A. V., Guglielmelli, P., Tarpey, P., Harding, H. P., Fitzpatrick, J. D., Goudie, C. T., Ortmann, C. A., Loughran, S. J., Raine, K., Jones, D. R., Butler, A. P., Teague, J. W., O'Meara, S., McLaren, S., Bianchi, M., Silber, Y., Dimitropoulou, D., Bloxham, D., Mudie, L., Maddison, M., Robinson, B., Keohane, C., Maclean, C., Hill, K., Orchard, K., Tauro, S., Du, M. Q., Greaves, M., Bowen, D., Huntly, B. J. P., Harrison, C. N., Cross, N. C. P., Ron, D., Vannucchi, A. M., Papaemmanuil, E., Campbell, P. J. and Green, A. R. (2013). "Somatic CALR mutations in myeloproliferative neoplasms with nonmutated JAK2." N Engl J Med **369**(25): 2391-2405.

Nervi, B., Link, D. C. and DiPersio, J. F. (2006). "Cytokines and hematopoietic stem cell mobilization." J Cell Biochem **99**(3): 690-705.

Nunes, V. and Ferreira, J. G. (2021). "From the cytoskeleton to the nucleus: An integrated view on early spindle assembly." Semin Cell Dev Biol **117**: 42-51.

Nunez, R. (2001). "DNA Measurement and Cell Cycle Analysis by Flow Cytometry." Curr. Issues Mol. Biol. **3**: 67-70.

O'Toole, E. T., McDonald, K. L., Mantler, J., McIntosh, J. R., Hyman, A. A. and Muller-Reichert, T. (2003). "Morphologically distinct microtubule ends in the mitotic centrosome of Caenorhabditis elegans." J Cell Biol **163**(3): 451-456.

Olschok, K., Altenburg, B., de Toledo, M. A. S., Maurer, A., Abels, A., Beier, F., Gezer, D., Isfort, S., Paeschke, K., Brümmendorf, T. H., Zenke, M., Chatain, N. and Koschmieder, S. (2023). "The telomerase inhibitor imetelstat differentially targets JAK2V617F versus CALR mutant myeloproliferative neoplasm cells and inhibits JAK-STAT signaling." Frontiers in Oncology **13**.

Pampalona, J., Roscioli, E., Silkworth, W. T., Bowden, B., Genesca, A., Tusell, L. and Cimini, D. (2016). "Chromosome Bridges Maintain Kinetochore-Microtubule Attachment throughout Mitosis and Rarely Break during Anaphase." PLoS One **11**(1): e0147420.

Pandey, G., Kuykendall, A. T. and Reuther, G. W. (2022). "JAK2 inhibitor persistence in MPN: uncovering a central role of ERK activation." Blood Cancer J **12**(1).

Patt, H. M. and Quastler, H. (1963). "Radiation effects on cell renewal and related systems." Physiol Rev **43**: 357-396.

Piltti, K. M., Cummings, B. J., Carta, K., Manughian-Peter, A., Worne, C. L., Singh, K., Ong, D., Maksymyuk, Y., Khine, M. and Anderson, A. J. (2018). "Live-cell time-lapse imaging and single-cell tracking of in vitro cultured neural stem cells - Tools for analyzing dynamics of cell cycle, migration, and lineage selection." Methods **133**: 81-90.

Pizzi, M., Croci, G. A., Ruggeri, M., Tabano, S., Dei Tos, A. P., Sabattini, E. and Gianelli, U. (2021). "The Classification of Myeloproliferative Neoplasms: Rationale, Historical Background and Future Perspectives with Focus on Unclassifiable Cases." Cancers (Basel) **13**(22).

Potapova, T. and Gorbsky, G. J. (2017). "The Consequences of Chromosome Segregation Errors in Mitosis and Meiosis." Biology (Basel) **6**(1).

Primorac, I., Weir, J. R., Chiroli, E., Gross, F., Hoffmann, I., van Gerwen, S., Ciliberto, A. and Musacchio, A. (2013). "Bub3 reads phosphorylated MELT repeats to promote spindle assembly checkpoint signaling." Elife.

Reddy, S. K., Rape, M., Margansky, W. A. and Kirschner, M. W. (2007). "Ubiquitination by the anaphase-promoting complex drives spindle checkpoint inactivation." Nature **446**(7138): 921-925.

Saurin, A. T., van der Waal, M. S., Medema, R. H., Lens, S. M. and Kops, G. J. (2011). "Aurora B potentiates Mps1 activation to ensure rapid checkpoint establishment at the onset of mitosis." Nat Commun **2**: 1 - 9.

Schindelin, J., Arganda-Carreras, I., Frise, E., Kaynig, V., Longair, M., Pietzsch, T., Preibisch, S., Rueden, C., Saalfeld, S., Schmid, B., Tinevez, J. Y., White, D. J., Hartenstein,

V., Eliceiri, K., Tomancak, P. and Cardona, A. (2012). "Fiji: an open-source platform for biological-image analysis." Nat Methods **9**(7): 676-682.

Schnerch, D., Schmidts, A., Follo, M., Udi, J., Felthaus, J., Pfeifer, D., Engelhardt, M. and Wasch, R. (2013). "BubR1 is frequently repressed in acute myeloid leukemia and its re-expression sensitizes cells to antimitotic therapy." Haematologica **98**(12): 1886-1895.

Schnerch, D., Yalcintepe, J., Schmidts, A., Becker, H., Follo, M., Engelhardt, M. and Wäsch, R. (2012). "cell cycle control in acute myeloid leukemia." American Journal of Cancer Research: 508-528.

Schooley, A., Moreno-Andres, D., De Magistris, P., Vollmer, B. and Antonin, W. (2015). "The lysine demethylase LSD1 is required for nuclear envelope formation at the end of mitosis." J Cell Sci **128**(18): 3466-3477.

Score, J., Calasanz, M. J., Ottman, O., Pane, F., Yeh, R. F., Sobrinho-Simões, M. A., Kreil, S., Ward, D., Hidalgo-Curtis, C., Melo, J. V., Wiemels, J., Nadel, B., Cross, N. C. P. and Grand, F. H. (2010). "Analysis of genomic breakpoints in p190 and p210 BCR–ABL indicate distinct mechanisms of formation." Leukemia **24**(10): 1742-1750.

Scott, L. M., Tong, W., Levine, R. L., Scott, M. A., Beer, P. A., Stratton, M. R., Futreal, P. A., Erber, W. N., McMullin, M. F., Harrison, C. N., Warren, A. J., Gilliland, D. G., Lodish, H. F. and and Green, A. R. (2007). "JAK2 Exon 12 Mutations in Polycythemia Vera and Idiopathic Erythrocytosis." The new england journal of medicine **356**: 459 - 468.

Simonetti, G., Bruno, S., Padella, A., Tenti, E. and Martinelli, G. (2019). "Aneuploidy: Cancer strength or vulnerability?" Int J Cancer **144**(1): 8-25.

Simovic, M. and Ernst, A. (2022). "Chromothripsis, DNA repair and checkpoints defects." Semin Cell Dev Biol **123**: 110-114.

Staal, F. J. and Clevers, H. C. (2005). "WNT signalling and haematopoiesis: a WNT-WNT situation." Nat Rev Immunol **5**(1): 21-30.

Sun, Z., Zhou, D., Yang, J. and Zhang, D. (2022). "Doxorubicin promotes breast cancer cell migration and invasion via DCAF13." FEBS Open Bio **12**(1): 221-230.

Tefferi, A., Guglielmelli, P., Larson, D. R., Finke, C., Wassie, E. A., Pieri, L., Gangat, N., Fjerza, R., Belachew, A. A., Lasho, T. L., Ketterling, R. P., Hanson, C. A., Rambaldi, A., Finazzi, G., Thiele, J., Barbui, T., Pardanani, A. and Vannucchi, A. M. (2014). "Long-term survival and blast transformation in molecularly annotated essential thrombocythemia, polycythemia vera, and myelofibrosis." Blood **124**(16): 2507-2513.

Thompson, S. L. and Compton, D. A. (2011). "Chromosome missegregation in human cells arises through specific types of kinetochore-microtubule attachment errors." Proc Natl Acad Sci U S A **108**(44): 17974-17978.

Tie, L., Xiao, H., Wu, D. L., Yang, Y. and Wang, P. (2021). "A brief guide to good practices in pharmacological experiments: Western blotting." Acta Pharmacol Sin **42**(7): 1015-1017.

Vagnarelli, P. (2021). "Back to the new beginning: Mitotic exit in space and time." Semin Cell Dev Biol **117**: 140-148.

Vainchenker, W. and Kralovics, R. (2017). "Genetic basis and molecular pathophysiology of classical myeloproliferative neoplasms." Blood **129**(6): 667-679.

Visintin, R., Prinz, S. and Amon, A. (1997). "CDC20 and CDHI: A Family of Substrate-Specific Activators of APC-dependent Proteolysis." Science **Vol 278**: 460 - 463.

Voorhees, J. J., Duell, E. A., Chambers, D. A. and Marcelo, C. L. (1976). "Regulation of cell cycles." J Invest Dermatol **67**(1): 15-19.

Waenphimai, O., Mahalapbutr, P., Vaeteewoottacharn, K., Wongkham, S. and Sawanyawisuth, K. (2022). "Multiple actions of NMS-P715, the monopolar spindle 1 (MPS1) mitotic checkpoint inhibitor in liver fluke-associated cholangiocarcinoma cells." Eur J Pharmacol **922**.

Weaver, B. A. and Cleveland, D. W. (2005). "Decoding the links between mitosis, cancer, and chemotherapy: The mitotic checkpoint, adaptation, and cell death." Cancer Cell **8**(1): 7-12.

Wilhelm, T., Olziersky, A. M., Harry, D., De Sousa, F., Vassal, H., Eskat, A. and Meraldi, P. (2019). "Mild replication stress causes chromosome mis-segregation via premature centriole disengagement." Nat Commun **10**(1).

Wilhelm, T., Said, M. and Naim, V. (2020). "DNA Replication Stress and Chromosomal Instability: Dangerous Liaisons." Genes (Basel) **11**(6).

Williams, N., Lee, J., Mitchell, E., Moore, L., Baxter, E. J., Hewinson, J., Dawson, K. J., Menzies, A., Godfrey, A. L., Green, A. R., Campbell, P. J. and Nangalia, J. (2022). "Life histories of myeloproliferative neoplasms inferred from phylogenies." Nature **602**(7895): 162-168.

Winkelmann, J. C., Ward, J., Mayeux, P., Lacombe, C., Schimmenti, L. and Jenkins, R. B. (1995). "A translocated erythropoietin receptor gene in a human erythroleukemia cell line (TF-1) expresses an abnormal transcript and a truncated protein." Blood **85**(1): 179-185.

Wolanin, K., Magalska, A., Kusio-Kobialka, M., Podszywalow-Bartnicka, P., Vejda, S., McKenna, S. L., Mosieniak, G., Sikora, E. and Piwocka, K. (2010). "Expression of oncogenic kinase Bcr-Abl impairs mitotic checkpoint and promotes aberrant divisions and resistance to microtubule-targeting agents." Mol Cancer Ther **9**(5): 1328-1338.

Yamada, H. Y. and Gorbsky, G. J. (2006). "Spindle checkpoint function and cellular sensitivity to antimitotic drugs." Mol Cancer Ther **5**(12): 2963-2969.

Zhang, C. Z., Spektor, A., Cornils, H., Francis, J. M., Jackson, E. K., Liu, S., Meyerson, M. and Pellman, D. (2015). "Chromothripsis from DNA damage in micronuclei." Nature **522**(7555): 179-184.

Zjablovskaja, P., Danek, P., Kardosova, M. and Alberich-Jorda, M. (2018). "Proliferation and Differentiation of Murine Myeloid Precursor 32D/G-CSF-R Cells." J Vis Exp(132).

7. Appendix

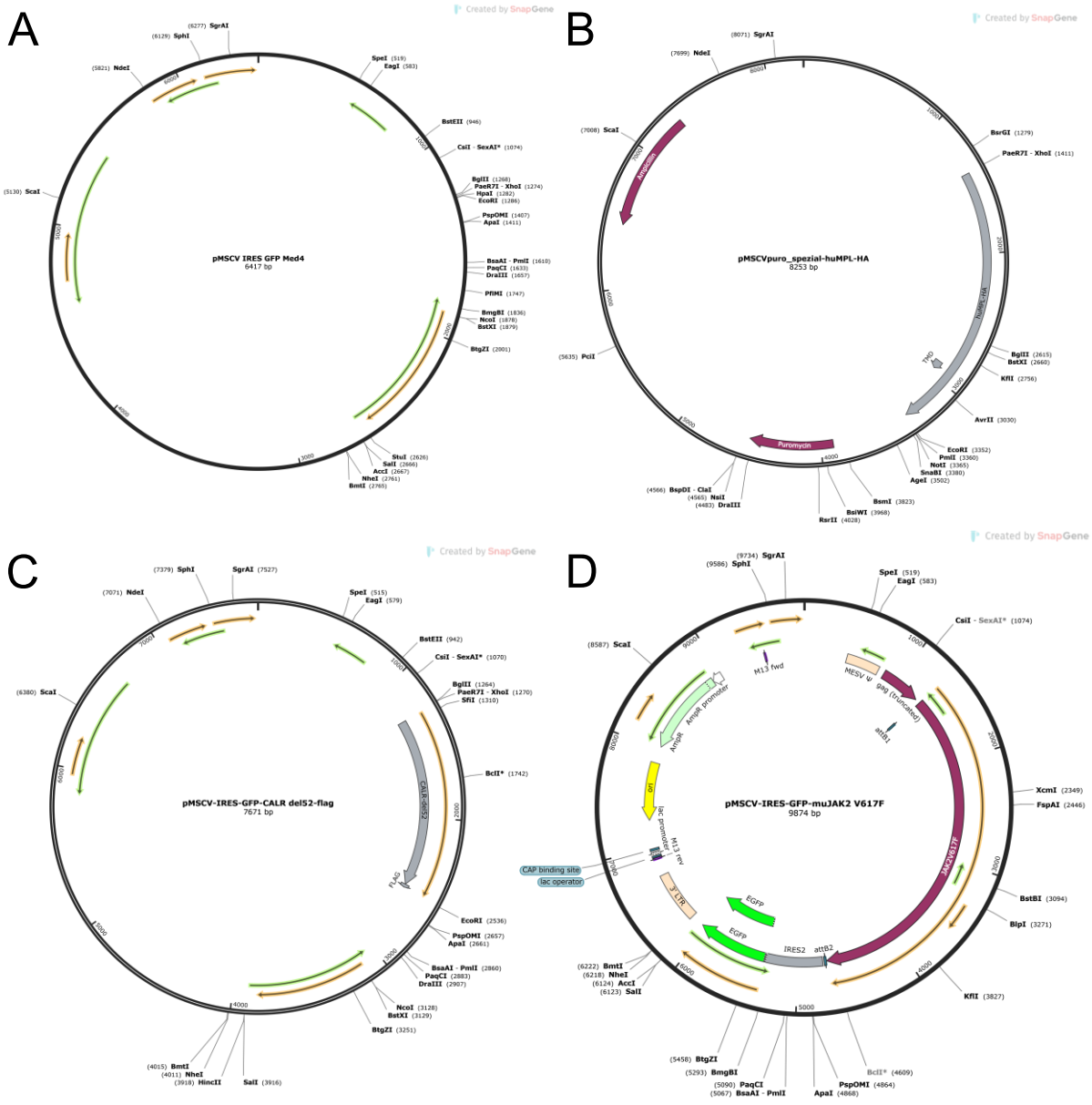

Supplemental Figure 18: vector sheets for transfection and transduction

Supplemental Table 9: Raw compression of Cyclin B1 / GAPDH between 0 h and 3h of nocodazole incubation

		0h	3h
control	**Exp 1**	0,94	0,89
	Exp 2	0,76	1,04
	Exp 3	1,01	1,35
	Exp 4	0,88	1,09
CALRdel52	**Exp 1**	0,85	1,10
	Exp 2	1,17	1,14
	Exp 3	0,56	0,63
	Exp 4	0,27	0,57
JAK2V617F	**Exp 1**	1,12	1,08
	Exp 2	1,18	0,96
	Exp 3	1,67	1,93
	Exp 4	0,39	0,73

Supplemental Table 10: Results of the Cyclin B1 time course experiments

		3h	6h	9h	12h	15h	18h
control	**Exp 1**	1,00	1,11	1,20	1,12	1,18	1,15
	Exp 2	1,00	0,92	0,98	1,03	0,97	0,44
	Exp 3	1,00	0,73	0,65	0,36	0,18	0,13
	Exp 4	1,00	0,93	0,91	0,54	0,36	0,18
CALRdel52	**Exp 1**	1,00	0,96	0,89	0,83	0,89	0,46
	Exp 2	1,00	0,72	0,59	0,51	0,45	0,46
	Exp 3	1,00	1,27	0,87	0,43	0,24	0,17
	Exp 4	1,00	0,69	0,69	0,44	0,32	0,30
JAK2V617F	**Exp 1**	1,00	1,13	1,13	0,73	0,84	0,68
	Exp 2	1,00	0,69	0,64	0,71	0,69	0,46
	Exp 3	1,00	0,58	0,61	0,34	0,26	0,12
	Exp 4	1,00	1,16	1,16	0,88	0,49	0,84

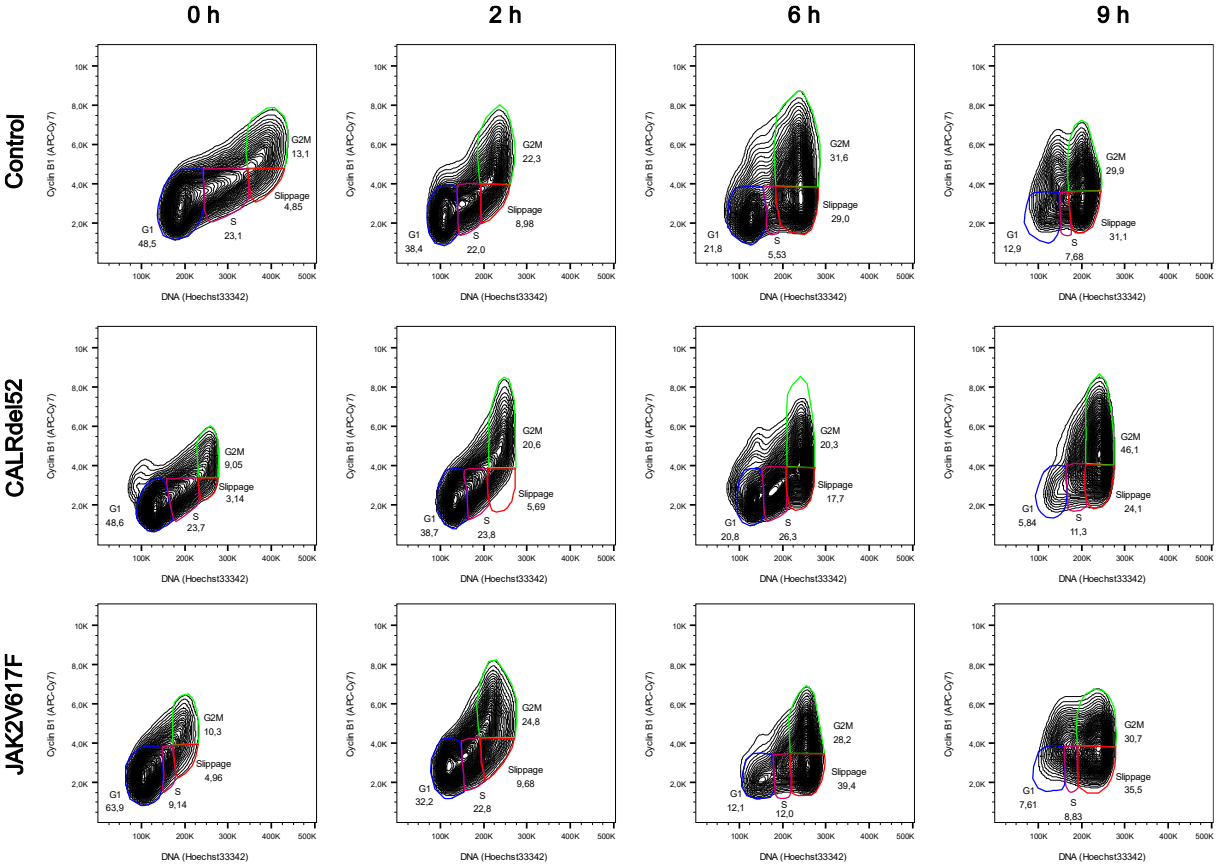

Supplemental Figure 19: Overview of results of the first cytometry experiment

Supplemental Table 11: Results of cytometry analysis

G1	CONTROL		CALRDEL52		JAK2V617F	
	Exp1	Exp2	Exp1	Exp2	Exp1	Exp2
0 H	48,5 %	49,5 %	48,3 %	40,3 %	63,2 %	51,0 %
2 H	38,2 %	52,1 %	38,2 %	35,3 %	32,1 %	24,3 %
6 H	21,6 %	37,8 %	20,7 %	19,5 %	12,0 %	15,1 %
9 H	12,8 %	32,1 %	5,8 %	9,7 %	7,2 %	7,2 %
S	**CONTROL**		**CALRdel52**		**JAK2V617F**	
	Exp1	Exp2	Exp1	Exp2	Exp1	Exp2
0 H	29,3 %	16,8 %	31,7 %	25,1 %	13,3 %	21,4 %
2 H	26,2 %	16,4 %	32,1 %	22,4 %	29,5 %	11,7 %
6 H	8,0 %	7,9 %	32,5 %	8,5 %	15,8 %	7,4 %
9 H	11,6 %	9,6 %	19,7 %	11,5 %	15,2 %	13,4 %
G2M	**CONTROL**		**CALRdel52**		**JAK2V617F**	
	Exp1	Exp2	Exp1	Exp2	Exp1	Exp2
0 H	13,1 %	11,0 %	9,1 %	15,3 %	10,8 %	13,2 %
2 H	22,3 %	15,0 %	20,6 %	26,9 %	25,5 %	13,7 %
6 H	31,6 %	25,9 %	19,0 %	41,6 %	28,2 %	47,0 %
9 H	29,8 %	31,9 %	46,9 %	23,6 %	30,7 %	22,1 %
SLIPPAGE	**CONTROL**		**CALRdel52**		**JAK2V617F**	
	Exp1	Exp2	Exp1	Exp2	Exp1	Exp2
0 H	4,9 %	6,4 %	2,9 %	3,0 %	5,0 %	3,2 %
2 H	9,0 %	8,2 %	5,7 %	4,2 %	8,9 %	1,8 %
6 H	29,0 %	22,6 %	18,7 %	22,0 %	39,2 %	20,2 %
9 H	31,5 %	22,3 %	24,0 %	42,2 %	35,1 %	50,6 %

Supplemental Table 12: Exact data from SAC factor western Blotting experiments

		0 h			18 h		
		control	CALRdel52	JAK2V617F	control	CALRdel52	JAK2V617F
cdc20	Exp 1	1,00	0,48	0,57	0,25	0,13	0,17
	Exp 2	1,00	0,77	0,58	0,18	0,20	0,41
	Exp 3	1,00	1,01	0,53	0,61	0,11	0,19
	Exp 4	1,00	0,85	0,48	0,56	0,28	0,34
MAD1	Exp 1	1,00	0,93	0,66	0,50	0,39	0,37
	Exp 2	1,00	0,73	0,57	0,42	0,48	0,51
	Exp 3	1,00	1,12	1,24	0,65	0,39	0,73
	Exp 4	1,00	1,35	1,66	0,77	1,45	1,92
Cyclin B1	Exp 1	1,00	0,64	1,01	0,56	0,21	0,28
	Exp 2	1,00	0,70	0,67	0,21	0,17	0,39
	Exp 3	1,00	0,47	0,34	0,53	0,29	0,29
	Exp 4	1,00	0,65	0,45	0,62	0,31	0,34
Au	Exp 1	1,00	0,42	0,97	0,67	0,40	0,39

	Exp 2	1,00	1,33	1,02	0,24	0,16	0,53
	Exp 3	1,00	1,08	0,97	1,80	0,98	0,76
	Exp 4	1,00	0,95	0,84	1,80	1,07	0,70
MAD2	Exp 1	1,00	1,03	1,10	1,20	0,86	0,63
	Exp 2	1,00	0,71	0,80	0,34	0,29	0,31
	Exp 3	1,00	0,50	0,36	0,53	0,43	0,31
	Exp 4	1,00	0,72	0,54	0,51	0,40	0,32
BUBR1	Exp 1	1,00	0,48	0,90	0,94	0,42	0,52
	Exp 2	1,00	0,78	0,70	0,36	0,25	0,51
	Exp 3	1,00	0,37	0,33	0,47	0,28	0,33
	Exp 4	1,00	0,42	0,42	0,51	0,21	0,27
MPS1	Exp 1	1,00	0,42	0,97	0,67	0,40	0,39
	Exp 2	1,00	0,94	1,05	0,56	0,31	0,83
	Exp 3	1,00	1,16	0,85	0,32	0,11	0,29
	Exp 4	1,00	0,86	2,06	1,37	0,94	0,73
PP2A	Exp 1	1,00	0,95	0,80	0,76	1,34	1,05
	Exp 2	1,00	0,78	1,18	1,13	2,10	1,69
	Exp 3	1,00	0,52	0,49	0,42	0,23	0,41
	Exp 4	1,00	0,61	0,51	0,23	0,17	0,28
PLK1	Exp 1	1,00	1,23	1,30	1,81	1,25	1,13
	Exp 2	1,00	0,79	1,01	1,41	1,04	1,18
	Exp 3	1,00	0,56	0,61	1,03	0,36	0,94
	Exp 4	1,00	0,40	1,10	0,84	0,72	1,43

Supplemental Table 13: Mitotic time and errors of 32D^{MPL} cells after doxorubicin NMS-P715 treatment

Doxorubicin	**control**	**CALRdel52**	**JAK2V617F**
Chromosome bridges	17.38 ± 5.73 %	22.50 ± 3.55 %	25.63 ± 5.78 %
Lagging Chromosome	5.63 ± 3.07 %	8.00 ± 4.11 %	8.00 ± 3.25 %
Micronuclei in telophase	0.25 ± 0.46 %	1.25 ± 0.89 %	1.50 ± 1.20 %
NMS-P715	**control**	**CALRdel52**	**JAK2V617F**
Chromosome bridges	15.67 ± 4.76 %	31.17 ± 6.18 %	32.50 ± 5.43 %
Lagging Chromosome	6.33 ± 1.86 %	14.33 ± 6.65 %	14.00 ± 4.52 %
Micronuclei in telophase	1.00 ± 0.89 %	3.00 ± 1.90 %	3.50 ± 2.07 %

Supplemental Table 14: Signal ratio between the different SAC factors and CREST

SAC Factor/ CREST		Control	CALRdel52	JAK2V617F
MAD1	Exp 1	1,04	1,53	0,84
	Exp 2	1,11	1,79	0,88
	Exp 3	1,23	1,69	0,73
CENPE	Exp 1	1,02	1,09	0,90
	Exp 2	1,01	1,18	1,07
	Exp 3	1,02	1,21	1,08
cdc20	Exp 1	1,03	1,44	0,64
	Exp 2	1,18	1,35	0,72
	Exp 3	1,08	1,14	0,50
Cyclin B1	Exp 1	1,21	5,64	0,57
	Exp 2	1,33	2,81	0,39
	Exp 3	1,06	2,10	0,32
MPS1	Exp 1	1,39	0,93	0,62
	Exp 2	1,09	0,65	0,40
	Exp 3	1,12	1,09	1,05
Aurora B	Exp 1	1,04	1,46	1,00
	Exp 2	0,99	1,25	1,16
	Exp 3	1,04	1,26	0,79
	Exp4	0,98	1,05	- / -
MAD2	Exp 1	1,00	1,72	1,37
	Exp 2	1,03	1,33	1,33
	Exp 3	1,03	1,23	0,80
BUBR1	Exp 1	1,05	0,81	0,74
	Exp 2	1,04	0,79	0,87
	Exp 3	1,02	0,94	0,87

8. This thesis would not have been possible without the input of the following people:

Dr Daniel Moreno-Andrés closely supervised this PhD work. He assisted me with guidance and scientific discussion of ideas, concepts, experiment protocols, and in the creation of the pipelines for the analysis of all experiments.

The 32D^{MPL} and TF-1^{MPL} cell lines, which were transduced with Empty vector, CALdel52 and JAK2V617F, were provided to me by Dr Nicolas Chatain and Prof Stefan Koschmieder. I was assisted in performing the flow cytometry by Dr Nicolas Chatain.

Anja Scheufen assisted me by applying nocodazole three hours prior to the subsequent processing of the samples in select kinetochore recruitment experiments (3.2.3). Additionally, she modified the HeLa cells that were utilized in this study.

Dr Ramona Jühlen provided the Studio R code for the evaluation of the mitotic time experiments [3.1 / 3.1.1 / 3.3.2].

As part of her Bachelor's thesis, Nathalie Brock conducted the immunofluorescence experiment examining MAD1 in TF-1^{MPL} cells [3.3.3].

Susanne Krapp (technical assistant) helped me to perform the fixation and pre-treatment of the samples for some of the quantitative immunofluorescence experiments [3.2.3].

9. Acknowledgments

I would like to take this opportunity to thank everyone who has supported and motivated me in writing this dissertation.

First and foremost, I would like to thank Prof Dr Wolfram Antonin and Dr Daniel Moreno-Andrés, who supervised and reviewed my dissertation. I would like to express my sincere thanks for their helpful suggestions and constructive criticism during the preparation of this thesis. I would also like to thank Prof Dr Gabriel Pradel for her helpful and scientific support as a second reviewer.

I would also like to thank the Faculty of Medicine's research funding programme (START) for their financial support of my research.

Special thanks also go to Prof Stefan Koschmieder and Dr Nico Chatain for their cooperation and helpfulness in carrying out the experiments and for providing the 32D and TF-1 cell lines.

I would also like to thank all the staff at the Institute of Biochemistry and Molecular Cell Biology for the many interesting discussions and ideas that have contributed significantly to the fact that this dissertation is available in this form. In particular, I would like to thank Dr Ramona Jühlen for providing the Studio R code and Anja Scheufen for providing the HeLa cells.

And finally, special thanks are owed to my family, who always believed in me and who kept me on the right path throughout my studies with infinite patience and loving care.

29.08.2024

Kristin Joana Holl

10. Publications as part of the doctoral thesis

Daniel Moreno-Andrés, **Kristin J. Holl**, Wolfram Antonin (2023), The second half of mitosis and its implications in Cancer Biology, Seminars in Cancer Biology, Volume 88, page 1-17.

Parts of this thesis were pre-published in this paper and on this poster:

Kristin J. Holl, Nicolas Chatain, Susanne Krapp, Julian Baumeister, Tiago Maie, Sarah Schmitz, Anja Scheufen, Nathalie Brock, Steffen Koschmieder, Daniel Moreno-Andrés (2024), "Calreticulin and JAK2V617F driver mutations induce distinct mitotic defects in myeloproliferative neoplasms." Sci Rep **14**(1): 2810.

Kristin J. Holl, Nicolas Chatain, Nathalie Brock, Susanne Krapp, Julian Baumeister, Steffen Koschmieder, Wolfram Antonin, Daniel Moreno-Andrés (2023), Mutant calreticulin and JAK2V617F driver mutations induce distinct mitotic defects in myeloproliferative neoplasms, *Poster at the EHA Frankfurt*

Eidesstattliche Erklärung

Kristin Joana Holl erklärt hiermit, dass diese Dissertation und die darin dargelegten Inhalte die eigenen sind und selbständig, als Ergebnis der eigenen originären Forschung, generiert wurden.

Hiermit erkläre ich an Eides statt

1. Diese Arbeit wurde größtenteils in der Phase als Doktorand dieser Fakultät und Universität angefertigt
2. Sofern irgendein Bestandteil dieser Dissertation zuvor für einen akademischen Abschluss oder eine andere Qualifikation an dieser oder einer anderen Institution verwendet wurde, wurde dies klar angezeigt
3. Wenn immer andere eigene- oder Veröffentlichungen Dritter herangezogen wurden, wurden diese klar benannt
4. Wenn aus anderen eigenen- oder Veröffentlichungen Dritter zitiert wurde, wurde stets die Quelle hierfür angegeben. Diese Dissertation ist vollständig meine eigene Arbeit, mit der Ausnahme solcher Zitate
5. Alle wesentlichen Quellen von Unterstützung wurden benannt
6. Wenn immer ein Teil dieser Dissertation auf der Zusammenarbeit mit anderen basiert, wurde von mir klar gekennzeichnet, was von anderen und was von mir selbst erarbeitet wurde
7. Teile dieser Arbeit wurden zuvor veröffentlicht und zwar in:
   Kristin J. Holl, Nicolas Chatain, Susanne Krapp, Julian Baumeister, Tiago Maie, Sarah Schmitz, Anja Scheufen, Nathalie Brock, Steffen Koschmieder, Daniel Moreno-Andrés (2024), "Calreticulin and JAK2V617F driver mutations induce distinct mitotic defects in myeloproliferative neoplasms." Sci Rep **14**(1): 2810.

29.08.2024

Kristin Joana Holl